

**Small-conductance calcium-dependent potassium channel
(SK) function: studies in transgenic mice harboring
conditional alleles at three *SK* loci**

by

Chris T. Bond

A Dissertation

Presented to the Cell and Developmental Biology Department
and the Oregon Health and Sciences University School of Medicine

in partial fulfillment of the requirements

for the degree of

Doctor of Philosophy

April 2004

School of Medicine
Oregon Health and Sciences University

CERTIFICATE OF APPROVAL

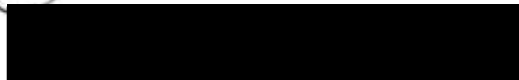
This is to certify that the Ph.D. thesis of

Chris T. Bond

has been approved



Professor in charge of thesis



Committee Member



Committee Member



Committee Member

Table of Contents

Acknowledgements	iii
Abstract	iv
List of figures	vi
Abbreviations	viii
Chapter I. Introduction	1
1. Small-conductance calcium-activated (SK) channels	1
2. Potassium channel clones	12
3. Potassium channel transgenic mice	18
Chapter II. <i>SK</i> transgenic mice	23
1. Introduction	23
2. <i>SK2 tTA</i> mice	32
3. Floxed alleles	39
4. Summary	48
Chapter III. <i>SK</i> knockout mice and hippocampal AHP currents	51
1. Abstract	52
2. Introduction	53
3. Methods	55
4. Results	61
5. Discussion	65
Chapter IV. <i>SK1</i> ; the enigma	68
1. Introduction	68
2. Materials and methods	73
3. Results	76
4. Discussion	81

5. Summary and hypotheses for SK1 function	86
Chapter V. Discussion	87
1. <i>SK</i> genetic loci	87
2. Conditional transgenes	88
3. SK Physiology and <i>SK</i> transgenic mice	96
Chapter VI. Summary and conclusions	103
References	105
Appendices	
A. Supplemental manuscripts	
B. Derivation of formula for comparative C_T method for quantitative PCR.	

Acknowledgements

I wish to acknowledge, foremost, John Adelman. John has served as mentor, boss, friend, teacher, motivator and reality check for eighteen years. John allowed and helped me to become a scientist without the benefit of a Ph.D. but then was encouraging and supportive when the need to acquire the advanced degree was no longer avoidable. Thank you John, I look forward to more science and more (though not too much) reality.

Many thanks also go to all members, past and present, of the Adelman lab; in particular Jim Maylie and my longtime friend Paco Herson. Thanks to Paco for e-phys on the KO mice. Thanks to Tim Strassmaier for biochemistry for the KO paper and beyond. Thanks to Zhongying Yang for lots of genotyping, southern blots and cell staining.

I also wish to acknowledge colleagues here at OHSU for their help, encouragement, and trust, in particular Mike Forte, Bruce Megun, Gary Thomas, Phil Copenhaver, and Gail Clinton.

Last but not least, I want to acknowledge my daughter Anna for reminding me what I taught her but then forgot: namely that we can do anything we set our minds to, our happiness is in our own hands and minds, and that age is irrelevant. And I thank Anna and Noah and all that is holy for my granddaughter, Zarah, who reminds me of the pure joy of living and loving.

Abstract

Small-conductance calcium-activated potassium (SK) channels, being voltage-independent, are activated solely by elevation of intracellular calcium. Use of apamin, a bee venom peptide toxin which blocks SK channels potently and specifically, has led to characterization of SK roles and activity in numerous central nervous system and peripheral organ physiologies. Activation of SK channels is coupled to varied sources of calcium: voltage-dependent calcium channels, 1,4,5 inositol trisphosphate receptors, or ionotropic neurotransmitter receptors among others; but irrespective of the source of calcium, activation of SK channels exerts a hyperpolarizing influence, thereby modulating excitability.

Three genes encoding SK channel subunits have been found in mammalian organisms and cDNAs representing each of these loci, *SK1*, *SK2*, and *SK3*, have been cloned and functionally characterized from mouse, rat and human. In situ hybridization experiments demonstrated that the three genes are expressed in distinct yet overlapping patterns throughout the brain.

Heterologous expression of the cloned cDNAs resulted in potassium currents that were activated by elevation of intracellular calcium from human SK1, rat, mouse or human SK2, and rat, mouse or human SK3. The calcium sensitivity and kinetics of activation and deactivation were virtually identical for all these channels. The pharmacological profile of the expressed currents showed that SK2 was most sensitive to block by apamin and *d*-tubocurarine, SK3 has

intermediate sensitivities and SK1 is least sensitive to these blockers of calcium-activated currents; the $I.C_{50}$ for apamin block of SK currents spanning from 60 pM to greater than 12 nM. Structure-function studies have shown that calmodulin associates with the SK pore-forming subunits and that binding of calcium to calmodulin mediates channel opening.

In order to allow discrimination of individual SK channel gene contribution to apamin-mediated effects, and to allow separation of SK channel roles in different brain regions and organ systems, transgenic mice have been created by homologous recombination that allow separate regulation of each of three *SK* genes. Studies of these mice have shown the important role of SK3 in control of vascular tone and bladder continence, and a role for SK3 in regulation of respiratory rhythm. Resolution of longstanding questions regarding the molecular identity of channel subunits mediating kinetically distinct afterhyperpolarizing currents in principle neurons of the hippocampus has been attained by study of these *SK* transgenic mice: *SK2* gene products are necessary for the channel underlying the medium component of the AHP; SK1, SK2 and SK3 do not form channels underlying the slow AHP.

Future studies of mice derived from these conditional allele mutants through cross breedings with region-specific *Cre* transgenic mice will play a major role in our growing understanding of the many roles served by SK channels and the specific subunits serving those roles.

List of Figures

Chapter I. Introduction

Figure 1. AHP currents in frog motoneuron.

Figure 2. Dendrogram of the potassium channel superfamily.

Figure 3. Membrane topology and tetramer assembly.

Figure 4. Homology of mammalian SK subunits.

Figure 5. Calcium gating of SK channels.

Chapter II. *SK* Transgenic Mice

Figure 1. Tet cassette.

Figure 2. 5' mapping of SK2 transcript.

Figure 3. *SK2 tTA* schematic.

Figure 4. B-Galactosidase activity dependent detection of SK2 and SK3 expression.

Figure 5. *SK1 flox*.

Figure 6. *SK2 flox*.

Figure 7. SK1 RT-PCR.

Figure 8. Hippocampal EEGs.

Chapter III. *SK* Knockout Mice Knockout Mice Reveal the Identity of

Calcium dependent AHP Currents.

Figure 1. *SK* transgenic mice.

Figure 2. Voltage clamp analysis of the AHP.

Figure 3. SK channels in medium and slow AHPs.

Figure 4. Quantitative analysis of SK mRNA levels.

Table 1. Cell parameters for different transgenic mice.

Table 2. AHP current amplitudes.

Chapter IV. SK1; the enigma

Figure 1. Alternative splicing at the *SK1* locus.

Figure 2. Schematic of topology and alternate exons of *SK1*.

Figure 3. Quantitative analysis of SK1 splice form expression in brain and kidney.

Figure 4. Western blot of SK1 alternative proteins expressed *in vitro*.

Figure 5. Western blot of SK1 alternative proteins with monoclonal antibodies.

Figure 6. Surface expression of SK subunits.

Chapter V. Discussion

Figure 1. Conservation of *SK* locus structure across isotype and species.

Abbreviations

ACh	acetylcholine
ACSF	artificial cerebrospinal fluid
AHP, IAHP	afterhyperpolarization, afterhyperpolarization current
AP	action potential
ATP/ADP	adenosine tri-phosphate/adenosine di-phosphate
B-Gal	beta-galactosidase
BK	large conductance calcium and voltage-dependent potassium channel
bp, kbp	base pair, kilobase pair
Ca ²⁺	divalent calcium ion
CaM	calmodulin
[Ca ²⁺] _i	intracellular calcium concentration
CaM-BD	calmodulin binding domain
cAMP	cyclic adenosine mono-phosphate
CMV	cytomegalovirus
CNS	central nervous system
DM	myotonic dystrophy
DNA, cDNA,	deoxyribonucleic acid, complementary DNA,
EA	episodic ataxia type 1
EEG	electroencephalogram
eGFP	enhanced green fluorescent protein
ES cell	embryonic stem cell
flox	flank with loxP sites
GnRH	gonadotropin releasing hormone
I/O	inside out
IK	intermediate conductance potassium channel
I _{KCa}	calcium-dependent potassium current
IP3	1,4,5-inositol trisphosphate

K ⁺	monovalent potassium ion
Kir, IR	inwardly rectifying, voltage-independent potassium channel
KO	knock out
Kv	voltage-dependent potassium channel
LTD	long term depression
LTP	long term potentiation
mAChR	muscarinic acetylcholine receptor
mEF	mouse embryonic fibroblasts
Met	methionine
mM, μ M, nM, pM	millimolar, micromolar, nanomolar, picomolar
mV	millivolt
Na ⁺	monovalent sodium ion
neo	neomycin resistance gene
NMDA	n-methyl-d-aspartate
OHC	outer hair cell
OMP	oscillating membrane potential
PBS	phosphate buffered saline
PCR, RT-PCR	polymerase chain reaction, reverse-transcription-PCR
pS	picosecond
RACE	rapid amplification of cDNA ends
RNA, mRNA	ribonucleic acid, messenger RNA
SK	small-conductance calcium activated potassium channels
Tet, dox	tetracycline, doxycycline
TM	transmembrane domain
TRP	tryptophan
URA	uracil
UTR	untranslated region
VDCC	voltage-dependent calcium channel
WT	wild type
μ g	microgram

CHAPTER I. Introduction

1. *Small-conductance calcium-activated potassium (SK) channels*

Potassium and calcium

Many atomic and molecular ions serve diverse functions in living organisms, as signaling molecules, co-factors, modulators, regulators of osmolarity, and mediators of excitability. Arguably the most important of all the biological ions is calcium (Ca^{2+}). Ca^{2+} ions are the central player in many signal transduction cascades, mediating responses from fertilization to cell death [1]. The intracellular concentration of calcium ($[\text{Ca}^{2+}]_i$) is under tight control; free ions are rapidly chelated by a host of calcium-binding proteins. Sources for calcium and the molecules that mediate flux of calcium into the cytoplasm from those sources are highly regulated. In response to incoming signals, Ca^{2+} ions flow into the cytoplasm from the extracellular space and/or from intracellular stores, which include at least the endoplasmic reticulum, mitochondria, and sarcoplasmic reticulum (muscle cells). Membrane-spanning proteins, including voltage-dependent calcium channels and ionotropic neurotransmitter receptors on plasma membranes, inositol 1,4,5-tris phosphate (IP3) receptors and ryanodine receptors on intracellular membranes, mediate influx of calcium to the cytoplasm, where elevation of $[\text{Ca}^{2+}]_i$ in a microdomain surrounding the entry site initiates a signaling cascade. Calcium influx can be stimulated by diverse signals, including membrane depolarization, stretch, noxious stimuli, and a multitude of

extracellular ligands. Different calcium signaling pathways can interact to control the source and characteristics of the cytosolic Ca^{2+} signal.

In excitable cells, three other major ions, Na^+ , K^+ , and Cl^- , contribute to the bulk ion concentration that results in a voltage gradient across the plasma membrane. Through the action of pumps and exchangers, the intracellular concentration of Na^+ is kept low while the K^+ concentration is maintained higher inside the cell than out. Because the cell is somewhat leaky for K^+ through numerous potassium or cation permeant “leak” channels, K^+ ions escape through the plasma membrane down the potassium concentration gradient. The negative ions that cannot permeate the leak channels are left as a negative charge cloud along the intracellular face of the plasma membrane. The net result of the distribution of these ions is that the inside of the plasma membrane is more negative than the outside by a range of 45 to 90 millivolts (mV). Membrane-spanning proteins containing pores permeant to specific ions respond to changes in the potential gradient by opening and allowing flux of ions across the membrane. When an input signal depolarizes a region of membrane by as little as 10 mV, voltage-dependent sodium channels open and the rapid influx of Na^+ ions, which constitute the primary component of an action potential (AP), results in a bulk depolarization of the cell plasma membrane. Voltage-dependent potassium channels open in response to the depolarizing wave of the action potential and potassium ions flood out of the cell, repolarizing the membrane and causing voltage-dependent channels to close. Opening of voltage-dependent

calcium channels (VDCC) in response to the depolarization yields an influx of Ca^{2+} ions. Possible responses to the influx of calcium ions include activation of Ca-sensitive channels on intracellular stores resulting in further elevation of cytosolic calcium, activation of signaling cascades such as through calcium/calmodulin dependent kinases, or opening of calcium-activated potassium channels that hyperpolarize the cell and thereby blunt the influx of calcium through the VDCC.

Of all the membrane proteins controlling the flux of ions, potassium channels are the most abundant and diverse. There are over seventy genes encoding potassium channel pore-forming subunits in the mammalian genome. Within the potassium channel super family are the “leak” channels that set up the polarity of the plasma membrane and contribute the resting membrane potential, voltage-dependent potassium channels that rapidly repolarize the membrane following an action potential, and other potassium channels that are gated or modulated by intracellular ligands such as ATP and calcium.

Calcium-activated potassium channels

In 1958, Gardos made the first observation that intracellular Ca^{2+} could exert control on the permeability of the cell membrane to K^+ ions by measuring efflux from red blood cells [2]. In the early 1970's, Meech and Strumwasser observed that micro-injection of calcium into an *Aplysia* neuron resulted in hyperpolarization of the cell membrane [3]. The observed response was accompanied by an increase in membrane conductance that had a reversal

potential consistent with a potassium conductance. With the advent of the patch clamp technique [4] the prevalence and diversity of calcium-sensitive potassium currents ($I_{K(Ca)}$) began to be appreciated. $I_{K(Ca)}$ currents have been observed in virtually all tissues examined. Characteristics of these currents are quite diverse: conductances range from a few to several hundred picosiemens (pS); calcium, voltage and pharmacological sensitivities vary broadly. $I_{K(Ca)}$ channels came to be loosely classified into three categories, large-conductance, intermediate-conductance and small-conductance families. Large conductance (BK) $I_{K(Ca)}$ channels have unitary conductances ranging from 180-240 pS, are gated by both calcium and voltage, and most are blocked by charybdotoxin. Intermediate-conductance (IK) channels exhibit unitary conductances between 40-60 pS, are voltage independent and are resistant to blockers of the other subgroups. Small-conductance (SK) (4-20 pS) $I_{K(Ca)}$ channels are more sensitive to calcium than BK channels, are voltage-independent and are selectively blocked by the bee venom peptide toxin, apamin, and by *d*-tubocurarine [5]. By careful use of this differential pharmacology, functional roles for the calcium-dependent potassium channels in a wide array of physiological systems have been postulated.

SK channels in physiology: excitability.

The potency and selectivity of apamin for blocking SK channels has allowed characterization SK channel activity in a wide array of cell types. Apamin binding or apamin block of an $I_{K(Ca)}$ have been demonstrated in neurons and glia from the central nervous system [6-8], in smooth muscle of the gut [9], bladder

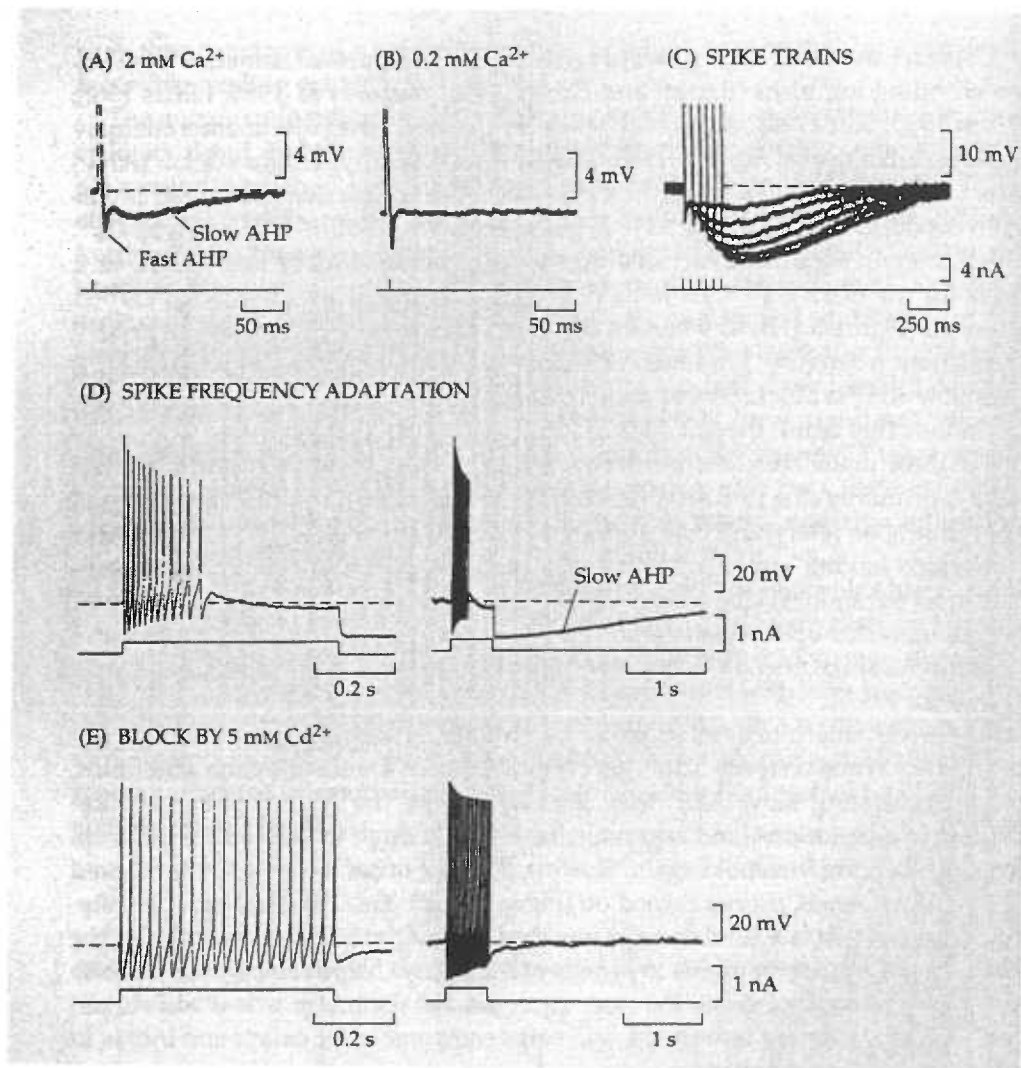


Figure 1.

Current clamp recording of a frog spinal motor neuron. A. Following an action potential which goes far above the edge of the figure, there is a multi-component AHP. B. The AHP is dependent on extracellular calcium. C. The amplitude and duration of the slow AHP grows with each additional action potential. D. A vagal motoneuron shows spike frequency adaptation and a large slow AHP during and following a long duration depolarizing current pulse. E. Addition of 5 mM Cd^{2+} to the medium eliminates spike frequency adaptation and most of the slow AHP.

Hille: Ion Channels of Excitable Membranes, Third addition, 2001

[10, 11], and vasculature [12, 13], in the adrenal [14] and pituitary [15, 16] glands, in hepatocytes [17] and in cultured skeletal muscle cells [18].

The high calcium-sensitivity of SK channels, coupled with voltage-independence, gives these channels an important role in controlling membrane excitability near the resting membrane potential. In excitable cells, SK channels are activated by calcium ions flowing into the cell through VDCCs [19] during the depolarized phase of the AP, causing an afterhyperpolarization (AHP). The hyperpolarizing current mediated by SK channels decays slowly, following the decline in calcium concentration. The effect of the AHP is to regulate the interspike interval and may also contribute to setting bursting patterns, thereby exerting control on the basic excitability of neurons. An apamin-sensitive component of the AHP has been characterized in cortical pyramidal cells [20] and in hippocampal pyramidal cells by whole cell voltage clamp experiments [21].

Apamin has been shown to affect learning and memory [22-24]. In hippocampal-dependent learning tests, intraperitoneal injection of apamin prior to training resulted in accelerated acquisition of relevant memory compared to performance of animals not receiving apamin. Neither retention nor consolidation of memories was affected by apamin injection. Field recordings from the CA1 region of the hippocampus in brain slice preparations revealed that apamin shifted the threshold for synaptic plasticity, both for long term depression (LTD) and longterm potentiation (LTP) to lower stimulus frequencies [24]. Thus SK channels modulate cellular responses to synaptic transmission as well as to APs

In addition to activation by influx of calcium through VDCCs, SK channel activation is coupled to neurotransmitter and neuromodulator activation of ionotropic and metabotropic receptors that result in elevation of intracellular calcium concentration. Coupling of muscarinic acetylcholine receptors to SK channel activity has been demonstrated in ventral midbrain dopamine neurons [25] and in pyramidal neurons in layers 2/3 of the visual cortex [26]. In dopamine neurons, activation of the muscarinic receptor stimulates production of IP₃, activating IP₃ receptors on intracellular membranes and releasing calcium from stores that then activates SK channels, hyperpolarizing the cell. The activation of SK channels happens with brief activation of mACh receptors, longer activation or higher concentrations of agonist results in activation of a depolarizing conductance. Thus the SK channels are dynamically regulated by acetylcholine, being phasically activated during periods of relatively low cholinergic activity, but tonically closed during periods of sustained cholinergic input [25]. In the neocortical neurons, SK channels were activated by calcium entry through VDCCs in response to a 5 ms depolarization. SK channel activity was elevated and prolonged by activation of the mACh receptor by carbachol in conjunction with the depolarization. The carbachol effect was mediated by IP₃-assisted calcium induced calcium release (CICR) [26].

SK channels are coupled to nicotinic ACh receptors in neonatal inner hair cells. Calcium influx through nAChRs containing $\alpha 9$ subunits activates SK channels. The inner hair cells are transiently synaptically innervated by ACh

fibers in mice, during the period between birth and the onset of hearing. The ACh innervation is not detected in inner hair cells of older animals [27]. The developmental consequences or function of this transient ACh innervation of inner hair cells is not known.

ACh innervation of outer hair cells (OHC) in mature mice is also coupled to activation of SK channels. Activation of SK channels in cochlear outer hair cells in response to Ca^{2+} influx through nicotinic acetylcholine receptors results in a fast inhibitory post synaptic current (IPSC) [28]. This is an example of fast inhibitory synaptic transmission that is not due to activation of ionotropic GABA or glycine receptors, but rather relies on the rapid coupling of excitatory and inhibitory ion channels. Again, although the functional significance of this coupling is not completely understood, calcium-dependent processes downstream of AChR activation play a role in regulating electromotility of the OHC; electromotility being part of the amplification and motor output process of the OHC [29].

A number of ionotropic neurotransmitter receptors are permeable to calcium, and SK channels are widely distributed throughout the CNS; co-localization of the receptors and SK channels in microdomains may yield a general mechanism for generating inhibitory synaptic transmission from activation of otherwise excitatory neurotransmitters [28].

SK channel function in oscillating systems.

In rat pituitary gonadotrophs, application of gonadotropin-releasing hormone (GnRH) resulted in IP₃-dependent oscillatory release of Ca²⁺ from intracellular stores. The resulting increase in [Ca²⁺]_i activated an apamin-sensitive potassium channel, causing periodic hyperpolarization of the plasma membrane. The oscillatory behavior was independent of extracellular calcium, although rundown occurred ultimately, probably due to depletion of calcium in stores. Relief of inactivation of voltage-dependent Na⁺ and Ca²⁺ channels by the period of hyperpolarized potential resulted in firing of one to three action potentials. Calcium entry during the APs served to replenish stores, allowing oscillations to continue as long as GnRH was present. Although gonadotropin release was not concurrently measured, it is likely that the oscillatory response to GnRH is an important element of the stimulation-secretion coupling in these cells. The authors also postulate this oscillatory behavior may be important for the calcium economy of the cell, allowing for release of calcium from stores for signaling but coupled to influx of extracellular calcium to replenish stores [16]. A possible role for SK channels in other types of oscillatory systems have been described and may define a function for SK channels in pattern generating pacemaker cells [30] or in intracellular calcium dynamics [31]. Some types of amacrine cells of the retina show oscillatory membrane potentials (OMPs) in response to light. These OMPs result from intrinsic properties of the cell and are dependent on coupling of calcium channels to SK channels [32].

SK channel function has been implicated in a brain-wide oscillation between non-REM and REM sleep. REM sleep propensity is accumulated during non-REM sleep, rather than during waking [33]. One hypothesis for the role of REM sleep is that REM sleep may occur to permit replenishment of neuronal intracellular K^+ , following destabilization of the Na^+/K^+ balance due to the increased somal and dendritic potassium flux [34] during non-REM sleep. Intracerebroventricular injection of small doses of apamin in rats produced a dose-dependent reduction of REM sleep without an increase in the frequency of attempts to enter REM sleep, suggesting that accumulation of REM sleep propensity is suppressed in response to block of SK channels [35].

SK function in skeletal muscle.

In the dominantly inherited human disease, myotonic muscular dystrophy (DM, Dystrophia Myotonica 1, OMIM #160900), skeletal muscles show stiffness and difficulty in relaxing after voluntary contractions. Electrophysiological analysis of myotonic muscles shows an increased excitability with a tendency to fire repetitive action potentials in response to stimulation (myotonia). I^{125} apamin bound to muscle cells from DM patients [36]. This binding of apamin was absent in normal human muscle tissue. These results implicate up-regulation of expression of an SK channel in DM. Injection of apamin into the muscles of DM patients eliminated the myotonic run; myotonia induced in muscles of patients suffering from Myotonia Congenita (OMIM # 160800), a disorder due to defects

in a chloride channel, was unaffected by apamin injection [37]. Although expression of hyperpolarizing currents in muscle cells might be expected to reduce excitability rather than increase it, the special architecture of the t-tubules of muscle may result in sequestration of extruded K^+ ions in the tubule extracellular space, resulting in a localized depolarization that could lead to a lowered threshold for AP generation. Denervation of normal skeletal muscle also results in hyperexcitability and appearance of apamin binding sites [38]. The relationship between up-regulation of SK expression in denervation and that in DM is still under investigation. Although the genetic lesion responsible for DM is not in any of the SK loci, up-regulation of SK expression is central to the major symptom of DM, and pharmacology directed at control of SK channel activity may be a valuable therapeutic approach for this disorder.

SK current details, as characterized in adrenal chromaffin cells.

SK channel activity was studied in detail in I/O patches from cultured rat adrenal chromaffin cells. The $[Ca^{2+}]$ necessary for half-maximal activation was $0.69 \mu M$, and was independent of membrane potential. SK currents were blocked by external application of apamin with a K_D of $4.4 nM$, tubocurarine (K_D $20 \mu M$), and tetraethylammonium (TEA) (K_D $5.4 mM$). SK channel activation in these cells is postulated to regulate muscarine-evoked release of catecholamines [39]. SK channels control some of the electrical activity of bovine chromaffin cells and modulate stimulated secretion of catecholamines [40].

Summary

In summary, SK channel activation is coupled to calcium entry through VDCCs [41, 42], ionotropic glutamate [43] and acetylcholine receptors [44]; activation of SK channels in response to calcium elevation results in hyperpolarization of the membrane and a dampening of excitability. Activation of nAChRs may be directly coupled to SK channels leading to a fast inhibitory response to the normally excitatory neurotransmitter, ACh [28]. SK channels are activated in response to calcium released from stores in response to activation of IP3 receptors [15, 16, 26]. Activation of SK from stores is coupled to metabotropic receptor (mAChR or mGluR) activation. SK activity, which depends on magnitude and duration of the metabotropic receptor activation, exerts a modulatory influence on the membrane potential, tuning the cell's excitability [25, 26, 45]. SK channels participate in intrinsic cell properties of rhythmically firing cells or oscillatory systems. Furthermore, SK channels may have an important role in calcium dynamics and the refilling of intracellular calcium stores in these oscillating systems [16, 32]. Most likely, the different sources of calcium and SK channels are discretely assembled into macromolecular complexes, or microdomains, that provide specificity of calcium signaling to particular pathways. Thus SK channels are poised to participate in regulation of membrane excitability and stimulus-secretion coupling in divergent systems throughout the organism.

2. Potassium channel clones

Historical perspective

The *Drosophila* mutant *Shaker*, named for the behavior of the flies when recovering from anesthesia [46], expresses an aberrant voltage-dependent potassium channel [47]. In an elegant combination of genetics and electrophysiology, the first cDNA clones encoding a potassium channel were isolated from *Shaker* flies [48]. Subsequent to this initial cloning success, the floodgates were opened, and cDNAs encoding potassium channel subunits of many different types were cloned. Homology screens, using *Shaker* cDNA in low-stringency hybridization on mammalian cDNA libraries, or probes consisting of degenerate oligonucleotide pools encoding amino acids conserved across different clones, led to isolation of mammalian potassium channel cDNAs [49-51]. Functional analysis by heterologous expression in *Xenopus* oocytes allowed correlation of individual cDNAs with channel types previously distinguished only by kinetic or pharmacological profiles [52-54]

In another *Drosophila* mutant, *slowpoke (slo)*, a fast, calcium-activated potassium conductance that contributes to repolarization of the flight muscle membrane following APs is missing. Genetic analysis of multiple independent *slo* flies resulted in identification of the locus and ultimately to the cloning of the channel coding sequence [55]. Molecular analysis and functional expression in *Xenopus* oocytes of cDNAs derived from this locus revealed that the channel

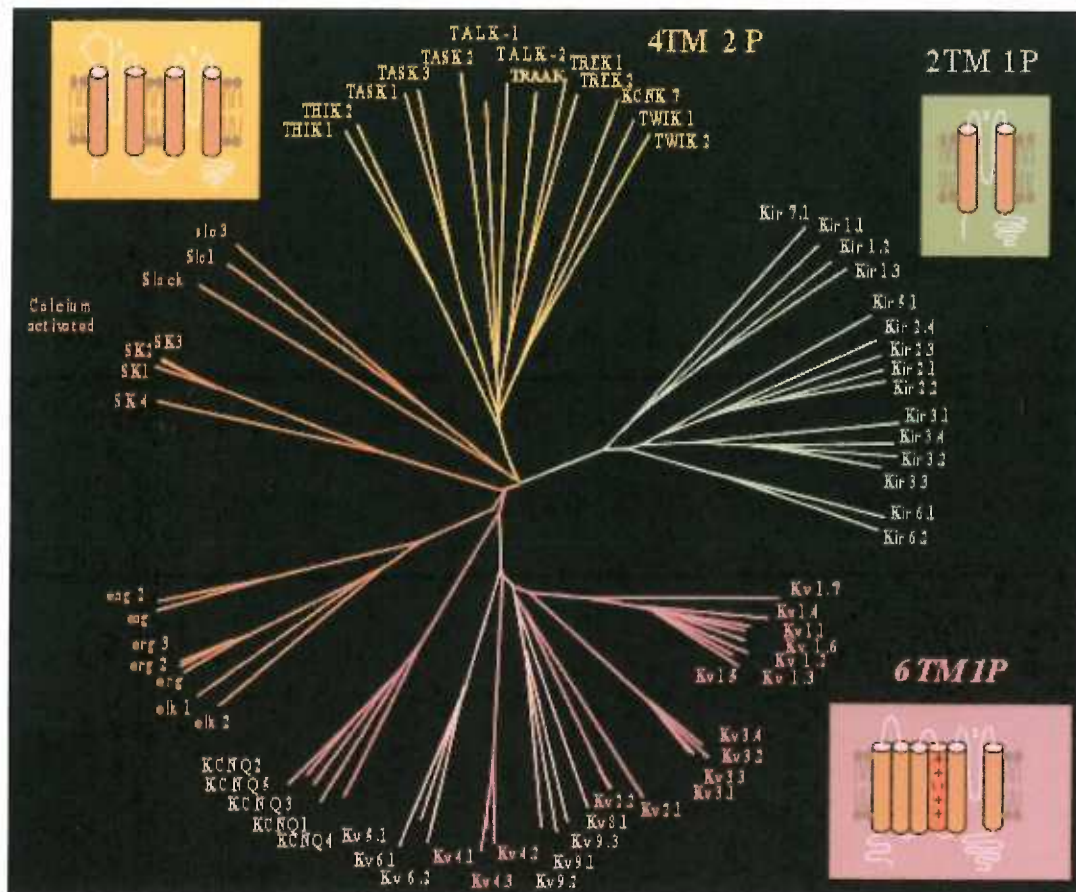


Figure 2.

Dendrogram of 71 mammalian potassium channel α -subunit genes. The largest subfamily is comprised of genes encoding subunits of voltage-dependent channels, having the classic membrane topology of 6 TMs (purple). Another large subfamily is comprised of the inward rectifiers with 2 TMs (aqua). The subfamily of two-pore, 4TM (yellow) subunits form background or leak channels. *SK* and *IK* genes comprise a small, distinct subfamily; *BK* and related genes form yet another small subfamily (tan).

Pharmacol Rev (2003) 55 (4):583-586

encoded by the *slo* gene is a multiply alternatively spliced, large-conductance, calcium- and voltage-activated potassium channel [56, 57].

All of the potassium channel cDNAs cloned using homology to voltage-dependent channels shared a predicted membrane topology of six membrane-spanning regions, with the N- and C-terminal sequences predicted to lie intracellular. Further, the most highly conserved region, between TMs 5 and 6, contained the amino acid sequence GYGD, residues which were postulated and later shown to line the permeation pathway, or pore, and to confer selectivity for potassium ions [58]. Functional potassium channels were comprised of a tetrameric assembly of pore forming subunits [59, 60]. Sequence comparison of cloned subunits and co-expression studies defined subfamilies within the potassium channel superfamily [61-63]. Subfamily delineations for these early clones followed the pattern in *Drosophila* that has four major loci encoding voltage-dependent potassium channels: *Shaker*, *Shab*, *Shal*, and *Shaw*. Even with the plethora of cloned potassium channel cDNAs, functional analysis revealed that several types of potassium channels known from studies of a variety of cells were not represented by the known sequences. Among those not yet cloned were the inward rectifier (IR) potassium channels; channels that are not gated by voltage, which allow K⁺ influx but very little K⁺ efflux. These channels had been characterized in multiple cell types, including skeletal and cardiac muscle cells [64], neurons [65] and endothelial cells [66] and were known

to be important in maintaining the resting membrane potential near the equilibrium potential for potassium.

Two groups [67, 68] isolated cDNAs encoding inward rectifier potassium channels by expression cloning. Size-fractionated A⁺ RNA from tissues enriched in inward rectifier currents was injected in to *Xenopus* oocytes that were then tested for the presence of the potassium current. RNA fractions positive for the activity were converted to cDNA, and functional analysis of cDNA pools led to isolation of inward rectifier (IR) coding sequences. Subsequent cDNA library screening with degenerate oligo pools designed against consensus pore sequences led to cloning of five more highly related subunits [69] indicating that the IR channels comprise a large subfamily of related potassium channels. All of the IR potassium channel clones shared a unique membrane topology consisting of only two TMs flanking the pore sequence. Functional characterization revealed, within the IR subfamily, ATP-sensitive channels [67, 70, 71], G-protein coupled channels [72-74] and subunits sensitive to pH [75]. However, none of the cloned sequences expressed channels with the characteristics of SK channel.

SK Channel clones

In the mid 1990's, the laboratory of John Adelman at the Vollum Institute in Portland, Oregon began efforts to isolate cDNAs encoding SK subunits. Two strategies were launched; screening single-stranded cDNA from brain with degenerate oligonucleotide primers (a strategy that had already yielded five

unknown IR sequences), and a virtual screen of the ever-growing public database with a loose consensus amino acid sequence representing the potassium channel pore and flanking regions (FXSIPXXXWWAXVTMTTVGYGDMXP). Among the many known potassium channel sequences found was one intriguing, new and significantly different partial sequence from a human hippocampal cDNA library. One translation frame of this sequence had the potential to be a unique potassium pore: LGAMWLISITFLSI?YGDMVPHTYCGKGVCLLTGIMRAGFTALVVAVVA?. Although the homology to the consensus pore sequence was weak, the presence of a stretch of hydrophobic amino acids that might form a transmembrane domain C-terminal to the partial pore sequence piqued interest. Oligonucleotide primers were designed and used to isolate a fragment from human cDNA. This fragment, which when sequenced verified the presence of the GYGD codons, was subsequently used to probe human hippocampal and rat brain cDNA libraries. Three distinct but highly related cDNAs, SK1, SK2 and SK3, were isolated that, when expressed heterologously, yielded calcium-dependent potassium currents with all the hallmarks of classic SK channels [76].

The three SK cDNAs predict proteins of 561, 580 and 732 amino acids (for hSK1, rSK2 and rSK3 respectively) that are highly related to one another, with six TMs and a potassium-selective pore, analogous to the structure of the voltage-dependent class of subunits. This was surprising in the face of predictions that the SK subunits might be members of the IR family because of

their voltage-independence and slightly inward-rectifying currents. However, except for the conserved pore sequence and 6 TM topology, the SK subunits show very little homology to the voltage-dependent or IR subunits. Dendrogram analysis placed the SK and subsequently cloned IK subunits in a new potassium channel subfamily.

Biophysical and biochemical studies of the SK channels clones revealed that calmodulin, the most abundant calcium-binding protein in the brain, serves as a beta subunit to the channel. Calmodulin is bound with high affinity to the membrane proximal portion of the intracellular C-terminus, the calmodulin binding domain (CaM-BD); binding of calcium to calmodulin mediates channel gating [77, 78]. Structural determination by X-ray diffraction of crystals formed of the CaM-BD and Ca^{2+} -calmodulin [79] correlates well with functional data indicating that the two N-terminal EF hands of calmodulin bind calcium while the two C-terminal EF hands do not. Again this was a surprising result because the C-terminal EF hands of calmodulin bind calcium at higher affinity than the N-terminal domains. The CaM-BD/calmodulin co-crystal showed that interaction with the CaM-BD forces a conformation on the C-terminal EF hands that is unique, and does not allow calcium binding. Further, the crystal structure visualizes a dimer formed of two CaM-BD/calmodulin complexes. Whether this is an artifact of crystallization with the CaM-BD unconstrained by its relation to the rest of the channel, or whether a dimer of dimers actually mediates gating of the channel upon binding of calcium is currently under investigation. All three of the

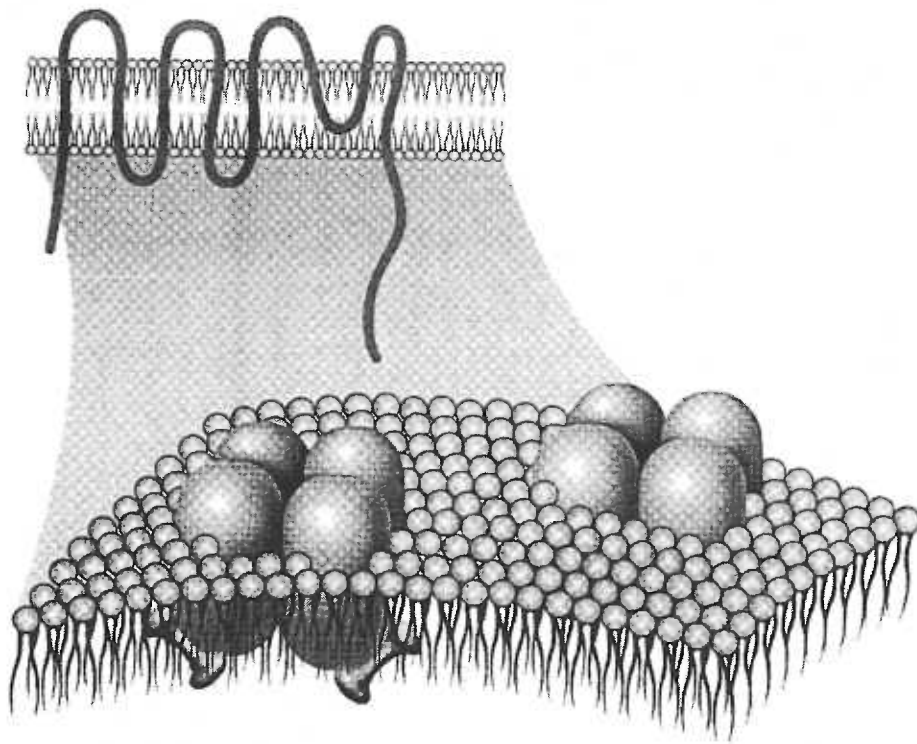


Figure 3.

Representation of the six transmembrane topology predicted for SK subunits and tetramers of subunits in a membrane with calmodulin (dumbell shape) associated with intracellular domains.

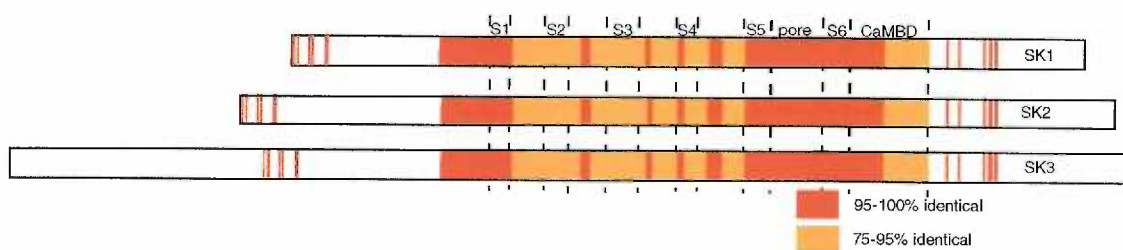


Figure 4.

Schematic showing high degree of amino acid conservation between mammalian SK1,SK2 and SK3 in the core domain from proximal to TM1 through the CaM-BD. Some small islands of identity are found in the otherwise unsimilar termini.

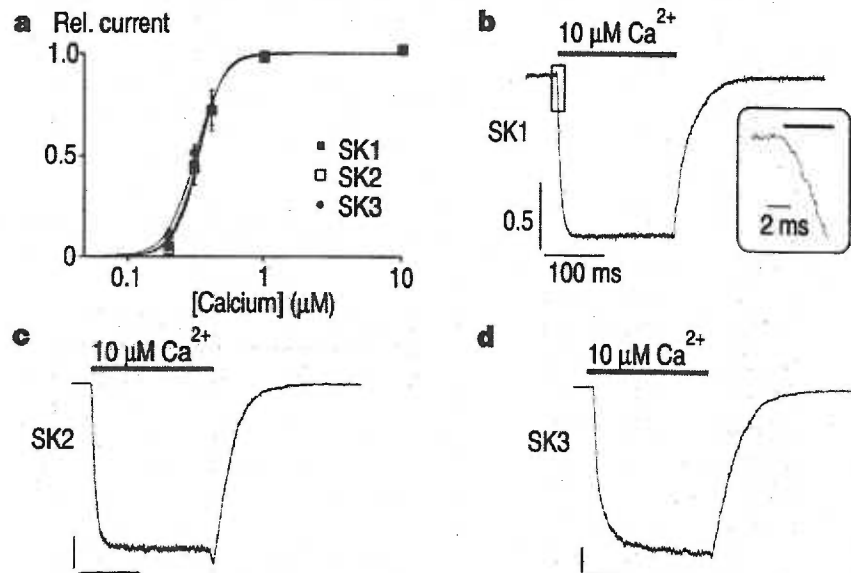


Figure 5. Calcium gating of SK channels

a. Calcium dose response relationships for hSK1, rSK2, and rSK3 channels. Relative amplitude of steady-state currents at -100 mV is plotted as a function of calcium concentration.

b-d. Fast piezo-driven application of Ca²⁺ (10 μM) to inside out patches expressing b. hSK1, c. rSK2, and d. rSK3 channels. The holding potential was -80 mV; current and time calibrations are 0.5 nA and 100 ms. Inset for hSK1 shows a current increase within 1 ms after Ca²⁺ application.

Nature (1998) 395:503-507

SK channel subtypes share the same calcium sensitivity, gating by calcium binding to associated calmodulin, and kinetics of activation and deactivation. Only in the sensitivities to pharmacological blockers did the SK subunits differ from one another. The K_D values for blocking of heterologously expressed SK channels by apamin, *d*-tubocurarine and dequalinium depend on the cell type in which the study is performed, with results from SK1 expression varying most widely (see Chapter IV). When expressed in *Xenopus* oocytes, SK2 has an IC_{50} of 60 pM for apamin, SK3; 1 nM, hSK1; >100 nM [76]. When expressed in HEK293 cells, the IC_{50} of hSK1 for apamin was found to be 8nM; 12 nM when expressed in COS cells [80]. When SK2 was expressed alone in HEK293 cells, the IC_{50} was found to be 94 pM, when co-expressed with SK1 the IC_{50} dropped to 1.4 nM [81]. Thus pharmacology of SK channel activity in endogenous expression sites cannot serve to identify the channel subtype.

In situ hybridization on rat brain sections for the three SK mRNAs showed that each gene is expressed in a wide array of central neurons [76, 82]. Although the expression pattern for each gene is distinct, there are multiple structures in which expression of two *SK* genes overlap, and even some structures where all three mRNAs are detected. High levels of all three mRNAs were detected in entorhinal cortex, the subiculum, and some thalamic nuclei. SK1 and SK2 mRNAs are both expressed at high levels in layer V of the cortex and in CA1-3 neurons of the hippocampus, both regions in which the principle neurons express both apamin-sensitive and apamin-insensitive AHP currents. In the amygdala,

only SK2 mRNAs were detected in the anterior amygdaloid area, SK2 and SK1 were found in the anterior cortical amygdaloid nucleus and all three SK mRNAs were expressed in the amygdalohippocampal area and the medial and basal amygdaloid nuclei. Only apamin-insensitive AHPs have been characterized in these neurons [82].

3. Potassium channel transgenic mice

Non-SK potassium channel transgenic mice

As with the SK channels subunits, clones for other potassium channel subtypes could be catalogued into potassium channel subfamilies by amino acid homology and basic functional characteristics. However, direct correlation of individual clones with endogenous channel functions was complicated by overlapping expression patterns and inexact recapitulation of function in heterologous systems. Co-expression with cloned beta subunits, the first of which was cloned by amino acid sequencing of peptide fragments from purified potassium channel complexes from bovine brain [83], resolved some differences between *in vivo* and *invitro* channel function [84, 85]. In some instances, co-expression of related pore-forming subunits resulted in functional channels with characteristics not seen with either subunit alone, but that closely paralleled *in vivo* channel features [86]. Thus the entire potassium channel field was faced with a plethora of cloned subunits, many of which could not be correlated with *in vivo* functions. In order to resolve this dilemma, many researchers turned to

genetic strategies. A few examples of the variety of approaches taken, the results obtained and a discussion of the interpretation or conflicting results are presented.

The large-conductance calcium- and voltage-activated potassium channel, BK, or *slo*, as the *Drosophila* gene and its products are named, was first cloned from *Drosophila*, and the alternative splicing of transcripts from the locus were subsequently characterized. The various splice forms yield channels that differ in functional characteristics such as calcium sensitivity, conductance and kinetics of activation and deactivation [56]. Null mutations of the *slo* locus exhibit multiple behavioral abnormalities. Brenner *et al* created transgenic flies by expressing one *slo* splice form on the background of the null allele. Their results show that this one splice form corrects some but not all of the dysfunction seen in the null flies, supporting the hypothesis that each splice form has characteristics necessary to specific function in particular cell types [87].

Dominant negative or overexpression transgene strategies have been employed for a number of potassium channel clones to test their *in vivo* function. A beta-cell K_{ATP} subunit, (a member of the inward-rectifier family, Kir6.2), mutated to reduce its sensitivity to ATP, was over-expressed in transgenic mice under control of the insulin promoter. In normal mice, elevation of cytoplasmic ATP/ADP in response to glucose metabolism closes K_{ATP} channels, causes cell depolarization, calcium entry and insulin release. The transgenic mice, however, developed severe hyperglycemia and hypoinsulinemia within five days of birth,

without gross morphological changes in the pancreas or islet cells [88]. These results supported the hypothesis that activity of an ATP-sensitive potassium channel is important in regulation of insulin release in glucose metabolism, and identified the cloned subunit as the likely gene product serving that function.

In the heart, inwardly rectifying potassium channels of the Kir 2 family contribute to repolarization of the action potential and to regulation of the heart rhythm. In mice, knock out of the Kir 2.1 subunit, the one of four members of this subfamily that most closely matches the functional characteristics of the native heart channels, causes severe health problems and early death, complicating study of heart function in the knockout animals [89]. To circumvent this difficulty, a dominant negative non-conducting mutant of Kir 2.1 was expressed in transgenic mouse heart under control of the α -myosin heavy chain promoter. In a manner not yet completely understood, this dominant negative channel causes a slower heartbeat in the transgenic animals [90]. These mice and isolated myocytes from them will serve as valuable tools for future study of Kir function in the heart.

Single amino acid mutations in the Kv1.1 delayed rectifier channel subunits have been found to underlie the human inherited disease Episodic Ataxia Type I (EA, OMIM #160120) [91], symptoms of which include stress-induced myotonia and ataxia. Heterologous expression studies of channel subunits containing point mutants found in human EA patients revealed a dominant negative affect of the mutant subunits on channel function [92]. Mice in

which the *Kv1.1* gene has been knocked out are viable as homozygotes, suffer increased susceptibility to seizures and decreased analgesia, but do not exhibit the symptoms of EA [93]. In contrast, knock-in mice that express *Kv1.1* channels containing an EA point mutant are not viable as homozygotes; embryos die sometime between embryonic days 4 and 9. Heterozygous mice show decreased motor coordination in response to stress that is ameliorated by acetazolamide, the only therapeutic agent available for treatment of human EA sufferers [94]. Thus the knock-in and knock-out mice give very different results and serve as an example of the care that must be exerted in interpretation of the study of genetically engineered animals.

SK transgenic mice

SK channels are expressed in a wide array of cell types. In neurons and smooth muscles, SK activity regulates and tunes excitability, coordinating responses to AP firing and neuromodulatory action that cause elevations of intracellular calcium. In neuroendocrine and gland cells, SK channels participate in stimulus-secretion coupling. Cloned SK subunits form homomeric or heteromeric channels with virtually identical kinetics of activation, calcium sensitivity and unit conductance. The pharmacology of heterologously expressed SK channels ranges widely and depends on the cell type in which the channels are expressed. In situ hybridization shows extensive overlap of sites of expression in the brain. Thus, ultimately, determination of which *SK* gene

underlies an apamin-mediated effect in any particular neuron or system requires animal models wherein separate control of *SK* gene expression can be exerted. This is the goal of the work described in this dissertation. Herein I detail the production and characterization (Chapter II) and initial physiological assays (Chapter III) of mice created by homologous recombination in which the genes expressing SK1, SK2, and SK3 can separately be regulated or ablated. These mice will serve as valuable tools for many future studies of SK function.

CHAPTER II. SK Transgenic Mice

1. Introduction

Homologous recombination

Development of technology for homologous recombination in mice, used to produce gene-specific knockout or knock-in animals, has led to an explosion in our understanding of the functions of many gene products. Homologous recombination has been routinely achievable in mice since the discovery that embryonic stem (ES) cells isolated from blastocysts of the 129 strain can be manipulated in culture and yet remain diploid and maintain pluripotency [95-98] (i.e. the ability to differentiate into all the structures of a viable mouse, including germ cells). A targeting vector, comprised of cloned genomic DNA with the genetic modification to be introduced and a selectable marker, is electroporated into ES cells. The cells are then cultured in the presence of the selection agent. During cell division in culture, the exogenous DNA is inserted into the genome, either integrating randomly or by homologous recombination; in which case one allele of the endogenous gene is replaced by the targeting vector. DNA from G418 resistant ES cell colonies are analyzed for correct integration at the gene of interest by molecular techniques such as genomic Southern blot analysis or polymerase chain reaction (PCR). ES cells containing the desired genetic change are injected into blastocysts that are then implanted in pseudopregnant female mice. The resulting chimeric offspring, containing structures differentiated

from both endogenous and injected ES cells, are bred and the offspring analyzed for the presence of the genetic change. To assist in tracking the success of contribution from implanted ES cells, the host blastocysts are usually chosen from a strain having either black or white coat color. Contribution from the ES cells (from the agouti 129 line) is then readily detected in the coat color of the chimeric pups. Although greater percentage of agouti hair on the chimeras implies greater contribution from implanted ES cells, the only true measure of success is transmission of the genetic change to the germ cells of the chimera. Offspring of the chimeric mouse having agouti coat color indicate that the ES cells contributed to the population of germ cells. Because the ES cells are diploid, only 50 % of the agouti offspring are expected to carry the genetic modification, and those animals will be heterozygous. These heterozygous founders can then be crossed to obtain animals that are homozygous for the transgenic allele.

This technology of homologous recombination in ES cells has been used to generate many different mouse lines that are lacking (knocked out, KO, null) different gene products by replacing the endogenous sequence with a targeting construct lacking essential exons. In many cases, studies of these KO animals have led to greater understanding of the function of the gene [99, 100]. However, in some instances, little can be learned, due to an embryonic lethal phenotype, or to compensation by a related gene, or due to canalization, a genetic buffering whereby developmental pathways are stabilized by overlapping

functions of many genes, thus obscuring the loss of function of the ablated gene [101-103]. In order to avoid these potential pitfalls of gene ablation, we chose to construct conditional KO alleles at the *SK* loci.

Conditional alleles

Two basic strategies are available for the production of a conditional allele; insertion of a regulatable element to control expression from the gene, or insertion of sequences recognized by recombinases, allowing deletion of intervening sequences following exposure to the recombinase [104, 105]. This dissertation describes the construction and study of *SK* alleles using both of these basic approaches; a tetracycline-sensitive gene switch was inserted into the *SK2* and *SK3* genes, recombinase recognition sites flanking coding exons were inserted into the *SK1* and *SK2* genes.

Tetracycline-sensitive gene switch

Regulatory elements that control tetracycline resistance in *Escherichia coli*, and a viral transcription element were combined to produce a highly specific transcription regulation system that functions in eukaryotic cells [106, 107]. Specifically, the DNA binding domain of the *E. coli* tet-repressor protein was fused to the C-terminal portion of the Herpes Simplex Virus transcription factor, VP-16, to yield the fusion protein tTA. The tTA protein binds specifically to the operator sequence from the *E. coli* tet operon, which, when fused to a minimal promoter such as that from the human cytomegalovirus (CMV), mediates

transactivation of transcription from that minimal promoter. Binding of the tet-repressor protein to the tet operator is blocked in the presence of tetracycline and its analogs, due to the interaction of the drug with the DNA binding domain of the repressor. In like manner, the binding of the tTA protein to the tet operator is blocked by tetracycline, and transcriptional transactivation by the tTA protein is prevented.

The tTA coding sequence and the tet operator were combined in a cassette [108] which also contains the selectable marker neo^R , for selection of ES cells, and the yeast URA3 gene for selection of recombinants in yeast, a tool for use in constructing the targeting vector [109]. These two selectable markers are flanked by lox P sites, allowing their excision by the Cre recombinase (see below) after proper integration into the targeted gene. This cassette does not supply a promoter to drive transcription of the mRNA encoding the tTA protein. Instead, insertion of the cassette into the 5'UTR of a gene of interest results in a chimeric transcript, driven by the targeted gene promoter elements, initiated at the endogenous CAP site and containing some 5'UTR fused to the tTA coding sequence. The cassette provides a 3' UTR and poly-adenylation signal to this transcript for efficient translation of the tTA protein.

Located at the 3' end of the cassette are concatenated (five copies) tet operator (tet_{O5}) repeats fused to the CMV minimal promoter. When the cassette is inserted into the 5'UTR of a gene, the tet_{O5} CMV_{min} are in position to, when transactivated by the tTA protein, drive transcription of an mRNA that encodes

the protein product of the targeted gene. In the absence of transactivation by tTA, (such as in the presence of tetracycline or a potent analog, doxycycline (dox)) the tet_{O5} CMV_{min} is silent and the gene is off, yielding, in the homozygote, a null for the targeted gene. A minimum of two transcription stop signals reside between the gene promoter which drives expression of the tTA mRNA and the tet_{O5} CMV_{min}, preventing RNA polymerase read-through and unregulated transcription of the targeted gene. Thus, in the homozygous mouse, the targeted gene's promoter is unaltered, with the developmental and cell-specific expression profiles intact. In the absence of tetracycline, the expression of the protein of interest should parallel that of wild type animals. However, when dox is administered to the animal, the gene's transcription is blocked and subsequent to protein turnover, the animal must function in the absence of the targeted gene product (Figure 1).

Recombinases

Two DNA recombinases, one from bacteriophage P1 (Cre) [110], the other from *Saccharomyces cerevisiae* (FLP) [111], have been shown to function in mammalian cells [112, 113]. Each recognizes sequence specific palindromes, recombining the DNA at those sites and excising the intervening sequences. When the recombinase recognition sequences (loxP sites for Cre recombinase, *frt* sites for FLP recombinase) are present in an allele with essential coding exons in the intervening sequence, exposure to recombinase activity results in deletion of those coding exons. If recombinase activity is present very early in

development, the excision event will occur in all cell types, including germ cells, so the deleted allele is passed to offspring. However, tissue and developmental stage-specific promoters can be used to drive expression of the recombinase, resulting in excision in only a subset of tissues or cells at some later time in development. This conditional KO of gene expression can be used to avoid embryonic-lethal phenotypes that may result from KO of gene activity early in development. This also allows characterization of gene function in specific systems without the pleiotropic effects of whole organism KO.

SK3 tTA mice

The tetracycline-sensitive gene switch has been previously introduced into the 5' UTR of the *SK3* gene. [114]. These mice were the first example of application of the tetracycline gene switch in which the targeted gene's promoter elements were undisturbed, so that in transgenic animals timing and cell-specific expression of the targeted gene parallels that of wild type animals.

Administration of doxycycline, either via the drinking water or food pellets, blocked transcription, with *SK3* transcripts undetectable after three days administration of 100 µg/ ml dox in the drinking water. However, western analysis revealed that *SK3* protein was still detectable unless transcription was blocked for > three weeks. Whether the lingering presence of *SK3* protein reflects basal protein turnover rate for *SK3* or the retention of *SK3* in a subset of

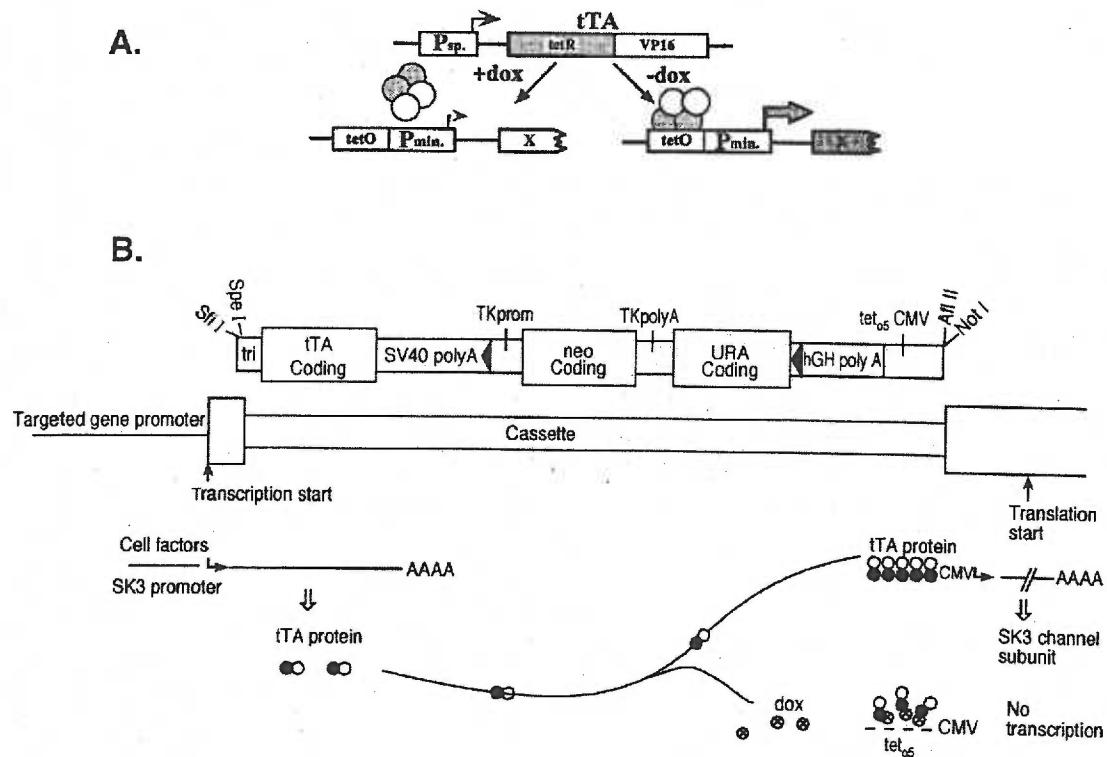


Figure 1.

A. The tTA protein is a fusion of the DNA binding domain from the *E. coli* tet repressor protein and the C-terminal domain of Herpes Simplex Virus transcription factor VP-16. In the absence of tetracycline, tTA binds the tet operator repeats from the *E. coli* tet operon, promoting transcription. Tetracycline interacts with the tTA protein, preventing binding to the operator, resulting in no transcription.

B. The tTA protein coding sequence, selectable markers and tet operator repeats were assembled into a cassette which can be inserted into the 5' UTR of the targeted gene in a single step. Transcription from the gene promoter yields a transcript encoding tTA which then transactivates transcription at the tet operator-CMV minimal promoter, producing an mRNA encoding the targeted gene product only where the gene promoter is normally active. The tetracycline analog doxycycline (dox) potentially binds to the tTA protein, preventing transcription.

cell types was not determined, due to the lack of an antibody that functions in immunohistochemical techniques.

In the absence of dox, *SK3 tTA* homozygotes overexpress the SK3 transcript three to five fold. This overexpression of transcript is paralleled by overexpression of protein by approximately five fold. The overexpression in these animals may result from disruption of control sequences due to the presence of the tet cassette in the 5'UTR of the gene, but more likely is simply due to the potency of transactivation of transcription by the tTA protein. When the neo and URA selectable markers were removed from the *SK3* allele by crossing the *SK3 tTA* mice with a Cre-deleter mouse, which expresses the Cre recombinase very early in development [115], SK3 expression increased even further, with transcripts at 5-10 fold higher than wild type. This increase in expression is consistent with the observation that the presence of the neo coding sequence in the genome reduces expression from neighboring loci [116, 117]. These higher levels of SK3 expression resulted in reduced viability and reproductive success in the *SK3 tTA_{Δneo}* mice, so the line is maintained with neo and URA still present in the allele. All results obtained by us and by collaborators have used mice retaining these selectable markers in the allele.

Knockout of SK3 expression by longterm administration of dox did not present any overt phenotype. However, in the absence of dox, SK3 overexpression resulted in compromised parturition. Because animals lacking oxytocin deliver pups successfully, this effect of SK3 overexpression is likely not

due to altered hormone secretion. SK3 protein is expressed in the uterus; overexpression of the hyperpolarizing current through SK3 channels may be sufficient to inhibit the development of a train of action potentials necessary to drive uterine contractions. This interpretation is supported by the observation that knock-down of SK3 expression by low concentration (5 μ g/ml) dox in the drinking water for only two days relieved the complications at parturition. Overexpression of SK3 also resulted in abnormal respiratory responses to hypoxia, introducing the possibility that regulation of SK3 channel activity may have a therapeutic potential in treatment or prevention of neonatal apnea, a potential contributing cause of Sudden Infant Death Syndrome [118].

More subtle roles for SK3 have been revealed by further studies of these mice in collaboration or by other investigators. SK3 is expressed in endothelial cells of the vasculature, and plays a role in regulating blood pressure [12]. Blood pressure is influenced by hormones such as estrogen [119]. SK3 expression is regulated by estrogen [120], and thus hormonal control of SK3 expression may have an integral role in the cardiovascular effects of estrogen. Consistent with this role of SK3 in smooth muscle function, SK3 channels are also expressed in both smooth muscle and urethelium of the bladder. Suppression of SK3 expression resulted in a marked increase in non-voiding contractions in conscious, freely moving mice, indicating that activation of SK channels may be a therapeutic approach for management of non-voiding contractions in urinary dysfunctions such as incontinence [11]. The suppression of SK3 expression by

dox administration also revealed a persisting apamin-sensitive conductance in the bladder, implying an additional role for SK2 channels.

SK2 and SK3 are both expressed in pancreatic islet cells, where they play a role in regulating intracellular calcium oscillations and insulin secretion in response to elevated glucose [121]. Once again, the ability to acutely regulate expression of SK3 revealed the expression and possibly overlapping function of SK2. More recently, SK3 channel function has been characterized in neurons of the vomeronasal organ (VNO). The VNO is an accessory olfactory system that mediates behavioral responses to pheromones. In the VNO, binding of pheromones to V1 and V2 receptors results in a signaling cascade of elevated IP3 and intracellular calcium that activates TRP2 and SK3 channels. The activation of these channels changes the basal firing rate of the VNO neurons, initiating transduction of the pheromone signal to higher brain structures (Yu, personal communication).

These results clearly demonstrate the efficacy of the *SK3 tTA* mice in a wide variety of studies and paradigms. The conditional regulation of SK3 expression has allowed demonstration of SK3 functions, as well as revealing overlapping roles for other SK channels in some systems. Future studies of these mice, as well as the other conditional *SK* alleles described in this dissertation will lead to greater understanding of the diverse and important roles served by SK channel function.

2. *SK2 tTA mice*

Introduction

SK2 and SK3 channel subunits share a high degree of amino acid homology (75% identity), greater than either compared to SK1 (67% identity). In addition, SK2 and SK3 are each virtually identical across mammalian species (>96% identity between mouse, rat and human). Sequencing of genomic fragments in preparation for constructing targeting vectors revealed that both *SK2* and *SK3* genes contain an extended, contiguous open reading frame (ORF) N-terminal to the initiator methionine (Met) characterized in the original cloned cDNAs used in heterologous expression studies. The putative amino acid sequences in the extended ORFs have domains of identity, consistent with the high degree of relatedness of SK2 and SK3. 5' RACE (Rapid Amplification of cDNA Ends), RT-PCR and northern analysis were applied to each gene to determine if the extended ORF is expressed. In the case of *SK3*, the transcription CAP site was mapped to ~840 nucleotides (nt) 5' of the heterologous expression Met. This extended transcript includes all of the contiguous ORF predicted from genomic DNA sequence, with the most N-terminal Met preceded by multiple stop codons in the ~300 bases of 5' untranslated region (UTR). Subsequent studies with an antibody generated against a peptide sequence from this extended N-terminus (Alomone) verified that this sequence is expressed in the SK3 protein.

In contrast to *SK3*, mapping of the CAP site of the *SK2* gene found that the *SK2* transcript initiates within the putative ORF ~520 nt 5' of the Met used in heterologous expression experiments. This transcript does not contain additional methionines, indicating that the expression Met is the likely start of the native protein.

Materials and methods

Recombination in yeast: Oligonucleotide primers were designed and used in PCR to amplify 250 bp fragments of the *SK2* gene flanking the site of cassette insertion. These gene fragments, the 5' and 3' recombinagenic arms (RAs), were cloned into unique restriction sites at the termini of the cassette, using sites provided by the primers. A donor fragment, consisting of the cassette with flanking RAs, was isolated and co-transformed with the yeast/bacteria shuttle vector containing a 7 kbp *SK2* gene fragment spanning the N-terminal exons into yeast made competent in lithium acetate. Transformants were selected on URA/TRP dropout media. Only those yeast harboring plasmids (TRP selection) that had undergone recombination and now carried the cassette and its URA gene were able to grow. Sequence analysis verified correct insertion of the cassette.

ES cell culture: Embryonic stem cells (gift of Richard Axel) were maintained in culture on mitomycin C inactivated mouse embryonic fibroblasts (mEF). 10×10^6 cells were electroporated with 0.7 mg of linearized DNA and

plated onto gelatin coated plates without mEFs. Cells were grown for 10 days in the presence of 175 mg/ml G418. Surviving colonies were picked into 0.5X trypsin, half the trypsinized cells were plated onto mEFs in 96 well format, half were pooled for DNA isolation and PCR analysis. Clones from positive pools were trypsinized, plated onto 24 well plates on mEFs and a portion of cells prepared as DNA for further analysis. Positive clones were further expanded on mEFs for frozen stocks and on gelatin plates for large scale DNA preparation for genomic Southern analysis.

Genotype PCRs: Genomic DNA from ES cell clones or mouse tail snips was prepared by proteinase K digestion followed by isopropanol precipitation. PCRs were performed in standard or nested format.

B-Gal staining: Animals were anesthetized by IP injection of 1 ml /100mg body weight 2% tribromoethanol, and transcardially perfused with 4% paraformaldehyde. Brains and other organs were removed and either stained directly or cryo-protected by incubation in 20% sucrose at 4°C overnight. Brains were sectioned by cryostat and thaw mounted onto glass slides. Slides or whole organs were then incubated in a solution comprised of 5 mM $K_3Fe(CN)_6$, 5 mM $K_4Fe(CN)_6$, 20 mM $MgCl_2$, 0.1 M PBS, 1 mg/ml X-Gal at 37°C for 10 minutes to 2 hours.

5' RACE: RNA-ligase mediated 5' RACE was performed using the GeneRacer kit (Invitrogen) according to manufacturers instructions.

RT-PCR: Total RNA was isolated using Tri-reagent (Sigma) according to manufacturer's recommendations. 10 µg total RNA was reverse-transcribed by 40 units MMLV in the presence of 40 mM KCl, 6 mM MgCl₂, 50 mM tris pH 8.3, 400 µM dNTPs, and 1 µg random hexamers at 37 °C. 0.5-1% of the resulting cDNA was used as substrate for the PCR.

Northern blot: 10-20 mg total RNA was electrophoresed through 1% agarose/ 6% formaldehyde gels and passively transferred to nylon membranes in 20XSSC. Blots were probed at 42°C in 50% formamide/5% SDS/50 mM NaPO₄ with ³²P-labeled random-primed DNA probes. Following high stringency washes in 0.1XSSC/ 0.1% SDS at 60 °C, signals were detected by radiography.

Results

The Cap and 5' UTR of the SK2 transcript from brain were mapped by 5' RACE, RT-PCR and Northern blot (Figure 2). Sequences of eight independently derived 5' RACE products, from nested PCR using primers specific to exon 2 in conjunction with the RACE oligo, all extended to within 10 nt ~ 520 nt 5' of the initiator Met. This region was concluded to comprise the CAP site for transcription of the *SK2* gene. RT-PCR on brain cDNA using primers successively further 5' of the Met, in combination with primers specific for exon 2, corroborated the RACE results, with primers 3' of the putative CAP site yielding products, primers 5' of the putative CAP site not yielding products. Northern blots of brain RNA, probed with sequences from within the CAP site showed

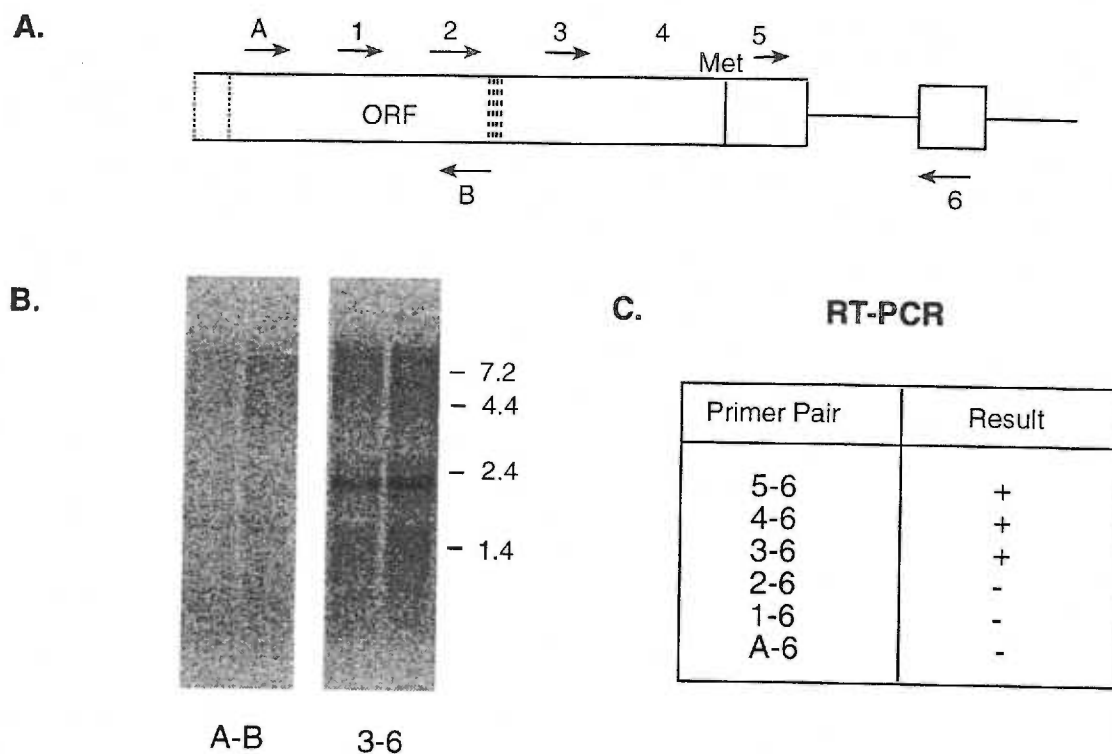


Figure 2.

Mapping the 5' extent of the SK2 transcript from brain.

A. Schematic showing the first two exons. Exon 1 is defined by a putative open reading frame (ORF) containing 2 methionines 5' of the Met defined by original cDNA clones and used for heterologous expression studies. Vertical dashed lines clustered near the middle of this exon indicate termini of 5' race products. Arrows above and below the exons indicate oligonucleotide primers used in RT-PCR and in generating DNA fragments used to make probes for Northern blots.

B. Mouse whole brain total RNA was probed with 5' fragments designated by primer pairs below the lanes. 20 μ g RNA was loaded per lane, 2 lanes are shown probed with each fragment. Molecular weight in kilobases on right.

C. Results of RT-PCR was performed on random-primed cDNA derived from mouse whole brain total RNA with indicated primer pairs.

positive hybridization to RNAs ~2.2 and 2.4 kb in length. No signal was detected with probes derived from 5' of the putative ORF.

A site 37 nt 5' of the initiator Met was chosen for insertion of the tet cassette (Figure 3.). The regulatory cassette was inserted by recombination in yeast. Sequence analysis verified exact insertion of the cassette into the gene fragment. This construct was linearized at unique flanking Not I site and electroporated into ES cells. One ES cellclone was found to have undergone homologous recombination into the *SK2* gene with no other insertions of cassette sequences into the genome. These ES cells were injected into blastocysts (University of Cincinnati Escore) and yielded chimeric males that subsequently transmitted the transgenic allele to their offspring, the heterozygote founders for the *SK2 tTA* line.

Heterozygotes were crossed and *SK2* expression in homozygous offspring on or off dox was assessed by RT-PCR. *SK2* transcripts were found in ~three fold excess of wild type levels, similar to the overexpression seen in *SK3 tTA* mice. However, in contrast to what had been found for *SK3 tTA* homozygotes, *SK2* transcripts could still be detected by RT-PCR in *SK2 tTA* homozygote brain RNA following two weeks or more of dox administration. 5' RACE was performed on this RNA; the dox insensitive *SK2* transcripts were found to have initiated from within the cassette, 5' of the tTA binding site. The unregulated transcripts are present at ~ 50% of the levels of *SK2* transcripts in wild type animals. The source of promoter elements

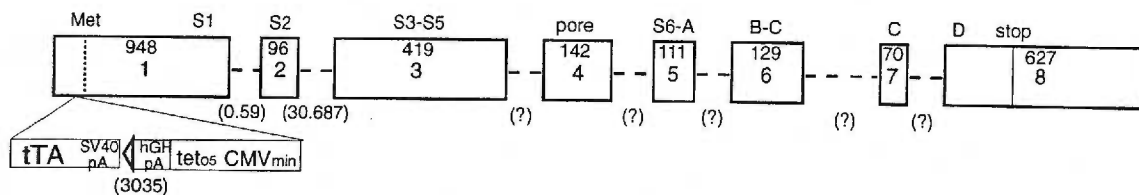


Figure 3.

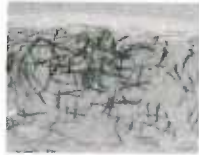
Schematic of the *mSK2* locus. Boxes represent exons, the size of each in base pairs is shown inside the box. The domains encoded by each exon are noted above. The size of introns, where known, is shown below in parentheses. The site of insertion and the structure of the tet cassette following Cre-mediated removal of neo and URA sequences is shown below exon 1.

responsible for expression of these anomalous transcripts is unknown. In an effort to remove possible read through or promotion from non-essential cassette elements, the *SK2 tTA* mice were crossed with the Cre-deleter mouse to excise the neo and URA coding sequences flanked by loxP sites. Consistent with what had been found in *SK3 tTA* mice, excision of neo resulted in even greater overexpression of SK2; transcript levels in heterozygotes were 5-6 fold higher than wild type levels. Heterozygote *SK2 tTA_{Δneo}* females give litters of only one or two pups, making breeding for homozygotes untenable. Assay of SK2 transcription from the cassette in *SK2 tTA +/T* animals treated with dox for three weeks still found a low level of anomalous transcripts. Thus it was determined that the *SK2 tTA_{Δneo}* mice could be used in models of overexpression, but would not serve as *SK2* null animals. Currently, this line is maintained by crosses between heterozygous *SK2 tTA_{Δneo}* males and wild type females and has been backcrossed into the C57Bl6/J background.

Characterization of the expression pattern from the SK2 promoter can be achieved by crossing the *SK2 tTA* mice with a reporter mouse containing a transgene consisting of the *lacZ* gene driven by the tet_{OS} CMV_{min} promoter [108]. In mice harboring both alleles, the tTA protein, expressed in cells where the *SK2* promoter is active, drives transcription of the *lacZ* gene. Resulting B-galactosidase activity can be detected by incubating tissues or sections in the presence of the chromogenic substrate, X-gal. X-Gal staining of brain slices recapitulated *in situ* hybridization results [82], indicating that cassette driven

A.

SK2

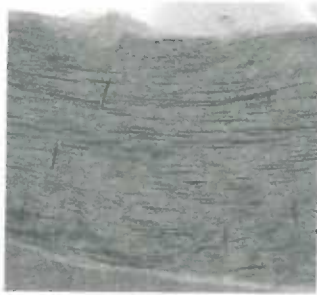


SK3



B.

SK2



SK3



Figure 4.

B-Galactosidase staining of whole mount tissues from *SK2 tTA/tetO-B-gal* and *SK3 tTA/tetO-B-Gal* mice.

A. A proximal segment of the epididymus

B. A segment of small intestine

overexpression of SK2 did not occur at ectopic sites. In addition, X-Gal staining of peripheral structures revealed previously unknown expression sites for *SK2* in the bladder, ovary (not shown), intestine and testis (Figure 4).

Discussion

The *SK2 tTA* mice are only the second known application of the tet cassette insertion in a gene, leaving the gene's promoter intact to preserve temporal and site -specific expression. As seen with the *SK3 tTA* mice, the strong transactivation by the tTA fusion protein results in overexpression of SK2 transcripts that is paralleled by overexpression of the SK2 protein. B-Gal staining confirmed that the tTA driven SK2 expression recapitulated the expression pattern revealed by *in situ* hybridization. Sites of expression of the anomalous transcript initiated from within the cassette were not investigated in detail. Further evidence of appropriate localization of overexpressed SK2 protein is provided by the increase of amplitude of the ImAHP in hippocampal Ca1 neurons (see chapter 3).

The inability to completely block SK2 transcription with dox rendered the *SK2 tTA* mice unusable for the study of SK2 KO. The unregulated initiation of transcripts from within the cassette would not appear to be a problem of the cassette itself, but perhaps reflects a specific characteristic of the *SK2* locus. If this is true, it is possible that even the anomalous transcripts are only expressed where the *SK2* promoter is active.

The cause of reduced fecundity of SK2 overexpressing females has not been investigated. SK2 is expressed in central nuclei that may participate in hormone cycling and in peripheral sites such as the pituitary and uterus. It is unlikely that the small litter size is due to decreased viability of the pups. SK2 expression in homozygous *tTA* mice was approximately the same as that from one allele in the *SK2 tTA_{Δneo}* mice. *SK2 tTA* homozygous pups were born in Mendelian ratios. *SK2 tTA_{Δneo} +/T* pups are born in the expected numbers from crosses between *SK2 tTA_{Δneo} +/T* males and wild type females.

3. Floxed alleles

Introduction

The Cre/lox system, where loxP sites that are recognized by the DNA recombinase Cre, are inserted into the targeted allele, offers a second strategy for producing conditional transgenic alleles. Commonly, loxP sites are used to allow excision of selectable markers, such as neo, from alleles that have been made into constitutive KOs by replacement of the endogenous gene by a targeting vector lacking essential exons. However, inserting loxP sites so that they flank essential exons allows for conditional KO of the allele following exposure to the recombinase. This exposure can be controlled by regulation of the expression of the recombinase. Many transgenic mice, in which Cre expression is driven by tissue- or developmental time-specific promoters, are now well characterized and available [122].

To obtain conditional floxed alleles at the *SK1* and *SK2* loci, a triple loxP site strategy was employed. For *SK2*, a single loxP site was inserted into the 5'UTR ~300 nt 5' of the initiator Met. A cassette, consisting of the coding sequence of the neomycin resistance gene flanked by two loxP sites in conjunction with the coding sequence for enhanced Green Fluorescent Protein (eGFP)(Clontech), was inserted into intron 2, approximately 2.3 kbp 3' of the end of exon 2. Following recombination by Cre, most of exon1 and all of exon 2, encompassing the Met through TM 2 of the SK2 protein, are excised, and the coding sequence of eGFP is transcribed as a chimeric transcript initiated by the *SK2* promoter. In the floxed allele, no promoter is provided for expression of eGFP so floxed animals should be negative for this fluorescence. Expression of GFP following Cre recombination should provide a clear marker for cells deleted for *SK2* which is detectable in live cells of brain slice preparations, as well as in fixed tissues used for immunohistochemical experiments.

For *SK1*, the single loxP site was inserted ~40 nt 5' of the initiator Met, the neo/GFP cassette was inserted into the intron between exons five and six. Cre recombination results in excision of exons three through five, encompassing the coding sequence from the Met through TM5, and, analogous to the *SK2* allele, puts eGFP expression under control of the *SK1* promoter. In addition, a hemagglutinin (HA) epitope tag was inserted in frame with the SK1 coding sequence in the loop between TMs one and two. In the absence of antibodies to

SK1 protein, this epitope tag may serve in immunohistochemical experiments to examine sites of SK1 protein expression.

Before the triple flox alleles can be used in region-specific KO experiments, the neo coding sequence must be removed. This is accomplished by partial Cre recombination, and is currently in progress through breedings between *SK flox* and *meuCre40* animals [123].

Breedings between *SK1* or *SK2 flox* and Cre-deleter animals results in total recombination of the loxP sites, yielding heterozygotes with one null *SK* (+/ Δ) allele which is transmitted through the germline. Crossing these heterozygotes yields *SK1* or *SK2* null (Δ/Δ) animals.

Materials and methods

Targeting vectors: SK1 flox and SK2 flox targeting vectors were constructed by standard molecular techniques.

ES cells: ES cell transfections and culturing were performed by the University of Cincinnati Escore. Genomic DNA prepared from clones was analyzed by nested PCR using standard methods described for the *SK2 tTA* mouse. Southern analysis of genomic DNA from ES cell clones or animals was performed by standard techniques.

EEG recordings: Field EEG activity was recorded (Robert Stackman) one week following stereotaxic placement of 125 μ m silver wires in the CA1 region of the hippocampus. Activity was filtered at 0.1 Hz high pass and 100 Hz low pass

and amplified 5000x. Recordings were conducted on freely moving mice, traces presented are from relatively quiet periods, wild type and *SK* null activity during recording were comparable.

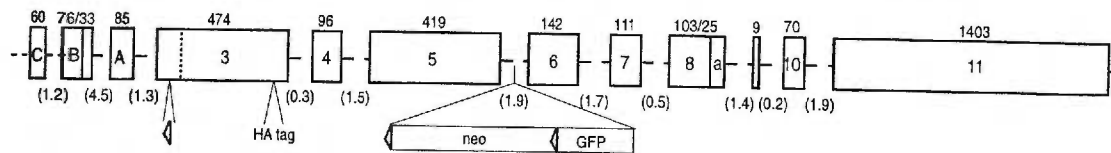
Results

Transgenic mice

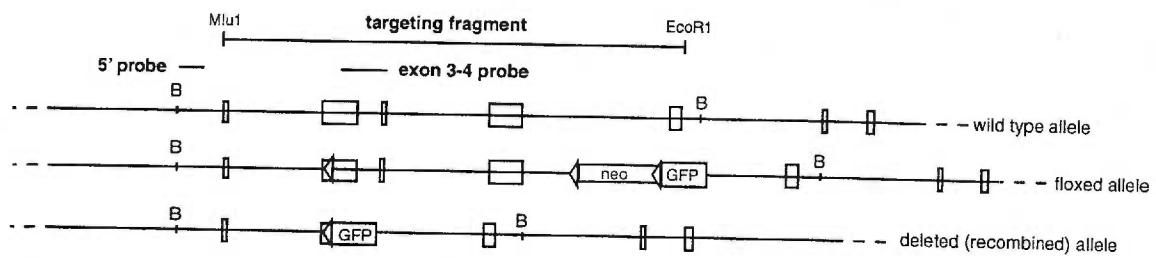
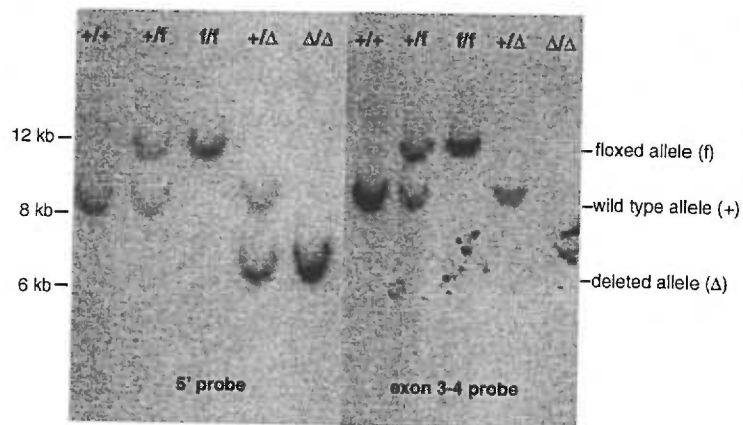
ES cells found by PCR and genomic southern analysis to harbor homologous recombination of the triple loxP vector were injected into blastocysts (UC Escore), chimeric offspring were bred, and their offspring were analyzed for presence of the floxed allele. Mice heterozygous for the floxed allele were bred to the Cre-deleter mouse, yielding heterozygous deleted animals that were then crossed to yield homozygous KO animals for *SK1* and *SK2*. Genomic Southern analysis (Figure 5) or PCR on genomic DNA (Figure 6) show the presence of the floxed or deleted alleles and the absence of the wild type allele in homozygous animals.

Neither homozygous floxed (*f/f*) *SK1* nor *SK2 f/f* animals exhibited any overt behavioral phenotype. RT-PCR analysis of transcripts from these animals was performed. In *SK1 f/f* brain RNA, PCR products of predicted size could be detected when primers for exon 3 and exon5 of *SK1* were used. However, when primers specific for exons 6 through 10, those 3' of the neo/GFP cassette, were used, no appropriately sized product was amplified (Figure 7). The implication of this result is that the presence of the neo/GFP cassette disrupts splicing of the

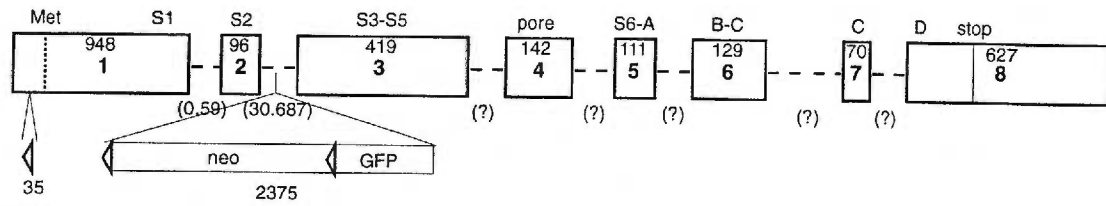
A.



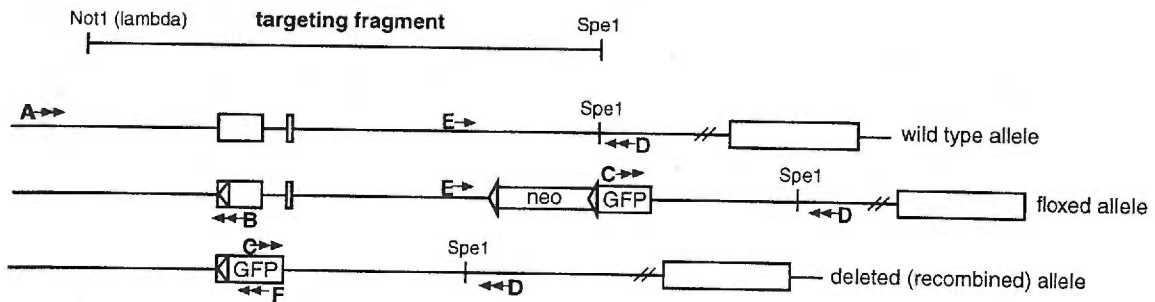
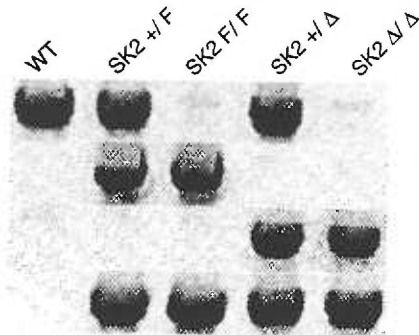
B.



A.



B.



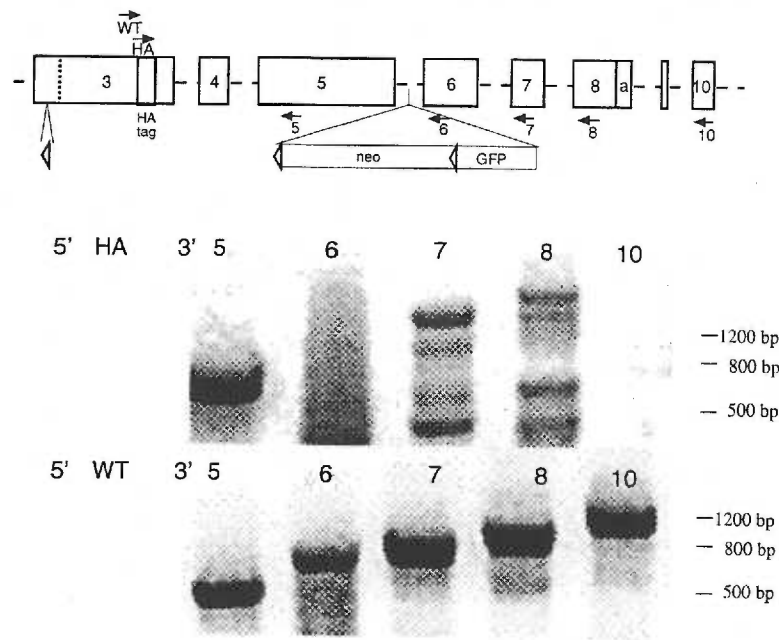


Figure 7.

RT-PCR on whole brain cDNA from an *SK1* $+/-$ mouse.

A. Schematic representation of the locus showing the sites of insertion of the 5' loxP site and the HA epitope tag in exon 3, and the floxed neo/ GFP cassette into the intron between exons 5 and 6. Sense primers that recognize either wild type (WT) or inserted epitope (HA) sequences are indicated above, antisense primers specific to each exon are shown below.

B. Ethidium-stained gel showing amplification products with designated primer pairs. Top panel shows amplifications using the HA primer. Only in combination with the primer to exon 5 is the expected product seen. Lower panel shows amplification with the WT primer, giving the expected product in all pairs.

SK1 hnRNA, a hypothesis consistent with the high degree of alternative splicing observed at this locus (see Chapter IV). Following partial Cre recombination to eliminate the neo coding sequences, *SK1 f/f_{Δneo}* animals will be retested for appropriate splicing of all transcripts. The lack of full length SK1 transcripts also implied that the *SK1 f/f* animals are essentially *SK1* KOs. Consistent with this, the *SK1 Δ/Δ* animals also show no overt behavioral phenotype. Western analysis of crude brain membranes from *SK1 f/f* animals using the HA antibody did not detect protein of the predicted molecular weight, again consistent with the lack of appropriately spliced mRNAs.

Analysis of SK2 transcripts from *SK2 f/f* animals revealed appropriate sized products that were expressed at ~ 20 % of the level in wild type animals. The reduction of expression is likely due to the presence of the neo coding sequences. These message levels will be re-evaluated following partial recombination to produce *SK2 f/f_{Δneo}* animals.

In contrast to *SK1*, *SK2 Δ/Δ* animals showed a complex, overt behavioral phenotype resulting from the loss of expression of SK2. Starting at postnatal day 7 (Pn7), *SK2* KOs were hyperactive and suffered a severe tremor. They are generally smaller than littermates at this age. There may be consequences for regulation of growth factors stemming from the loss of SK2, but it is also possible that the small size of the KO pups is due to poor competition with littermates for nutrition. This observation has not been quantified, but when litters are reduced in number by removing non-phenotypic WT and +/Δ pups, the KO pups rapidly

recover to normal size and weight. Adult *SK2* KO mice are not different in size from WT. During the period from Pn7 to Pn21, *SK2* KO pups also exhibit an odd gait or ataxia. The gait is characterized by “flipper foot”, a flinging of the hind foot up and out following each step. The combination of the ataxia and the tremor rendered young *SK2* KOs incapable of motor behavior assays such as the rotor rod or balance beam. As the *SK2* KOs grow older, severity of the ataxia declines and the overt phenotype is reduced to mild hyperactivity and whole body tremor. *SK2* Δ/Δ females are capable of reproducing and nurture their pups appropriately. However, *SK2* Δ/Δ males did not beget offspring, whether this is a problem of motor coordination or a deficit within the reproductive system has not been determined.

EEGs

Field electroencephalographic (EEG) activity was recorded from freely moving mice one week after stereotaxic placement of 125 μ m silver wires bilaterally in the CA1 region of the hippocampus. *SK2* Δ/Δ mice showed a marked increase in high frequency discharges compared to wild type animals, as well as an increase in the amplitude of the EEG signal. However, no evidence of behavioral seizures were observed during the recording, nor was any ictal activity, indicative of seizure [124], seen in the EEG of the *SK2* null mice (Figure 8).

Hippocampal EEG

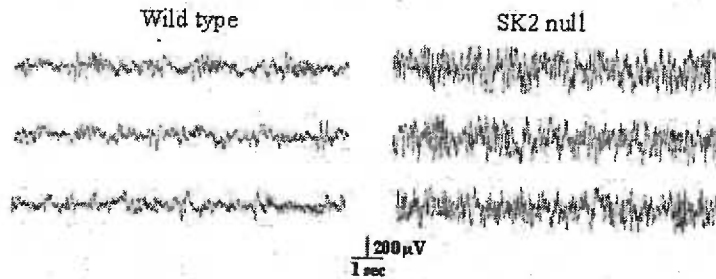


Figure 8. Hippocampal field electroencephalogram (EEG) recordings. Three representative ~10 second duration traces are shown for wildtype (left) and *SK2* null (right). Field EEG activity was recorded one week after stereotaxic placement of bilateral pairs of silver wires into the CA1. Activity was filtered at 0.1 Hz high pass and 100 Hz low pass, amplification is 5000X. All recordings were conducted while the mice were freely moving; traces shown are from episodes when the mice relatively quiet, so the behavior of the two animals was comparable. The scale bars are the same for both mice. The *SK2* null mouse shows a marked increase in high frequency discharges and the amplitude of the EEG signal is greater than in the wild type mouse. No evidence of ictal activity was seen in any of the EEGs.

GFP

Freshly prepared brain slices, used for electrophysiological characterization of neuronal function in *SK* KO animals, (see Chapter III), were examined for cell-specific fluorescence from the eGFP protein expressed under control of the *SK* promoter by excitation at 488nm, detecting emission at >495 nm. No GFP fluorescence signal was detected in fresh brain slices from *SK1* Δ/Δ or *SK2* Δ/Δ animals. Furthermore, no GFP signal was detected from six week old *SK2* *f/f* *CreR4* [125] mice, animals in which recombination at the *SK2* locus should have occurred in CA1 pyramidal cells by this age. This inability to detect GFP likely reflects the low basal activity of the *SK* promoters. A similar difficulty is encountered in detecting SK protein by immunohistochemistry, due to the low abundance of channels expressed.

Discussion

Triple loxP allele mice have been created for *SK1* and *SK2*. At the *SK1* locus, the presence of the neo and GFP coding sequences in an intron disrupts splicing of the mRNA, yielding mice that are likely *SK1* null in *f/f* genotype. Future experiments will determine if removal of neo sequence repairs the defect in the floxed allele.

The absence of a phenotype in the *SK1* *f/f* and Δ/Δ animals offers nothing to our understanding of the function of *SK1* in the rodent. However, as with the *SK3* *tTA* mice, more detailed characterization of various central and peripheral

physiologies may reveal differences between *SK1* null and wild type animals that will lead to new hypotheses and understanding of SK1 (see Chapter IV).

SK2 f/f mice exhibit no overt phenotype; SK2 expression in these homozygotes is normal in form but reduced in levels. Removal of neo coding sequences will likely result in near wild type levels of expression from the floxed allele, making these animals appropriate for studies of region-specific deletion of SK2 expression.

The overt behavioral phenotype of the *SK2 Δ/Δ* mice is consistent with *in situ* hybridization results that demonstrate expression of SK2 in principle neurons in many brain regions [82]. More detailed characterization of SK2 function in principle neurons of the hippocampus is presented in Chapter III. Predictions of phenotypic consequences for *SK2* null mice, based on known functions and expression sites, included the likelihood of seizure activity, due to the important role for SK channels in control of excitability. No seizures have been observed in the *SK2 Δ/Δ* mice, nor was ictal activity observed in hippocampal EEGs from freely moving *SK2* null animals. SK2 mRNA is also expressed in inhibitory interneurons of the hippocampus. It is possible that loss of SK2 hyperpolarizing currents in both excitatory pyramidal cells and inhibitory interneurons results in a new balance of excitation and inhibition that precludes spontaneous excitatory cycling that characterizes seizures. Alternatively, overlapping functions of the other SK channels, or other potassium conductances, serve to protect against the uncontrolled excitatory feedback. Future experiments on animals lacking

SK2 in only principle neurons of the hippocampus [125] may reveal roles served by SK2 in interneurons.

Apamin has been shown to affect acquisition of memory[22, 24, 126]. At this time, which of the apamin-sensitive SK channels underlie this effect is not known. Future behavior assays on all the *SK* KO mice will determine the contributions of each of the three genes. Due to the highly specific effect of *SK2* KO in the hippocampus (see Chapter III), it is likely that the learning affect of apamin is due purely to block of SK2 channels. Thus it is possible that future experiments on region-specific *SK2* nulls may shed light on the role of the hippocampus relative to the cortex in memory acquisition and retention.

The appearance and subsidence of an apparent motor control deficit exhibited as an ataxic gait in the *SK2* Δ/Δ mice parallels the developmentally regulated expression of SK2 in the purkinje neurons of the cerebellum [127]. Thus it is tempting to conclude that the ataxia is a result of no cerebellar SK2 channels. However, the change in motor control could also result from loss of SK2 function in cortical motor nuclei. However, at this time it is not clear what role is served by the limited temporal expression of SK2 in the purkinje neurons. Purkinje neurons exhibit complex spontaneous firing patterns of at least three different modes that are thought to reflect intrinsic properties of the neurons [128]. Switching between modes of firing is effected by apamin application [129]. The mechanism underlying apamin-induced firing-mode switch in the cerebellum is not known; elucidation of the mechanism is complicated by the expression of all

three SK subunits in the structure. *In situ* hybridization studies show that all three SK mRNAs are expressed in the cerebellum [82]. SK2 protein has been immunodetected in purkinje neurons. B-gal staining of *SK3 tTA/tet_oB-gal* mice revealed SK3 promoter activity in the Bergmann glia. Bergmann glia are astrocytes that are closely apposed to purkinje neurons and play an important role in purkinje cell firing through their uptake of glutamate [130]. Creating animals deleted for SK2 in only the cerebellum by crossing floxed animals with *pcp-Cre* mice [131], which express the recombinase only in the cerebellar purkinje cells, will provide a model in which to test the role of SK2 in cortical versus cerebellar motor control. Ultimately, the ability to regulate or ablate multiple SK isoforms may be necessary to dissect the complex relationship between purkinje cell firing properties and motor control.

4. Summary

We now have in hand a rich set of tools with which we can examine the function of each SK channel isoform. *SK3 tTA* mice give a range of expression of SK3 protein from ~5 fold more than wildtype to SK3 KO. *SK2 tTA* mice show overexpression of SK2 protein of ~15 fold greater than wild type mice. *SK1* and *SK2* floxed mice offer substrates for generating *SK1* or *SK2* null animals and for dissection of function by creating SK1 or SK2 region-specific KOs. New specificity in sites and timing for the expression of Cre are being developed using tissue-specific promoter and inducible systems [132], opening new possibilities

for study of SK function in discrete cell types or physiological systems. Finally, crossing *SK* conditional mice will yield animals in which we can test combined functions of the *SK* genes.

CHAPTER III.

SK Knockout Mice Reveal the Identity of Calcium-dependent AHP Currents

Chris T. Bond, Paco S. Herson, Timothy Strassmaier, Rebecca Hammond[^],

Robert Stackman[^], James Maylie^{\$}, John P. Adelman

Vollum Institute, Departments of [^]Behavioral Neuroscience, and ^{\$}Obstetrics and
Gynecology, Oregon Health & Science University

Portland, Oregon

Please send communications to:

Dr. John P. Adelman

Vollum Institute

Oregon Health & Science University

3181 SW Sam Jackson Park Road

Portland, Oregon 97239

1. Abstract

Action potentials in many central neurons are followed by a prolonged afterhyperpolarization (AHP) that influences firing frequency and affects neuronal integration. In hippocampal CA1 pyramidal neurons, the current ascribed to the AHP, I_{AHP}, has three kinetic components. The I_{fastAHP} (I_{fAHP}) is due to voltage-dependent K⁺ channels while Ca²⁺-dependent and voltage-independent K⁺ channels contribute to the I_{mediumAHP} (I_{mAHP}) and I_{slowAHP} (I_{sAHP}). Apamin, which selectively suppresses a component of the mAHP, increases neuronal excitability and facilitates the induction of synaptic plasticity at Shaffer collateral synapses and hippocampal-dependent learning. The Ca²⁺-dependent components of the AHP have been attributed to the activity of small conductance Ca²⁺ activated K⁺ channels (SK channels). Examination of transgenic mice each lacking one of the three *SK* channel genes expressed in the central nervous system reveals that mice without the SK2 subunit completely lack the apamin-sensitive component of the I_{mAHP} in CA1 neurons while the I_{sAHP} is not different in any of the *SK* transgenic mice. In each of the transgenic lines the expression levels of the remaining *SK* genes are not changed. The results demonstrate that only SK2 channels are necessary for the I_{mAHP}, and none of the SK channels underlie the I_{sAHP}.

Key words: SK channels, apamin, CA1 neurons, I_{mAHP}

2. Introduction

A principal determinant of neuronal excitability is the AHP that follows an action potential. In hippocampal CA1 pyramidal cells, and many other neurons, three overlapping kinetic components of the AHP, frequently recorded as the IAHP in voltage clamp, have been distinguished. Reports using pharmacological agents to examine the underlying channels have suggested that BK channels (large conductance voltage- and Ca^{2+} -dependent K^+ channels) contribute to the IAHP with time constants on the order of 50 ms [133-135]. The ImAHP is largely if not completely eliminated by apamin, a selective blocker of SK channels, and the apamin-sensitive current decays with time constants of ~200 ms [21] [136]. BK channels, KCNQ (I_M) and HCN (I_h), channels have also been reported to contribute to the medium component [137] although many of these studies were performed prior to the relatively recent discovery of the apamin-sensitive component [138] [21]. The channels underlying the slow component, IsAHP, are also K^+ selective, voltage-independent, and require Ca^{2+} influx through voltage-dependent Ca^{2+} channels for activation [133]. These characteristics have suggested that SK channels are responsible for the sAHP, although the IsAHP is not blocked by apamin [21, 136, 139].

Application of apamin to CA1 neurons increases excitability which can be seen as a shortened interspike interval, especially early in a burst of action potentials, and increases the number of action potentials for a given current injection. The action potential duration and the resting membrane potential do not

exchange in the slice is not optimal, the data support a major contribution of SK2 to the IAHP [21]. To determine the contribution of each of the SK channels to the IAHP in CA1 neurons, transgenic mouse lines were constructed, each lacking one of the *SK* channel genes and brain slice recordings were conducted.

3. Methods

Transgenic mice

SK1 Δ/Δ mice A 6.6 kilobase genomic DNA fragment encompassing exon 1 (5' UTR) to the intron between exons 6 (pore) and 7 was isolated from a 129/Sv mouse genomic library. A single loxP site was inserted into the 5'UTR 40 nucleotides 5' of the initiator methionine codon. A cassette consisting of the neomycin resistance gene flanked by loxP sites and the coding sequence for enhanced GFP was inserted into a unique Hpa1 site in the intron between exons 5 and 6. Recombination across loxP sites results in the loss of exons 3, 4, and 5 (encoding initiation of translation through TM5). The targeting construct was electroporated into ES cells (University of Cincinnati ES Core) and G418-resistant colonies were analyzed for homologous recombination by PCR and genomic Southern blot. One positive clone, when injected into C57Bl/6 blastocysts, yielded two chimeras that transmitted the targeted allele via the germline. Animals heterozygous for the floxed allele were bred to the *Cre deleter* mouse that expresses Cre recombinase ubiquitously from the two-cell stage

[115]. Offspring heterozygous for the recombined allele (+/ Δ) were bred to yield homozygous deleted *SK1* animals (Δ/Δ).

SK2 Δ/Δ mice A single loxP site was introduced into the 5'UTR 300 nucleotides 5' of the initiator methionine and a cassette consisting of the neomycin-resistance gene flanked by loxP sites, and the coding sequence for enhanced GFP was inserted into an EcoRV site in intron 2, ~2.3 kilobases from the end of exon 2. Recombination at the loxP sites yields an allele that is deleted for *SK2* exons 1 and 2. The targeting construct was electroporated into ES cells and several properly recombined ES cell clones were injected into C57Bl/6 blastocysts. One chimera gave germline transmission of the targeted allele. Crosses between heterozygous floxed *SK2* and the *Cre deleter* mouse yielded offspring that are heterozygous for the *SK2* deleted allele (+/ Δ). Crosses of *SK2* +/ Δ mice yielded *SK2 Δ/Δ mice*.

SK3 tTA mice The *SK3* mice used in this study have previously been reported [147]. The *SK3* gene was altered by homologous recombination, inserting a doxycycline (dox) sensitive gene switch into the exon encoding the 5'UTR. Using this strategy, temporal and spatial expression patterns are preserved while gene expression is controlled by dietary dox. The *SK3 tTA* mice have ~3-fold basal overexpression of *SK3*, and *SK3* expression is effectively eliminated by dietary dox from conception.

Western blotting

Mouse brains were homogenized in 320 mM sucrose, 10 mM HEPES, 1mM EGTA, pH 7.4 (HS), supplemented with a protease inhibitor cocktail. Nuclear material was removed centrifugation at 900Xg. Crude synaptosomal membranes were recovered in the pellet after centrifugation at 10,000Xg, washed once, and lysed in hypotonic solution 10 mM Hepes, 1mM EGTA, pH 7.4 (HE). The lysed synaptosomal membranes were collected by centrifugation at 25,000Xg, resuspended in HS and layered onto a sucrose step-gradient (1.2M, 1.0M, 0.8 M sucrose in 10 mM Hepes, 1 mM EGTA). After centrifugation at 150,000Xg for 90 minutes, membranes banding at the 1.0/1.2 M sucrose interface were recovered, diluted in HE and collected by centrifugation for 30 minutes at 150,000Xg. These membranes were stored in aliquots in HS at -80°C. Thirty micrograms of membrane protein were separated on 8% acrylamide-SDS gels and transferred to nitrocellulose. Primary antibody dilutions were: affinity purified rabbit anti-SK2, 2 μ g/ml; anti-SK3 1:1,000 (raised against DTSGHFHDSGVGDLDEDPKCP in the N-terminal domain; Alomone Labs, Jerusalem, Israel); anti-Na⁺K⁺ATPase 1:25,000 (courtesy of Dr. Svetlana Lutsenko). Protein-antibody complexes were visualized using Picosignal ECL reagents (Pierce, Rockford, IL). The polyclonal anti-SK2 antiserum was raised in rabbits against a sequence (ETQMENYDKHVTYNAE) in the C-terminal domain (Global Peptide Service, Fort Collins, CO). Anti-SK2 antibodies were purified using the peptide antigen immobilized on Sulfo-Link resin (Pierce, Rockford, IL).

Real-time PCR

Whole brain total RNA or total hippocampal RNA was isolated using Tri-reagent according to manufacturer's protocol. Total RNA was reverse-transcribed by MMLV reverse transcriptase (Invitrogen, Carlsbad, CA) in the presence of random hexamers but without dithiothriitol. Real-time PCRs were performed in triplicate for each SK transcript in each genotype, and expression levels were determined by comparison to 18S rRNA. The amplicon for 18S was 76 bp (primers: CCGCAGCTAGGAATAATGGA, CCCTCTTAATCATGGCCTCA); for SK1, 118 bp (primers: GCTCTTTTGCTCTGAAATGCC, CAGTCGTCGGCACCATTGTCC); for SK2, 151 bp (primers: GTCGCTGTATTCTTTAGCTCTG, ACGCTCATAAGTCATGGC); for SK3, 148 bp (primers: GCTCTGATTTTTTGGGATGTTTG, CGATGATCAAACCAAGCAGG ATGA). All SK amplicons span an intron. The efficiencies of the primer pairs were tested in a validation experiment using serial dilutions of a wild type cDNA (slope of ΔC_t (SK_{Ct} -18S $_{Ct}$) <0.1 ; not shown). C_t , the threshold cycle, indicates the fractional cycle number at which the amount of amplified target reaches a fixed threshold. The reaction master mix, consisting of 10X buffer, Mg (C_i = 4mM), dNTPs (C_i =200 mM), Platinum taq polymerase (Invitrogen, Carlsbad, CA) (0.6 units/ 20 ml reaction) and SYBR Green (Molecular Probes, Eugene, OR) (0.5X manufacturer's recommended concentration), was aliquoted, the cDNA substrates added, and then further aliquoted and primers added (C_i =200 nM).

Reactions were then split into triplicates for amplification in an MJ Research Opticon DNA Engine with cycling parameters 95°C, 2 minutes 1X; 95°C, 30 seconds/ 64°C, 45 seconds, with fluorescence read at 78°C for 40 cycles. A melting curve and gel electrophoresis analysis verified that a single product was amplified in all reactions.

Analysis For each run, the relative mRNA level was determined by the expression $2^{-\Delta\Delta Ct}$ (ΔCt (SK_{Ct}-18S_{Ct}) within each genotype, $\Delta\Delta Ct$ ($\Delta Ct_{SK\ transgene} - \Delta Ct_{wildtype}$) (ABO Prism 7700 Sequence Detection System, user bulletin 2). The mean and standard error of the value $2^{-\Delta\Delta Ct}$ for each SK mRNA in each genotype, across all runs, were plotted. Statistical significance was determined by 1-way ANOVA of ΔCt values across all genotypes followed by Bonferroni t-test.

Preparation of hippocampal sections and staining

Adult mice were transcardially perfused with PBS followed by 4% paraformaldehyde, brains removed, then post-fixed in 4% paraformaldehyde overnight. Brains were cryoprotected by soaking in 20% sucrose/PBS overnight at 4°C. 25 mm thick sections were cut on a cryostat and thaw mounted onto glass slides. Sections were delipidated by passage through ascending alcohol concentrations, followed by 10 min. incubation in Xylene. After re-hydrating through descending alcohol concentrations, the sections were briefly stained in a 0.25% thionin solution, dehydrated and mounted with Cytoseal 60.

Preparation of hippocampal slices

Mice (16-20 days old) were used for all studies in accordance with guidelines approved by the department of animal care at Oregon Health and Science University. Mice were first sedated by i.p. injection of a ketamine/xylazine mixture, then perfused through the left ventricle with ice-cold oxygenated ACSF solution described below. Following decapitation, the hippocampus was removed and transverse slices (350 μ M thick) were cut with a vibratome (Leica VT 1000S) in ACSF. Slices were subsequently incubated at 35°C for 30 min in ACSF and allowed to recover at room temperature for 30 min prior to recording. All recordings were performed at room temperature. The ACSF solution contained (in mM): 119 NaCl, 2.5 KCl, 2.5 CaCl₂, 1 MgCl₂, 1 NaH₂PO₄, 26.2 NaHCO₃ and 11 glucose, saturated with 95% O₂/5% CO₂, pH 7.35

Electrophysiology

CA1 neurons were visualized with a microscope equipped with IR/DIC optics (Leica DMLFS). Whole-cell recording pipettes were fabricated from thin wall borosilicate glass having resistances of 1.5-3 MW. Pipettes were filled with an intracellular solution containing (in mM): 140 KMeSO₄, 8 NaCl, 1 MgCl₂, 10 HEPES, 2 Mg-ATP, 0.4 Na₂-GTP, 20 μ M EGTA. (pH 7.3, 290 mOsm), and slices were continuously superfused with ACSF saturated with 95% O₂/5% CO₂. Whole-cell patch-clamp currents were recorded with a Multiclamp 700A amplifier (Axon Instruments, Foster City, CA), digitized using an ITC-16 A/D converter (Instrutech Corp., Greatneck, NY), and acquired onto computer using Pulse software (HEKA

Electronics, Lambrecht, Germany).

For measurement of the IAHP, CA1 neurons were held at -55 mV and IAHP currents were evoked by depolarizing voltage commands to 20 mV for 100 msec followed by a return to -55 mV for 10 sec. All cells had a resting membrane potential more hyperpolarized than -55 mV and input resistances of 150-350 MW. Access resistance was stable at <20 MW and was 80% compensated. IAHP recordings were filtered at 1 kHz and digitized at a sampling frequency of 1 kHz; the records were further filtered offline with a 300 Hz Gaussian filter (for 1 pass). Data were analyzed in Igor Pro (Wavemetrics, Lake Oswego, OR). Data are expressed as mean \pm SEM. Statistical significance was tested using ANOVA where appropriate, and a $P < 0.01$ was considered significant. Apamin was obtained from Calbiochem.

4. Results

SK transgenic mice

Three SK channel genes, *SK1*, *SK2*, and *SK3* are expressed in the central nervous system and each gene shows a distinct tissue and cell type expression profile [76, 82]. The mRNAs for each of the *SK* genes have been detected in CA1 neurons by in situ hybridization [21]. To determine the contributions of each of the genes to the IAHP in CA1 neurons, conditional knockout alleles were constructed by homologous recombination (Fig. 1A). For *SK1* and *SK2*, flanking coding exons with loxP sites (floxing) created conditional alleles. For *SK1*, loxP

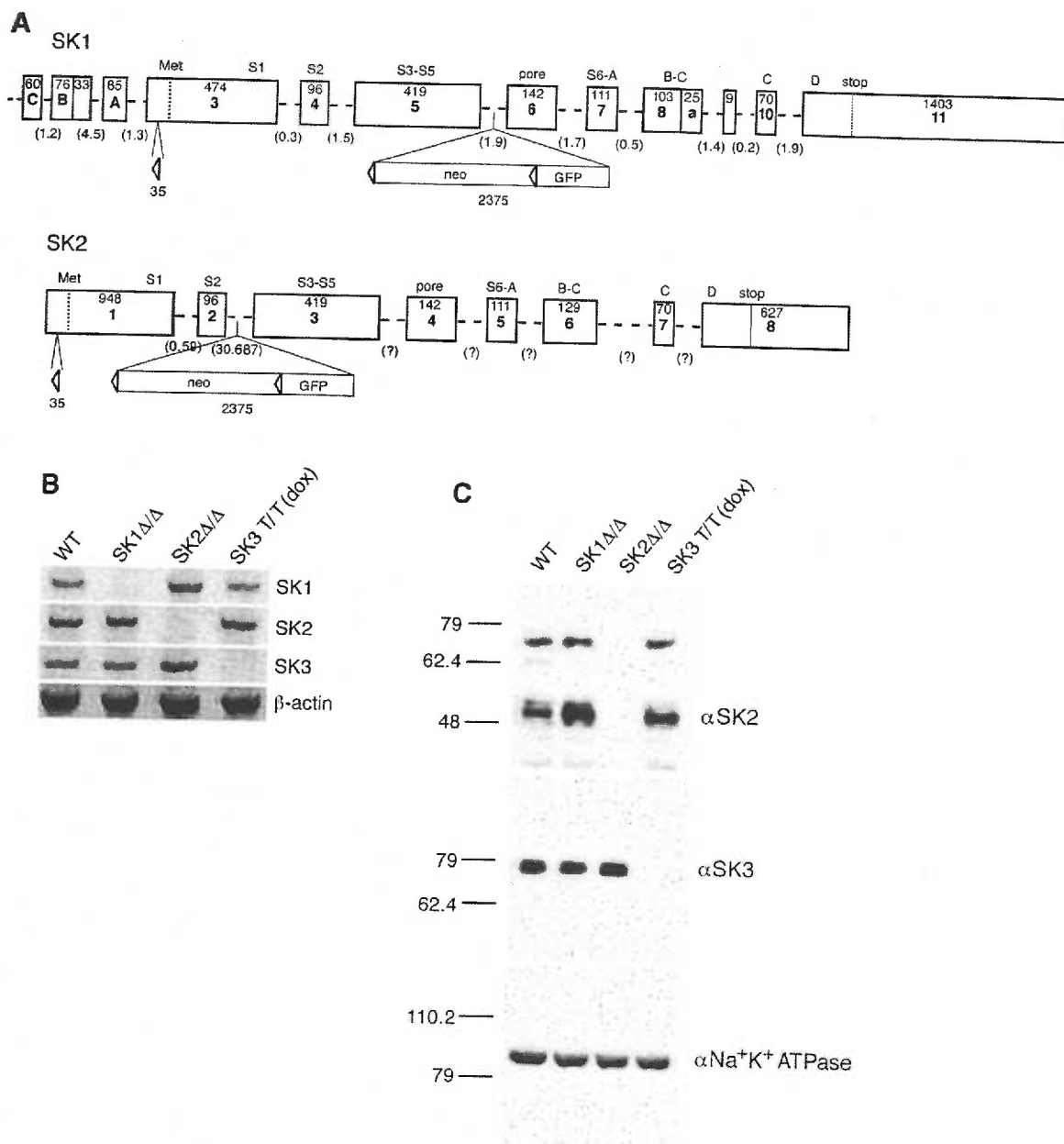
Figure 1. *SK* transgenic mice

A) Schematic representations of the *SK1* and *SK2* transgene loci; *SK1 flox* (top) and *SK2 flox* (bottom) alleles. The sizes of the exons (bps) and the channel domains they encode are presented and the sizes of the introns (kbps) are given for those that have been determined. The inserted elements (triangles represent loxP sites), their sizes and positions in the targeting constructs are shown below the exon-intron mosaic.

B) rt-PCR analysis using total brain cDNA shows the loss of each SK mRNA in the respective knockout mice. β -actin was amplified to approximate the relative amounts of cDNA from the different genotypes.

C) Western blots of brain proteins for SK2 and SK3. The same samples (30 μ g) were loaded in each lane for each of the blots. The top blot was probed with an affinity-purified polyclonal SK2 antiserum and shows the loss of SK2 in *SK2* Δ/Δ mice. The middle blot was probed with a polyclonal SK3 antiserum and shows the loss of SK3 protein in *SK3* *T/T* mice that had been administered dietary doxycycline. The bottom blot was probed with a polyclonal Na⁺-K⁺ ATPase antiserum and shows the relative sample loading across all lanes.

Fig. 1



sites were inserted within exon 3 and after exon 5, encompassing the sequences that encode the initiator methionine through transmembrane (TM) domain five. For *SK2*, loxP sites flanked exons encoding the intracellular N-terminal domain and TMs one and two. Excision of the SK coding exons in all cell types including germ cells was accomplished by crossing animals harboring the floxed allele with a *Cre-deleter* mouse [115] that ubiquitously expresses Cre recombinase very early following conception. Crossing heterozygous animals yielded homozygous-null offspring for either the *SK1* or *SK2* genes. *SK3* knockout mice have been previously reported and were achieved by insertion of a tetracycline-regulated gene switch into the exon encoding the 5' UTR. SK3 expression is abolished by dietary dox [114]; see below). Homozygous female transgenic mice lacking any one of the SK genes were viable and reproductively competent.

Analysis by rt-PCR and Western blotting verified effective genetic manipulations for each SK subunit. Brain cDNAs from *SK1* Δ/Δ , *SK2* Δ/Δ , and *SK3* *T/T(dox)* mice or wild type controls were used for PCRs specific for each of the SK mRNAs (Fig 1B, left). The results showed the loss of SK1, SK2, or SK3 mRNA expression in the respective mice. Western blotting was performed with brain membrane proteins using SK2- or SK3-specific polyclonal antibodies. The results showed an absence of the respective SK protein.

SK2 channels underlie the apamin-sensitive current in CA1 neurons

To determine the contributions of each of the SK subunits to the IAHP in

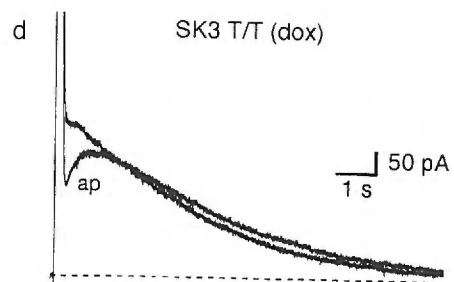
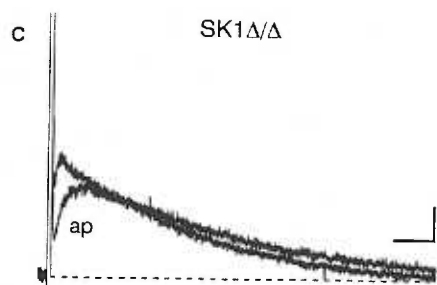
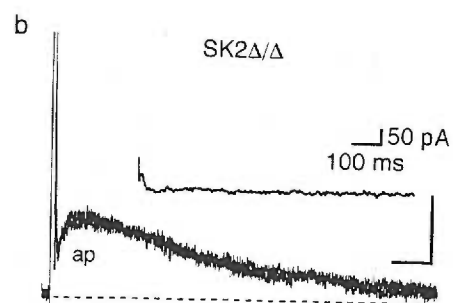
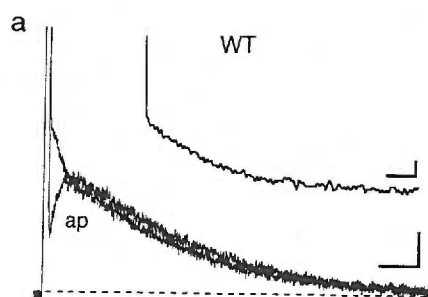
CA1 neurons, whole cell voltage clamp recordings were performed in hippocampal slices from the different *SK* transgenic mice. Anatomically, there were no obvious abnormalities in the hippocampi of any of the *SK* transgenic mice, and the CA1 region was not different than wild type (Fig. 2A). The IAHP was measured at -55 mV following a 100 msec depolarization to 20 mV (Fig. 2B). In slices from wild type mice, apamin blocked an early component of the IAHP and the apamin sensitive component of the ImAHP, obtained as the difference between the IAHP in control and after apamin application, decayed with a time constant of 192 ± 11 msec ($n=15$; inset Fig. 2B, Table 1). Apamin also blocked an initial component in each genotype except *SK2* Δ/Δ in which the difference trace was essentially flat. To quantify the apamin-sensitive component of the ImAHP and the IsAHP in each of the transgenic mice, the amplitude of the apamin-sensitive current was measured at 100 ms following the depolarizing pulse while the IsAHP was measured at 1 sec in the presence of apamin. The results show that in CA1 neurons the amplitude of the apamin-sensitive component was not significantly different in mice lacking SK1 or SK3. In contrast, *SK2* Δ/Δ mice completely lacked the apamin-sensitive component of the ImAHP (Fig. 3). The time constant of decay of the apamin-sensitive component of the ImAHP was not different from wild type in *SK1* Δ/Δ or *SK3* *T/T* (*dox*) mice. Although the amplitude of the IsAHP was more variable, the IsAHP amplitude in any of the transgenic lines was not different from wild type, showing that no member of the SK channel family is required for the IsAHP (Fig. 3). The time

Figure 2. Voltage clamp analysis of the IAHP

A. Thionin-stained hippocampal sections from *SK* knockout mice. No obvious anatomical abnormalities were observed in any of the genotypes.

B. Voltage clamp recordings of mouse CA1 neurons following a 100 ms depolarizing pulse to +20 mV. Apamin blocks an initial component of the IAHP in all of the genotypes except *SK2* Δ/Δ mice, which lack the apamin-sensitive current. Subtraction of the traces before and after apamin application yielded the ImAHP (shown for wild type and *SK2* Δ/Δ). Scale bars for full traces correspond to those for *SK3* *T/T* (dox); those for the insets correspond to the values shown for *SK2* Δ/Δ .

A.



constants for the decay of the apamin-sensitive component of the ImAHP, and IsAHP, as well as the half-rise time of the IsAHP are summarized in Table 1 and show that except for *SK2* Δ/Δ mice that lack the apamin-sensitive component of the ImAHP, these kinetic parameters, as well as membrane capacitance, were not different in any of the transgenic mice compared to wild type mice.

To evaluate whether there are changes in the expression levels of the remaining two SK channel genes in each of the null mice, mouse brain cDNA was used for quantitative real-time rtPCR (see methods). The values for each of the SK amplicons were normalized to those obtained from wild type animals; 18S RNA was used as the internal reference. As shown in Fig. 4, mRNA levels for the two remaining intact *SK* genes were not significantly altered in any of the knockout animals.

While not significant, there was a clear trend to lower apamin-sensitive component ImAHP amplitudes in the *SK1* Δ/Δ mice (Table2). Recent reports show that heterologous co-expression of SK1 with either SK2 or SK3 results in heteromeric channels, and suggest that rodent SK1 subunits, themselves incapable of forming functional homomeric channels, may contribute to the levels of channels containing SK2 or SK3. To investigate the potential contribution of SK1, the levels of SK1 and SK3 mRNAs, normalized to SK2 mRNA levels, were determined from wild type whole brain or hippocampus. The results show that SK1 mRNA levels are ~20% of SK2 levels in either whole brain or hippocampus.

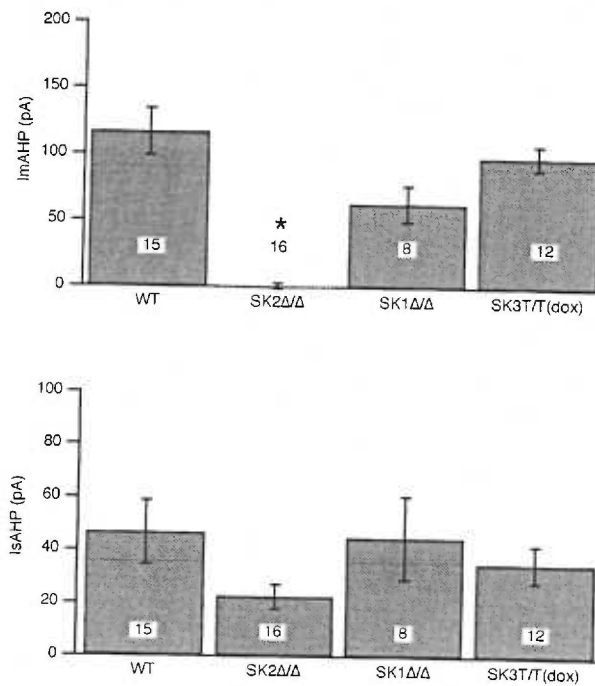


Figure 3. SK2 channels underlie the apamin-sensitive component of the ImAHP while the SK channels do not contribute to the IsAHP.

Top: The average amplitudes of the apamin-sensitive component of the ImAHP from the different genotypes, measured 100 ms after the pulse, are shown in the bar graph. Mice lacking SK2 channels do not express an apamin sensitive ImAHP. Statistical differences were determined by analysis of variance, yielding p-values < 0.001 for *SK2* Δ/Δ, 0.23 for *SK1* Δ/Δ, and 0.92 for *SK3* T/T (dox) mice compared to wild type. Statistical significances at 1% level are indicated by *.

Bottom: The IsAHP was measured, in the presence of apamin, as the current amplitude at 1s after the end of the pulse. Statistical differences were determined by analysis of variance, yielding p-values of 0.26 for *SK2* Δ/Δ, 1.00 for *SK1* Δ/Δ, and 0.90 for *SK3* T/T (dox) mice compared to wild type. There were no significant differences between groups (n>7), showing that none of the SK channels contribute to the IsAHP.

For both plots, ± SEM; n, are as indicated.

Figure 4. Quantitative analysis of SK mRNA levels in *SK* transgenic mice

Top panel: Real-time PCR performed with whole brain RNA from the different *SK* transgenic mice was used to evaluate the levels of each of the SK mRNAs, normalized to the levels determined for wild type (n=5 for each genotype; see methods). 18S ribosomal RNA was used as the internal reference. Relative expression compared to wild type was calculated as the mean of $2^{-\Delta\Delta Ct} \pm$ SEM and shows that mRNA levels derived from the unmodified *SK* genes are not significantly altered in any of the transgenic mice. Statistically significant differences ($P < 0.05$) in expression levels compared to wild type are indicated by *.

Bottom panel: Comparison of levels of SK1 and SK3 mRNAs to SK2 mRNA in whole brain and hippocampus of wild type mice by real-time PCR. 18S rRNA was used as the internal reference. (n=5)

Fig. 4 Quantitative PCR

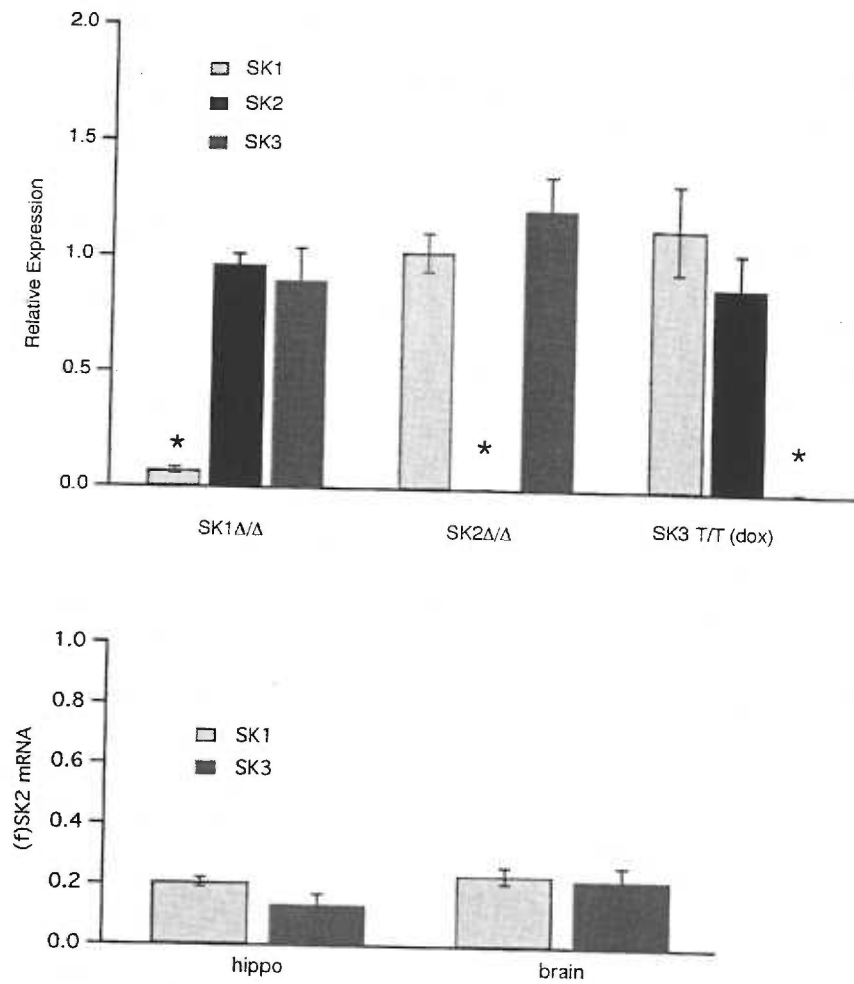


Table 1. Cell parameters for different transgenic mice.

genotype	Cap	Rinp	τ ImAHP	T1/2 IsAHP	τ IsAHP
	pF \pm SEM (n)	M Ω \pm SEM (n)	ms \pm SEM (n)	ms \pm SEM (n)	s \pm SEM (n)
wt	120.1 \pm 15.4 (15)	257.6 \pm 21.7 (15)	192.4 \pm 10.9 (15)	183.0 \pm 12.4 (3)	2.9 \pm 0.2 (7)
<i>SK2Δ/Δ</i>	130.5 \pm 14.0 (15)	270.0 \pm 25.5 (15)		244.2 \pm 98.9 (3)	3.2 \pm 0.2 (9)
<i>SK1Δ/Δ</i>	123.0 \pm 20.7 (8)	219.5 \pm 18.1 (8)	200.2 \pm 26.0 (7)	163.7 \pm 52.9 (2)	3.3 \pm 0.3 (5)
<i>SK3 T/T</i>	137.5 \pm 8.5 (12)	232.5 \pm 12.6 (13)	197.0 \pm 15.7 (11)	135.2 \pm 11.9 (2)	2.7 \pm 0.1 (8)
(dox)					

Data presented as mean \pm SEM, Cap represents cell capacitance, Rinp represents cell input resistance, τ ImAHP represents decay time constant of apamin sensitive component of IAHP, T1/2 IsAHP represent time to half peak of IsAHP, τ IsAHP represents time constant of decay of IsAHP in presence of apamin.

Table 2. AHP current amplitudes

Genotype	ImAHP (pA)	p-value	IsAHP (pA)	p-value
WT	116.7±68.2 (15)		46.6±46.8 (15)	
<i>SK2</i> Δ/Δ	0.9±8.4 (16)	<0.01	22.6±19.0 (16)	0.26
<i>SK1</i> Δ/Δ	63.0±38.5 (8)	0.23	45.0±44.8 (8)	1.00
<i>SK3</i> T/T dox	98.4±31.9 (12)	0.92	35.4±25.3 (12)	0.90

Data presented as mean±SD (n), p-value determined from analysis of variance (Tukey HSD) on current amplitudes between WT and each genotype.

SK3 levels are ~20% in whole brain, but reduced to ~10% relative to SK2 mRNA levels in hippocampus (Fig. 4).

5. Discussion

The results show that SK2 subunits are necessary for the apamin-sensitive component of the I_mAHP. In *SK1* Δ/Δ or *SK3* *T/T(dox)* mice, the apamin-sensitive component of the I_mAHP was not significantly different from control, there were no significant changes in the levels of SK2 mRNA, and SK2 protein levels were not obviously up-regulated, suggesting that only SK2 is necessary for the apamin-sensitive component of the I_mAHP. This is consistent with earlier suggestions that were based on the pharmacological profile of the current and on the high specificity of apamin [21, 145].

In heterologous expression studies mouse and rat SK1 subunits, different from human SK1 subunits, do not form functional homomeric channels in the plasma membrane but they are incorporated into heteromeric channels with SK2 or SK3 subunits [81, 146]. These data suggest that SK1 subunits may contribute to the number of functional SK2-containing channels, although the stoichiometry of SK1/SK2 heteromeric channels is not known. Quantitative PCR showed that in hippocampus SK1 mRNA is present at levels that are ~20% of SK2. Also, the SK1 mRNA population contains multiple splice variants [148]. Only two of these, co-assemble with SK2 into plasma membrane channels and only one of those two splice forms, comprising ~40% of the SK1 transcripts, is expressed in the

brain (unpublished). The native levels of the different SK subunit mRNAs are in contrast to heterologous expression studies where both subunit types are robustly co-expressed. Therefore, it is probable that in native neurons only a small percentage of heteromeric SK1/SK2 channels would form. If all of these heteromeric channels were absent in the *SK1* Δ/Δ mice, it is unlikely that more than a 10% reduction of the apamin-sensitive *I*_{mAHP} would be seen.

Nevertheless, we cannot unequivocally exclude a contribution of SK1 subunits.

In situ hybridization results show that in CA1 neurons SK2 mRNA is the most highly expressed of the SK channel mRNAs, SK1 is also abundant while SK3 is lower but detectable [21, 82]. The relative transcript levels detected by *insitu* hybridization are consistent with the quantitative PCR results presented here. Immunohistochemical studies showed SK1 and SK2 immunoreactivity in CA3 neurons, only SK2 immunoreactivity was prominent in CA1 neurons; SK3 was excluded from the pyramidal and granule cell layers of the hippocampus [145, 149]. Interestingly, SK3 immunoreactivity was found predominantly in the terminal field of the mossy fibers and in fine varicose fibers, and in hippocampal cultures SK3 was co-localized with presynaptic markers [149].

Indeed, the biophysical properties of the heterologously expressed SK channels are quite comparable, exhibiting essentially identical $E.C_{50}$ values for Ca^{2+} gating, and similar gating kinetics. It is likely that different functional roles for the channels are endowed by distinct subcellular localizations and interactions with different microdomain components. It is interesting that SK2 channels,

required for the apamin-sensitive I_{mAHP} , may also be responsible for the effects of apamin on the induction of synaptic plasticity in CA1 neurons. These dual roles may reflect spatially and functionally distinct subpopulations of SK2 channels within the same CA1 neuron.

Like the SK channels that contribute to the I_{mAHP} , the channels underlying the I_{sAHP} are voltage-independent and K^+ selective, and they require Ca^{2+} influx for activation [133] [41]. Indeed, SK channels have been suggested to underlie the $sAHP$ [139]. However, the results show that the cloned SK channels are not necessary for the I_{sAHP} that is responsible for spike-frequency adaptation. In particular the I_{sAHP} in mice lacking the least apamin-sensitive SK subunit, SK1, is similar to wild type and is not apamin-sensitive. In addition, the Ca^{2+} -dependence of the channels underlying the I_{sAHP} may not be mediated by the same calmodulin-dependent gating mechanism that is the molecular hallmark of SK channels [77, 136, 150-153]. Based upon the present results it seems likely that the I_{sAHP} channels have not yet been molecularly identified and that the channels underlying the $sAHP$ are distinct from SK channels.

CHAPTER IV: SK1; the enigma

1. Introduction

Cross-species comparisons from cloned cDNAs

The first full length SK1 cDNA clone was isolated from a human hippocampal cDNA library [76]. Inside-out (I/O) patches pulled from *Xenopus* oocytes injected with *in vitro* transcribed hSK1 mRNA displayed calcium-activated potassium currents, indicating that the hSK1 cDNA encodes subunits that form functional channels in the plasma membrane. These SK1 channels had the same calcium sensitivity and kinetics of channel activation as seen with expression of rat SK2 and SK3 cDNAs. However, the pharmacology of the SK1 channels appeared to differ from SK2 and SK3. Calcium-dependent currents in inside-out patches pulled from oocytes expressing SK2 were blocked by picomolar concentrations of extracellular apamin. In contrast, the currents from oocytes expressing hSK1 were resistant to block by 100 nM apamin. This result led to the hypothesis that SK1 subunits form the channel underlying the apamin-insensitive, calcium-dependent potassium current of the slow AHP described in Chapter 3. However, subsequent expression studies in transiently transfected cells showed that the channels formed by hSK1 subunits were blocked by 8 nM apamin when expressed in HEK293 cells or 12 nM apamin in COS cells [80]. These differences in sensitivity in different cell types suggest that there may be components supplied by the cell that contribute to the formation of hSK1

channels that influence the conformation of the channel, and thereby its pharmacological profile.

Even more striking results were observed when cDNAs for SK1 were isolated from rat and mouse. Neither the rat nor the mouse cDNA yields calcium-activated currents when expressed in oocytes or transfected cells. When the rSK2 cDNA with a triple myc epitope tag in the putative extracellular loop between TMs 3 and 4 is transfected into COS or HEK293 cells, live cell staining with the anti-myc antibody demonstrates the presence of the tagged SK2 channels on the plasma membrane [154]. Similar experiments performed on cells transfected with the analogously tagged rat or mouse SK1 showed that, although the protein was abundant within the cell, no extracellular epitope was detected, indicating that the SK1 channels do not reside in the plasma membrane. The myc tagged hSK1 could be detected in live cell staining, implying that the lack of staining of rat or mouse SK1 was not a function of epitope masking. Very recent results have shown that chimeric rSK1 channels, containing the intracellular C-terminus of either hSK1 or rSK2, express currents in transfected cells, and that these currents are apamin insensitive [155]. Co-expression of the chimeric rSK1 with rSK2 led to calcium-activated currents with reduced sensitivity to apamin, indicating that these two subunits can co-assemble, raising the possibility that SK1 subunits function as auxiliary subunits in SK2 channels.

The amino acid sequences of the three mammalian SK subunits are highly homologous, being 67-75% identical. The sequences for SK2 and SK3 are nearly (96-98%) identical when compared between rat, mouse and human. In contrast, the human SK1 protein differs from either rodent form substantially, sharing only 84% identity. These differences raise the questions; do the rodent and human clones for SK1 truly represent orthologs? Does SK1 serve functions in the human that are different than served by this protein in rodents? What is the function of the rodent SK1? Interest in these questions was further piqued by the discovery of alternative splicing at the *SK1* locus that could result in expression of as many as eight different protein forms [148](appendix paper #).

Alternative Splicing

The gene for the large-conductance calcium-modulated potassium channel, *BK*, has a complex array of alternative exons encoding the intracellular C-terminus of the protein [56]. Channel kinetics and conduction properties depend on the assembly of exons composing each subunit. These differences in functional characteristics contribute to tuning frequency responses in the inner hair cells [156]. Many of the variable exons represent one choice of two or three possibilities. Other exons are represented in an IN or OUT choice, i.e. the exon is included or excluded, but no alternative exon exists at that position. The alternative splicing characterized at the *SK1* locus includes alternative 5'UTR regions (Figure 1A), but also occurs at exons encoding the C-terminal portion of

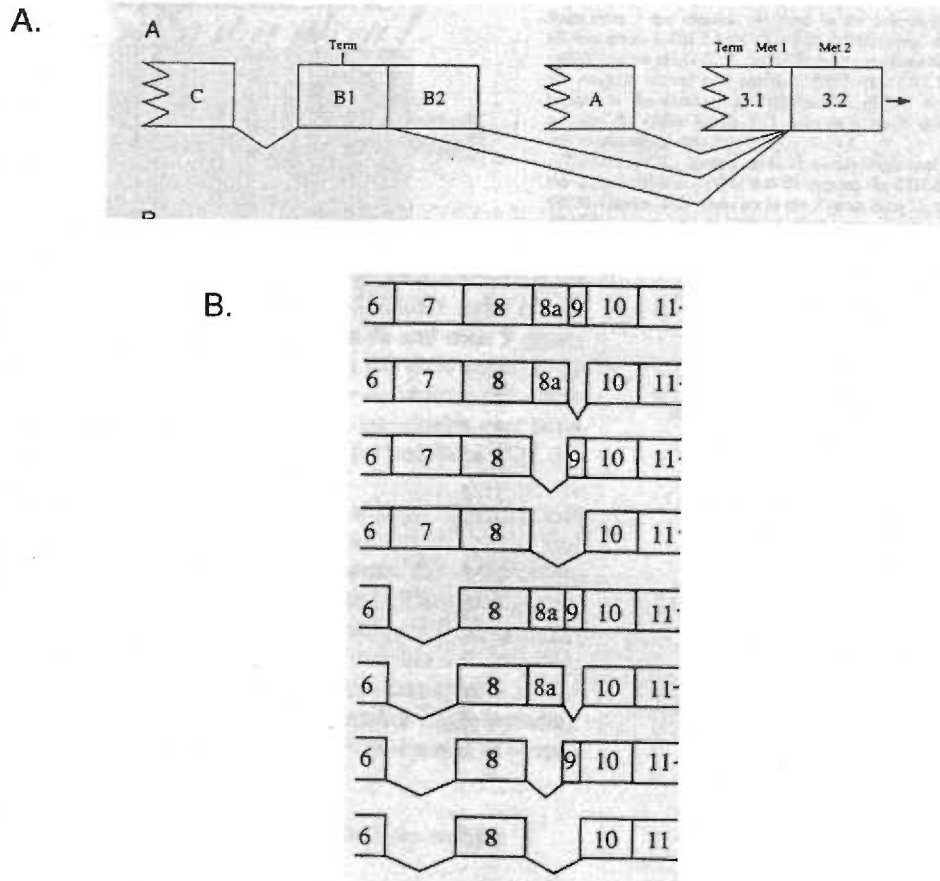


Figure 1.

Schematic representations of the alternative splicing at the *SK1* locus.

A. The 5' UTR consists of either exon A, C-B1-B2, or C-B1 spliced to exon 3.2 which contains the initiator methionine. 3.1 is most likely intronic and is found only in rare, partially spliced transcripts.

B. The C-terminal splice variants are formed by exclusion of exon 7, exon 8a, exon 9, or all possible combinations. Exon 8a is 25 bps of the C-terminal end of exon 8. Deletion of 8a causes a frame shift that results in truncation of the C-terminus.

the protein (Figure 1B). No evidence was found for alternative N-termini, pores, or TM domains (except in the case of deletion of exon 7, see below). All alternative splices in SK1 are of the inclusion/exclusion form. Mapping of the intron/exon mosaic of mouse and human *SK1* loci verified that all but one variable splice site occurred at canonical intron/exon boundaries. The one exception joins a noncanonical site within exon 8 to the splice acceptor site at the 5' end of either exon 9 or exon 10.

The variously spliced SK1 mRNAs have the potential to encode eight different proteins. All share the same N-terminus, TMs 1-5, pore and N-terminal half of TM 6. The smallest variation from the high homology shared by all three SK subunits is the inclusion of a nine nucleotide exon which encodes the amino acids AQK (alanine, glutamine, lysine) within the CaM-BD, residues not found in SK2 or SK3. In experiments where immobilized C-termini of SK1 (with AQK) and SK2 were exposed to cytoplasmic proteins from rat brain extracts, calmodulin was bound much more tightly to the C-terminus of SK2 than to SK1. Most of the calmodulin bound to SK1 was eluted in 2 M urea, while the calmodulin bound to SK2 remained bound in 2 M urea, but was eluted in 8 M urea (Tim Strassmeier, unpublished observation). These results demonstrate that the presence of the AQK exon in the Cam-BD weakens the interaction of CaM with SK1, and that CaM may not be present as a constitutive beta subunit, as predicted for SK2 and SK3.

The other SK1 splice variants result in more extreme changes in the SK1 protein. Exclusion of exon seven ($\Delta 7$) results in a putative translation product that lacks the C-terminal half of TM 6. The newly adjoined amino acids do not have the hydrophobic character normally found in membrane-spanning regions, raising the question of the topology of this form of SK1. Although the pore amino acids are still present, the absence of TM 6 may result in a completely novel conformation that does not participate as a pore-forming subunit. Splicing at the noncanonical site in exon 8 ($\Delta 8a$) results in a frame shift (this does not occur with any of the other exon exclusions) and the ORF terminates after only three ($\Delta 8a\Delta 9$) or six ($\Delta 8a$) residues. This truncated protein lacks the C-terminal portion of the CaM-BD; instead terminating in residues known in other proteins to interact with PDZ domains [157]. *In vitro* binding of calmodulin to these truncated forms is markedly diminished [158] (Figure 2).

These alternative SK1 transcripts, characterized here in the mouse, are also found in human (Lazdunsky, personal communication, [158]) and rat (unpublished observation). This conservation across species implies a functional basis for the multiple SK1 forms. Results described here include characterization of the mouse *SK1* locus, quantitative PCR assay of relative levels of the alternate transcripts in various tissues, tests of translation and trafficking of alternate SK1 proteins *in vitro*, and the development of monoclonal antibodies to recognize the long and the truncated C-termini. It is my hope that future experiments using

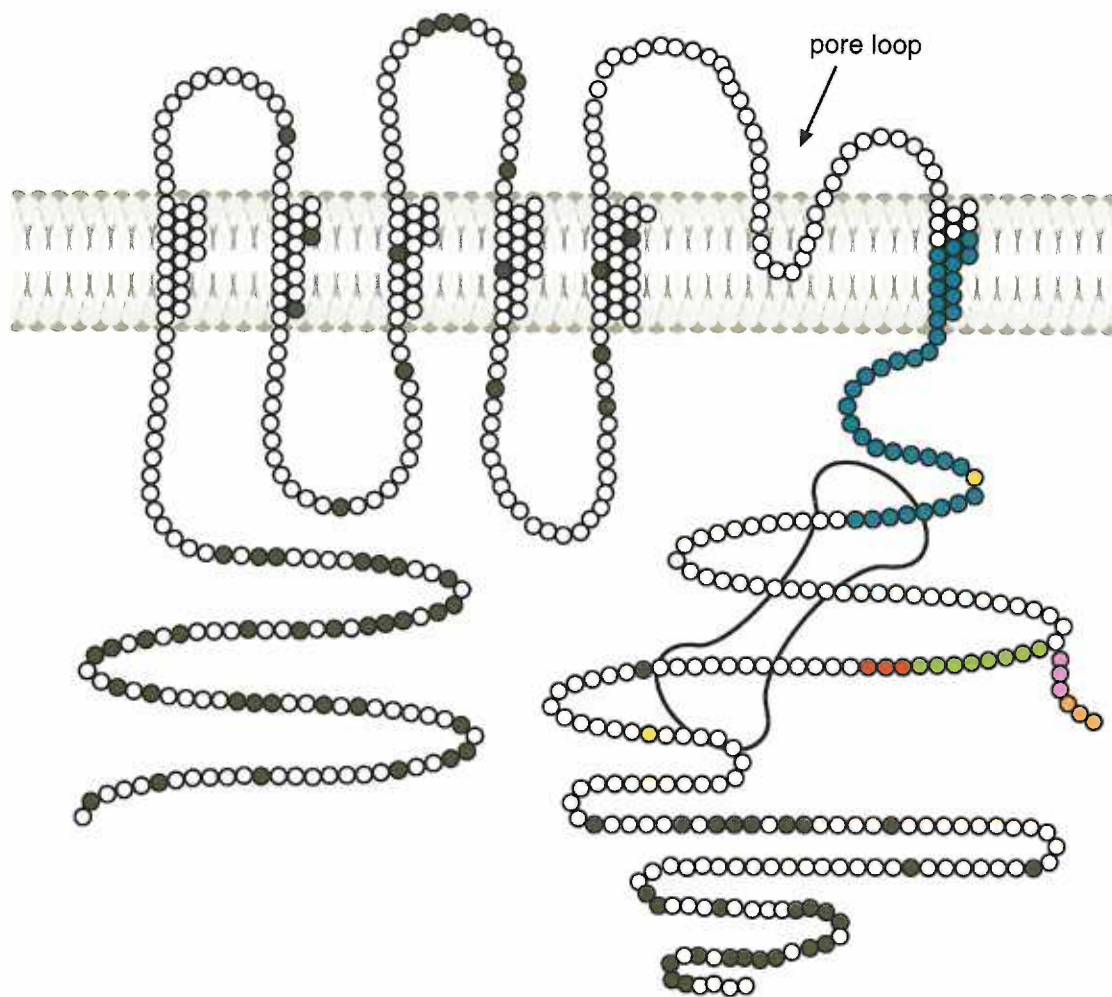


Figure 2.

Schematic representation of an SK1 subunit sitting in a membrane bilayer. Each circle represents an amino acid. The position of the pore loop is indicated. Calmodulin is represented by a dumbbell lying within the CaM-BD, the limits resolved in the CaM:CaM-BD co-crystal indicated by yellow. The SK1 alternate splice exons are indicated: exon 7 in blue, exon 8a in green, exon nine in red. The alternative C-terminus of the $\Delta 8a$ splice form is shown in pink and orange; $\Delta 8a\Delta 9$ would end with the pink residues. Charcoal residues indicate amino acids that are different between human and mouse SK1. Clearly, each of the alternatively spliced exons impacts the structure of the CaM-BD.

SK1 specific antibodies and the *SK1* conditional mice will contribute to our understanding of the functions served by SK1.

2. Materials and methods

5' RACE

Total RNA was reverse transcribed by MMLV (Invitrogen) in the presence of random hexamers. A poly-adenosine tail of 15-30 nucleotides was added to the single-stranded cDNA by incubation with terminal deoxy-transferase (BRL) in the presence of 250 μ M dATP in a suboptimal transferase buffer consisting of 25 mM tris (pH 8.3), 3 mM MgCl₂, 20 mM KCl, and 5 mM DTT. The tailed cDNA was then added as substrate for PCR for one cycle of 96°C for 30 sec. / 50 °C for 2 min. / 72°C for 2 min. in the presence of dTH3 primer (gacaccaagcttt₁₅) to render the cDNA double-stranded. The gene-specific primer was added to the reaction and cycling continued at 95°C for 30 sec. / 52-60°C for 30 sec. / 72°C for 1 min. X25 cycles. 0.5-5% of the outer reaction was used as substrate in a nested reaction with a second gene-specific primer in conjunction with the H3 primer (gacaccaagctttttt) for 25 cycles at 95°C for 30 sec / 55-60°C for 30 sec. / 72°C for 1 min. PCR products were then purified and cloned using sites conferred by the PCR primers and subjected to sequence analysis.

Immunofluorescence

COS cells were grown on poly-L-lysine coated coverslips to ~50% confluency. Cells were transfected with specific cDNAs plus 1/10th concentration

GFP as a marker of transfection using lipofectamine (Invitrogen). In all cases where different SK subunits were co-transfected the ratio of SK DNA concentrations was 1:1. One to two days following transfection, cells were fixed for 20 min. in 4% paraformaldehyde, washed with PBS and then incubated with sera or monoclonal supernatants at concentrations from 1:1 to 1:5 for 30 min. at room temperature. For live cell staining, α -myc monoclonal antibody (Upstate Biotechnologies) was added to the medium at a concentration of 1:250 at 37°C for 30 min. prior to fixation. Cells were then washed with PBS, fixed in 4% paraformaldehyde for 20 min. at room temperature, washed in PBS. A cy3-conjugated secondary antibody (either α -mouse or α -rat, as appropriate) diluted 1:250 was applied for 30 min, followed by PBS washes, mounting with Antifade (Molecular probes) and visualization by fluorescence microscopy.

Western blot

Membranes from transfected COS cells were isolated. Cells were homogenized in a glass dounce, nuclei pelleted at 5xg for 10 min. and membranes pelleted from the supernatant by high speed centrifugation (60 krpm, 30 min. at 4°C). Membranes were solubilized in 320 mM sucrose in PBS. Protein was quantified by Bradford assay. 10-20 μ g of protein were separated by PAGE, transferred to nitrocellulose membranes and incubated with the α -HA primary antibody at a dilution of 1:250 overnight at 4°C. Following washes in PBS, the membrane was incubated with an HRP-conjugated secondary antibody for 1 hour at room temperature. Immunoreactivity was visualized by ECL (Pierce

Pico-signal).

Realtime quantitative PCR

Total RNA was isolated using Tri-reagent (Sigma) according to manufacturer's recommendations, and reverse-transcribed by MMLV (Invitrogen) in the presence of 1 μ g random hexamers per 20 μ g RNA, 50 mM tris (pH 8.3), 6 mM $MgCl_2$, 40 mM KCl, and 200 μ M dNTPs. The single-stranded cDNA was added as substrate for PCR in the presence of 0.6 units/ reaction Platinum Taq Polymerase (Invitrogen), 10 X buffer, 4 mM $MgCl_2$, 200 μ M dNTPs, and SYBR Green (Molecular Probes) at 0.5x manufacturer's recommendation, and 200 nM primers. Reactions were then split into triplicates for amplification in an MJ Research Opticon DNA Engine with cycling parameters 95°C, 2 minutes 1X; 95°C, 30 seconds/ 64°C, 45 seconds, with fluorescence read at 84°C for 40 cycles. A melting curve and gel electrophoresis analysis verified that a single product was amplified in all reactions. Expression levels were determined by comparison to beta actin transcript levels. The efficiencies of the primer pairs were tested in a validation experiment using serial dilutions of pooled plasmid DNAs (slope of ΔC_t (SK1 splice_{Ct}-beta actin_{Ct}) <0.1. C_t , the threshold cycle, indicates the fractional cycle number at which the amount of amplified target reaches a fixed threshold.

Analysis For each run, the relative mRNA level was determined by the expression $2^{-\Delta\Delta C_t}$

(ΔCt ($SK1splice_{Ct}$ - $\beta actin_{Ct}$) within each tissue, $\Delta\Delta Ct$ ($\Delta Ct_{SK1splice} - \Delta Ct_{full\ length/brain}$) (ABO Prism 7700 Sequence Detection System, user bulletin 2, see appendix for derivation). The mean and standard error of the value $2^{-\Delta\Delta Ct}$ for each SK mRNA in each genotype, across all runs, were plotted.

3. Results

***mSK1* locus**

The intron/exon mosaic of the mouse *SK1* gene was mapped by B. Shmukler and S. Alper [148]. In the mouse *SK1* gene, the AUG that is analogous to the initiator Met codon in SK2 is preceded by a contiguous ORF of 43 amino acids, including an additional 5' Met. 5' RACE and RT-PCR analysis from mouse brain cDNA demonstrated that a complex of alternative 5' UTR exons are spliced to the coding exon downstream of the most 5' AUG (Figure 1A). None of the three alternative 5' exons contain in frame Met codons; thus the mouse SK1 protein likely initiates at the position most homologous to the start of the SK2 protein. In contrast, human SK1 has an additional 18 N-terminal amino acids that have no counterpart in the mouse protein. No bias in the combination of 5'UTR exon and downstream splice pattern was detected in RT-PCR experiments on brain cDNA. Currently, nothing is known about tissue- or developmental-specific choice of 5' UTR exon pattern.

Relative expression of SK1 splice variants

Quantitative real time PCR was used to compare relative levels of SK1 alternative splice transcripts. Real time PCR utilizes detection of fluorescence to indicate the formation of a double-stranded product. In contrast to standard PCR techniques, where the product detected is the end-point, real time PCR reports the first cycle at which product reaches the threshold of detection. Thus the variables that make end-point PCR non-quantitative, such as depletion of nucleotides or primers or saturation of detection, are avoided. Primer pairs were designed to produce amplicons that were each less than 150 bp in length. Primers spanned exon boundaries in such a manner that only one splice variant was amplified by each pair. The specificity of primer pairs was verified by amplification of plasmid DNAs of all of the possible variants, alone or pooled. End point gel electrophoresis verified that only the preferred product was amplified, that the primer pairs did not yield primer dimers or non-specific products, even when no substrate was included. Primer pairs that did not fulfill these criteria were redesigned and new pairs tested. Finally, primer pairs were tested in parallel on a standard curve comprised of pooled splice variant plasmid DNA constructs, along with a PCR fragment spanning the beta actin amplicon, serially diluted 8 times tenfold. This final control serves as validation that the efficiencies of amplification of the various primer pairs are equivalent, a necessary condition to using them to make quantitative statements.

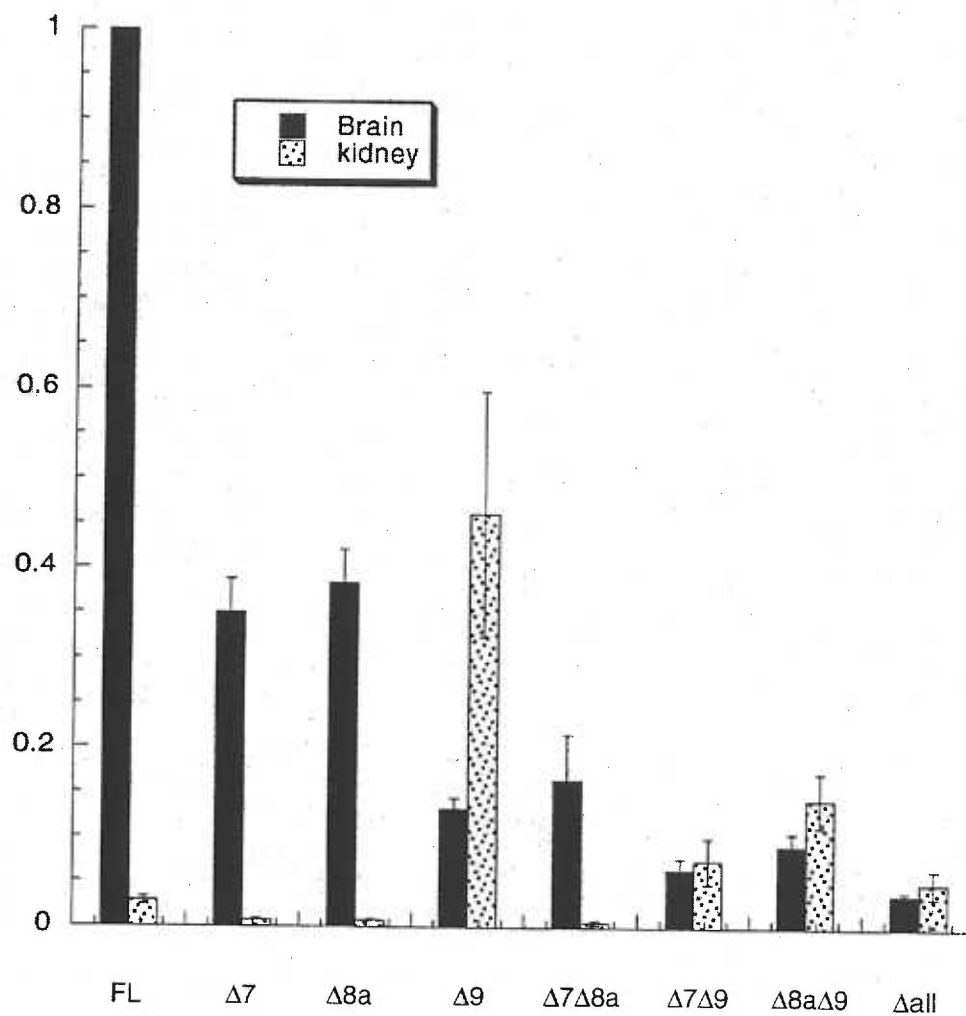


Figure 3.

Real time PCR of SK1 splice variants from whole brain and kidney. All results are relative to levels of the full length (FL) transcript in brain. Beta actin was the internal reference. Full length transcripts are almost undetectable in kidney where $\Delta 9$ is the predominant form. (n=4)

Finally, single-stranded cDNAs, transcribed from total RNA isolated from various central and peripheral tissues from prenatal, 4 week old and six month old mice, were amplified in triplicate and in parallel to the standard curve with primers for each splice variant. Initial experiments revealed that expression levels of most forms were very low in all tissues assayed, being at the lower limit of SYBR Green methodology for quantitation and thus giving variable and unreliable results. Exceptions to this were levels of full length, $\Delta 8a$, $\Delta 7$ and $\Delta 7\Delta 8a$ in the brain and $\Delta 9$ found in several peripheral tissues. Therefore in a second approach, SK1 splice variant mRNA levels were quantified relative to expression of beta actin transcripts from whole brain and kidney, and then normalized to the level of full length SK1 transcripts in the brain (Figure 3). In the brain, $\Delta 7$ and $\Delta 8a$ transcripts were found at ~35% of the levels of the full length transcript; $\Delta 7\Delta 8a$ was found at ~10% and all others tested were <10%. In the kidney, full length transcripts were less than 5% of the level of full length transcripts from the brain. Transcripts for $\Delta 9$ splice form were the most abundant form seen in the kidney, at ~45% of the levels of full length in the brain.

***In vitro* expression of SK1 proteins.**

To test whether the predicted proteins encoded by the various SK1 alternatively spliced mRNAs can be translated, expression constructs were engineered to insert an HA tag into the loop between TMs 1 and 2, at the position analogous to the HA tag in the SK1flox allele. Crude membranes prepared from

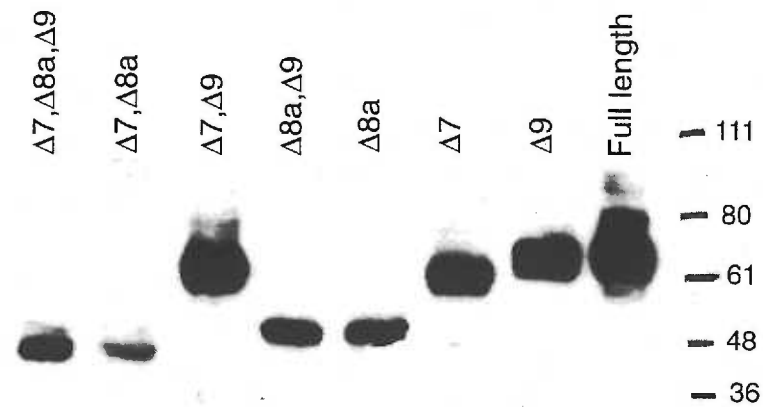


Figure 4.

Western blot of membranes from COS cells transfected with the HA-tagged SK1 splice variants probed with the α -HA antibody. 10 μ g of protein was loaded onto each lane. Molecular weight markers (K_D) are shown on the right.

COS cells two days after transfection were prepared as a western blot and probed with the anti-HA antibody. All forms of SK1 were translated into stable HA labeled proteins of the expected molecular weight (Figure 4).

Monoclonal antibodies

Peptides, twenty-five residues in length and chosen from sequences within the C-terminus to distinguish between full length SK1 (PGHLATATHSPQSHWLPTMGSDCG) and the truncated $\Delta 8a$ splice variant (HTRLVKKPDQGRVRKHQRLRSSEV) were synthesized, conjugated to KLH (Global Peptides, Fort Collins, CO) and injected into mice and rats (Monoclonal Antibody Core Facility, OHSU). Sera from injected animals was assayed by western analysis of membranes isolated from COS cells transfected with either HA-tagged full length SK1 or HA-tagged $\Delta 8a$. HA immuno-reactivity served as positive control for specificity. Sera were also tested in an immunofluorescence (IFC) assay of transfected COS cells immobilized on cover slips, with full length and $\Delta 8a$ transfected cells serving as negative controls for each other. Spleens from animals having positively reactive sera were fused to hybridoma cell lines (MACF), and supernatants from cell clones were retested. Using the western and IFC analysis to track positive reactivity, cells were cloned out and antibodies purified from supernatants. In this manner, one cell line from a rat fusion yielded monoclonal antibodies against full length SK1 (12B1), and two mouse fusion cell lines (6H7 and 7G9) are being processed for purified antibody against the $\Delta 8a$

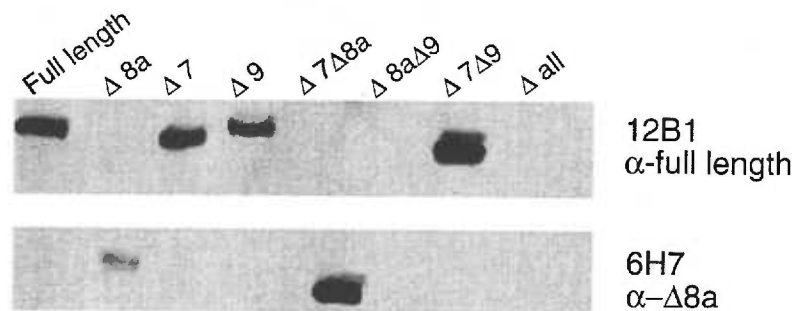


Figure 5.

Membranes from COS cells transfected with HA-tagged SK1 splice variants were probed with anti-peptide monoclonal antibodies directed against full length (12B1) or Δ8a (6H7). 12B1 recognizes all splice forms with an intact C-terminus, 6H7 recognizes splice variants Δ8a and Δ7Δ8a. Neither of the antibodies recognizes Δ8aΔ9 or Δall.

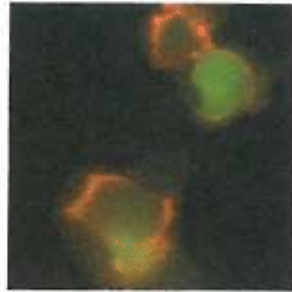
splice form. When tested on membranes from COS cells transfected with all SK1 splice forms, the 12B1 antibody detected full length, $\Delta 7$, $\Delta 9$, and $\Delta 7\Delta 9$ proteins. The 6H7 antibody detected only the $\Delta 8a$ and $\Delta 7\Delta 8a$ proteins (Figure 5). To date, purified 12B1 antibody applied to western blots of fractionated mouse brain membranes has not detected an appropriate molecular weight protein. In contrast, 6H7, one of the $\Delta 8a$ supernatants, detected a protein of expected molecular weight in wild type membranes that is not present in SK1 Δ/Δ brain membranes. This result lends optimism that antibodies with specificity for full length and truncated SK1 proteins may be in hand. Further work will determine if these monoclonal antibodies can be used in biochemical approaches, such as western analysis, immunohistochemistry and immunoprecipitation, to study SK1 protein distribution and function.

Surface Expression

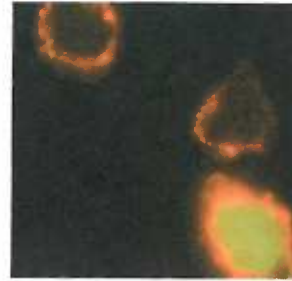
A triple myc epitope tag was engineered into the loop between TMs 3 and 4, analogous to the extracellular epitope in rSK2, in all eight mSK1 splice variants. COS cells transfected with the myc-tagged cDNAs were tested for surface expression by live cell staining. None of the mSK1 proteins, when expressed alone, were transported to the plasma membrane. In contrast, when myc-tagged full length mSK1 was co-expressed with rSK2, the myc tag was detected on the surface. Co-expression of mSK1 $\Delta 9$ with rSK2 also resulted in transport of the myc-tagged mSK1 subunits to the surface where the epitope

Figure 6. Surface expression of SK subunits.

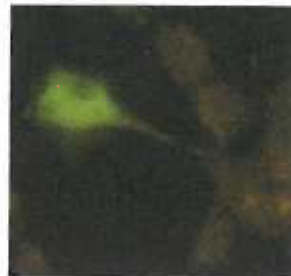
COS cells, transfected with the indicated constructs, were stained with the α -myc antibody either before (live) or after fixation and permeabilization. SK2 and SK3 extracellular myc tags were detected in non-permeabilized cells. None of the mSK1 myc-tagged constructs were detected on the surface in live cell staining, although the protein was detected in abundance in permeabilized cells (representative shown; SK1 FL myc). Co-transfection with either SK2 (not shown) or SK3 resulted in transport of mSK1 full length myc and mSK1 Δ 9 myc (not shown) to the surface where the myc tag was detected in live cell staining. None of the other mSK1 splice variants were detected at the surface in co-transfections with either SK2 or SK3. Furthermore, co-transfection of five fold excess of the Δ 7 or Δ 8a mSK1 splice variants with either SK2 myc or SK3 myc did not disrupt the appearance of SK2 or SK3 at the surface, indicating that these forms likely do not heteropolymerize with SK2 or SK3 (not shown).



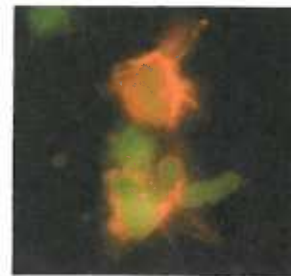
SK2 myc
live



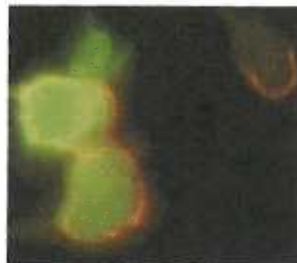
SK3 myc
live



SK1 FL myc
live



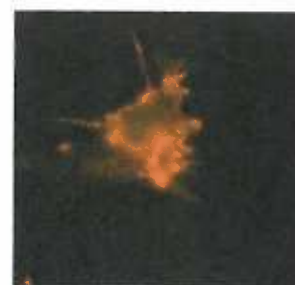
SK1 FL myc
permeabilized



SK3 +
SK1 FL myc
live



SK3 +
SK1 Δ 8a myc
live



SK3 +
SK1 Δ 8a myc
permeabilized

could be detected in live cell staining. However, none of the other mSK1 splice variants could be detected on the plasma membrane when co-expressed with rSK2. Furthermore, these splice variants did not apparently reduce the surface expression of the myc-tagged rSK2 subunits. Similar results were seen in experiments on cells co-transfected with mSK1 with rSK3. The myc tag on mSK1 full length and $\Delta 9$ splice variants was detected in live cell staining on the surface of the cells co-transfected with rSK3, but not when transfected alone. None of the other six mSK1 splice forms could be detected in live cell staining when co-transfected with rSK3 (Figure 6). The myc-tagged SK3 subunit could be detected on the surface in all co-transfections. These results indicate that mSK1 full length and $\Delta 9$ splice forms can heteropolymerize with either SK2 or SK3 subunits in order to be transported to the cell surface. Whether these heteromultimeric channels are functional is yet to be determined.

4. Discussion

SK1 is unique in the *SK* gene family in exhibiting complex and widely expressed alternatively spliced mRNAs. While the functions of these various splice forms are not currently known, the conservation of each of the splice variants in mouse, rat and human transcriptomes suggests that each form serves an important function. The relative levels of expression in human tissues of four splice forms (full length, $\Delta 8a$, $\Delta 8a\Delta 9$, and $\Delta 9$) parallel the realtime PCR results described here for mouse: full length and $\Delta 8a$ transcripts were most abundant in

the brain, with $\Delta 8a\Delta 9$ at low levels and $\Delta 9$ not found; $\Delta 8a\Delta 9$ and $\Delta 9$ transcripts were most abundant in erythropoietic tissue [158]. *In vitro* experiments demonstrated that the eight different mSK1 proteins are translated and are stable in heterologous systems. Whether native proteins of each of these forms exist is still to be discovered. Rat brain synaptosomal membranes prepared as a western and probed with an amino-terminal epitope revealed three bands of sizes approximating the molecular weights of proteins predicted by full length, $\Delta 7$ and $\Delta 8a$ SK1 transcripts, suggesting that all three forms are indeed present in rat brain. A C-terminal epitope SK1 antibody detected only two bands in the synaptosomal membranes, bands that closely parallel the predicted molecular weights of full length and $\Delta 7$ forms. This is consistent, as the truncated C-terminus of $\Delta 8a$ does not contain the C-terminal epitope [145].

Recent reports describe functional co-expression of rSK1 (full length) and rSK2 subunits in heterologous systems. Co-transfection of 2 μg rSK1 cDNA with 1 μg rSK2 cDNA resulted in a 77% increase in current amplitude over that seen with 1 μg rSK2 transfected alone [81]. This result is not inconsistent with our results showing that mSK1 and rSK2 can heteropolymerize and that co-expression of rSK2 with full length mSK1 and $\Delta 9$ mSK1 mediates translocation of the mSK1 subunit to the plasma membrane. However, nothing is currently known about the subunit stoichiometry of these heteromultimers. In the brain, mSK1 transcripts are present at $\sim 20\%$ of the level of mSK2 transcripts (Chapter III). Of those mSK1 transcripts, less than two thirds are likely to be the full length splice

form. It is not known how many mSK1 subunits will be tolerated in a functional hetero-tetrameric assembly with SK2. Our results indicate that full length mSK1 and $\Delta 9$ mSK1 can also heteromultimerize with rSK3. Also here, nothing is known about the stoichiometry of the hetero-tetrameric channels, or whether they produce functional channels. Levels of mSK3 in the brain are approximately equivalent to the levels of mSK1 (total of all splice forms) but *in situ* hybridizations have shown that there is very little overlap in the sites of expression of mSK1 and mSK3 [82]. Thus the participation and contribution of SK1 to SK channel function in the brain may be very subtle, a hypothesis supported by the lack of overt phenotype in the *SK1* KO mice.

What role might be played by the $\Delta 8a$ mSK1 is even more enigmatic. Transcripts for $\Delta 8a$ are found at ~40% of levels for full length mSK1 in the brain. Co-expression with SK2 or SK3 did not result in translocation of the $\Delta 8a$ subunits to the cell surface in heterologous systems. Is it possible that this (and/or the other, rarer splice forms) function on intracellular membranes? The $\Delta 8a$ splice form has a truncated C-terminus due to a frame shift introduced by the splicing out of 25 nucleotides of exon 8. The truncated sequence lacks eleven amino acids of the CaM-BD. *In vitro* tests of calmodulin binding to hSK1 splice variant C-termini found that the $\Delta 8a\Delta 9$ form did not bind calmodulin [158]. Thus if this subunit can participate in formation of tetrameric channels, even intracellularly, the gating mechanism may be very different from our understanding of classic SK channels.

A role for an apamin sensitive, calcium-activated potassium channel has been postulated in oscillatory release of calcium from intracellular vesicles. IP₃-induced release of calcium from mucin granules or endoplasmic reticulum of airway goblet cells was visualized by confocal imaging of cells or isolated vesicles loaded with fluorescent calcium probes. IP₃ induced oscillatory waves in calcium concentrations within the intracellular organelle were followed, out of phase, by oscillations in the cytoplasm adjacent to the organelle. A mechanism was proposed whereby Ca²⁺ released in response to IP₃ binding the IP₃ receptor activates a apamin-sensitive calcium-dependent potassium channel, K⁺ flows into the organelle, ionically balancing the matrix that binds calcium, allowing calcium to be freed and subsequently to flow out of the organelle to the cytoplasm via the IP₃ receptor. The oscillatory behavior was blocked by apamin [31]. Could the intracellular retention of SK1 splice variants be a part of the mechanism for localization of an SK channel on intracellular membranes and vesicles? This is among the questions we hope to be able to address with the various and combined SK transgenic mice.

The Δ9 SK1 is the predominant splice form expressed in kidney. Further experiments are necessary to quantify relative expression levels in other peripheral tissues. Co-expression of SK2 and SK3 with Δ9 SK1 resulted in translocation of Δ9 SK1 to the cell surface, indicating that it may participate in functional heteromeric channels. What is the function of the three amino acids AQK encoded by exon nine; that it is essential in the brain, but excluded in the

periphery? The presence or absence of the AQK does not result in any known canonical motif such as a kinase site or signal for other post-translational modification. Channel activity recorded from HEK293 cells expressing full length hSK1 or $\Delta 9$ hSK1 did not reveal any differences in calcium sensitivity or kinetics of activation (unpublished results). This three amino acid exon is one more enigma of the SK1 locus.

The $\Delta 7$ splice form of SK1 is lacking the C-terminal half of TM 6. TM six in potassium channels participates in forming the ion pore and the gating structure [159]. It is not possible to predict what the consequences for the topology of a $\Delta 7$ subunit might be, or how it might participate in a heteromeric assembly. The transcript levels for $\Delta 7$, $\Delta 7\Delta 9$, and $\Delta 7\Delta 8a$ splice forms are very low in the brain and peripheral organs. However, the conservation of all these forms across species from mouse to human implies they likely have functional significance. Future experiments, perhaps creating mice that express only one of the possible forms, are necessary to further understanding.

The initial SK1 enigma, that hSK1 subunits can form functional channels in heterologous expression while the mouse and rat do not, still abides. Why have the amino acid sequences of this gene product drifted significantly more than the other SK genes, while the alternate splicing has been preserved? What is the function of SK1 in human, is it the same function served in mouse and rat? Do SK1 variants participate in intracellular SK channels? Are SK1 subunits only

auxillary to channels formed of SK2 or SK3 subunits, and as such, dispensable?

5. Summary and hypotheses for SK1 function

With each detail learned about the *SK1* locus; gene expression, splicing, distribution, and functional characterization, the enigma of SK1 as a member of the SK family remains. At this time the list of questions is longer than the accumulation of understanding. Simple modulatory/accessory roles for full length and $\Delta 9$ splice forms can be proposed, based on observations that these subunits have the capacity to heteropolymerize with SK2 or SK3. Overlap of sites of expression suggest that SK2 is the more likely partner. Perhaps inclusion of one or more SK1 subunit in a hetero-tetramer confers a specific subcellular, or macromolecular complex localization. Or, inclusion of SK1 subunits may alter modulation of channel function by kinases, nucleosides, or other cytoplasmic factors. However, there is as yet no demonstration of *in vivo* evidence to verify the proposal. Intracellular functions for other SK1 splice forms may be postulated, but to date no specific results corroborate these speculations. Our future understanding of SK1, as well as that of SK2 and SK3, will greatly benefit from the study of the mice in which *SK* genes can be regulated.

CHAPTER V: Discussion

1. *SK genetic loci*

Based on nucleotide and amino acid homologies, small-conductance and intermediate-conductance calcium-activated potassium channels comprise a distinct subfamily within the potassium channel superfamily [76]. Although SK and IK proteins share with voltage-dependent potassium channels the classic serpentine topology of six membrane-spanning domains and re-entrant ion selective pore loop, with N- and C-termini intracellular, very little amino acid homology can be found other than in the ion selectivity sequence lining the pore and the hydrophobic nature of TM domains. Nor is there significant homology between SK or IK proteins and inward rectifier potassium channels, despite functional similarities of voltage independence, small conductance, inward rectification and modulation by intracellular ligands.

Evolutionarily, SK channel genes show both conservation and drift. The nematode genome contains four *SK* genes (L. Salkoff, personal communication), although neither functional studies nor mutant analysis have confirmed function or roles for these sequence-identified loci. Calcium-dependent, small-conductance potassium currents were observed in body wall muscle cells after rundown of other potassium conductances, but this current was not tested pharmacologically or genetically to verify its relationship with *SK* genes [160]. Putative translation products from *C. elegans SK* genes do not share distinct

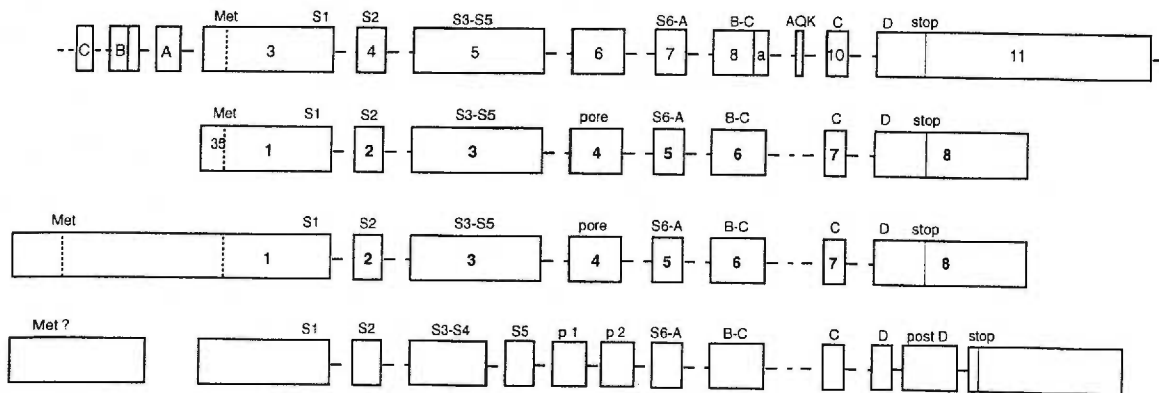


Figure 1.

Schematics of the intron-exon mosaics of *SK* loci showing the conservation of exon boundaries across isotype and species. Order of loci, from top to bottom is mammalian *SK1*, *SK2*, and *SK3* and *Drosophila SK*. Boxes indicate exons, protein domains encoded by each exon are indicated above the box.

homology with any one of the three mammalian SK proteins, and in fact have very much less homology between them than the mammalian family (unpublished observation). *Drosophila melanogaster* has one *SK* gene (unpublished observation) that encodes more than one protein through the use of alternative exons, including an alternative pore exon. However, once again functional characterization has not been reported. The *Drosophila* SK protein, like the nematode, does not closely match any one of the mammalian SKs. In contrast, genome database and EST (expressed sequence tag) database searches locate proteins highly homologous to SK2, but not SK3 or SK1, from zebrafish, trout and chicken.

Intron/exon mosaics of *SK* loci are highly conserved across species [148, 161, 162] (Figure 1). *Drosophila* and mammalian genes share precise exon boundaries over most of the coding sequence, with some exons further divided into multiple exons in *Drosophila* (unpublished observation). Even the boundaries of exons that participate in alternative splicing in the *SK1* locus are conserved, with the exception of the non-canonical splice in exon 8 and the nine nucleotide exon 9 [148, 162].

2. Conditional transgenes

Strategies and tools

Although there are an ever-growing number of strategies for generating animals having conditional expression of specific genes, all these strategies fall

into one of two basic categories; insertion of regulatory sequences that allow induction or repression of expression by administration of exogenous agents, or insertion of recognition sequences that direct recombination of genomic DNA when exposed to specific recombinases. Additional sophistication in gene control is achieved by combinatorial use of these two basic strategies. In one example, expression of the Cre recombinase was driven in a particular cell type by a specific promoter. The recombinase was expressed as a fusion protein with the mutant prolactin receptor (PLR). Upon administration of the ligand RU-486, the mutant receptor was transduced into the nucleus, carrying with it the recombinase, and thereby initiating recombinase-mediated excision of the floxed sequences. Thus in this example, gene knockout occurred in only the cells in which the promoter driving the CRE-PLR fusion protein was active, but then only after administration of the RU-486 ligand. In this manner, both site and timing of gene knockout was achieved [163].

The number and variations of regulatory elements that respond to exogenous ligands that are being used as tools in transgenesis continue to grow. The list includes, at least, tetracycline sensitive transcription, ecdysone (insect hormone) inducible transcription, tamoxifen inducible transcription, and RU-486 mediated translocation to the nucleus. In addition, an ever growing stable of tissue- and developmental time point-specific promoters are being characterized and employed in multi-layered transgenic strategies [122].

This expanding sophistication of tools impacts strategies for the use of recombinases. Greater specificity is being added to control of site and timing of recombinase expression. Recombinase function can also be modulated by modification of the recognition sites. Studies of the specificity of the recognition sites for both Cre and FLP recombinases have led to subtle control over the order and completeness of recombination within an allele based on the use of mutant loxP or frt sites [164] [113]. Combinatorial use of two recombinases and appropriately placed recognition sequences allows sequential or segregated excision events, directed by the controlled exposure of the floxed/frted allele to recombinase activity. At the very minimum, a dual recombinase strategy might be employed to remove selectable markers from the targeted allele while still leaving in place recognition sites for subsequent gene ablation.

The last few years have seen an explosion in conditional transgene strategies, as new tools are developed and combinations of tools are employed. We set out to derive mice expressing conditional alleles at the three *SK* loci at the very beginning of this revolution. Hence the strategies we employed, while sophisticated at the time, are simple in design compared to some of the multiple-layer strategies described above.

Tetracycline regulation of transcription

The tetracycline-sensitive transcription transactivator protein, tTA, described in Chapter II, has been employed in many forms in transgenic mice

[165, 166]. In most examples, expression of either the tTA protein alone or tTA and the $\text{tet}_0\text{CMV}_{\text{min}}$ promoter responsive gene were derived as classical transgenes, rather than through homologous recombination. The *SK3 tTA* mouse was the first (and still only published) example of a single step insertion of the tTA coding sequence and the responsive promoter into a gene by homologous recombination [114]. The goal of this strategy was to obtain a mouse model in which expression of the *SK3* gene paralleled that in wild type animals until intervention through dietary administration of doxycycline, allowing for acute knockout of gene expression that could be recovered by removal of the drug. Thus each animal would serve as its own control in behavioral or physiological assays.

In the *SK3 tTA* mice, some but not all of these goals were achieved. Tissue-specificity and timing of expression of SK3 transcripts and protein were preserved in the absence of drug. However, the tTA protein provides such strong transactivation at the $\text{tet}_0\text{CMV}_{\text{min}}$ promoter that, in all sites examined, SK3 was over-expressed 3-5 fold. This over-expression was exacerbated when the silencing effect of the neo gene was removed from the allele. It was not possible to titrate expression of SK3 in specific tissues by varying the dosage of tetracycline analogs because of the differential penetration of the drug into the brain and peripheral sites. However, since many transgenic models are based on over-expression of genes of interest, this characteristic of the tet cassette strategy might be considered a bonus, with the added benefit of over-expression

occurring at only normal sites, avoiding complications of exogenous sites of expression seen in classical transgenes.

The second goal of the strategy, the ability to regulate expression simply through the diet, was elegantly achieved. SK3 transcripts were not detectable in the brain after only three days of administration of 100 µg/ml dox in the drinking water. However, much longer drug exposure was necessary before the SK3 protein could not be detected. While knockout of SK3 completely was accomplished through the diet, recovery of expression depended on clearance of the drug from the system after removal from the diet. Due to retention of the drug in fatty tissues, the time to recover expression from the targeted gene took approximately twice as long as the period of drug administration necessary to achieve knockout. Thus the goal of having each animal serve as its own control was compromised or complicated by the time frame within which experiments could be performed.

Finally, the tet cassette strategy relies on placement of the cassette into the 5' UTR of the gene of interest. As seen with the *SK2 tTA* mouse and other, unpublished mice using this strategy, disruption of endogenous regulatory domains within the UTR may result in a targeted allele that cannot be regulated, or is null for expression even in the absence of drug. Thus success can only be guaranteed when a great deal of knowledge about the targeted locus is already in hand.

Floxed alleles

The second conditional strategy that we employed offers different benefits than the tet cassette approach. Because the recombination event is irreversible, knockout animals cannot serve as their own controls. However, the site and timing of gene knockout can be either organism-wide or limited in extent. In design, the strategy can be ultimately simple; insert loxP sites into an allele, and then provide sophistication of timing and sites of gene ablation by choice of Cre expressing mice to which to breed the floxed mouse. Three loxP sites were inserted into the *SK1* and *SK2* alleles, two flanking the neo-resistance gene, and the third flanking SK coding exons. Thus, in these mice, mosaic, or limited Cre expression is necessary to remove the neo gene without disrupting the *SK* allele. This requires multiple generations of mice crossed to mosaic Cre-expressing animals [123] to produce the desired line containing only two loxP sites flanking the gene of interest that will have expression profiles comparable to wild type prior to total or tissue-specific gene ablation. The tri-lox approach will in future be improved by the combined use of two recombinases or by insertion of mutant recognition sites to eliminate the need for limited and mosaic Cre-mediated recombination to separate excision of selectable marker genes from excision of targeted exons.

The coding sequence for GFP was inserted into the *SK1* and *SK2* alleles in conjunction with the loxP sites, such that, following complete Cre-mediated recombination, the GFP protein would be expressed under control of the SK

promoter, thus serving as a marker for those cells in which the *SK* gene had been ablated. This goal was not achieved in either *SK1* or *SK2* floxed mice. In animals where complete recombination in the germline yielded SK null animals, no GFP could be detected in cells where the SK promoter was known to be active. While GFP expression may be sufficient to be detected by immunodetection with α -GFP antibodies (experiments still in progress), no fluorescence could be detected in freshly prepared brain slices, such as would be used in electrophysiological assays of cellular function in the absence of SK expression. Therefore, characterization of the pattern of gene ablation in response to different profiles of Cre expression will rely on the use of Cre-sensitive reporter expression [167]. The reason for the lack of detectable GFP expression is unknown. GFP is a reporter that is being widely employed in transgenic mice. The protein has been genetically modified to give high levels of emitted fluorescence to improve detection [168] and high levels of expression [169] [170]. GFP protein is apparently stable; protein degradation has not been a problem in transgenic mice. It may be that the SK promoters are very weak, driving only low levels of transcription; an hypothesis that is consistent with the low-density of SK channels seen in wild type animals.

A second problem with the insertion of the GFP sequence was encountered in the *SK1* floxed mouse. The presence of neo and GFP coding sequences together in an intron resulted in disruption of appropriate splicing of *SK1* transcripts. Thus the *SK1 f/f* animals are essentially SK1 nulls. Once

mosaic Cre activity has removed the neo coding sequence, *SK1 flox_{Δneo}* mice will be reassessed to determine if the presence of the GFP coding sequence alone in the intron also results in disruption of splicing. This mouse line illustrates the hazards of insertion of foreign sequences of substantial extent into introns of limited size, particularly at loci that undergo complex regulation and splicing.

In summary, different conditional strategies offer different benefits and problems. The one step tet cassette insertion has the advantages of simple construction, fidelity of site and timing of expression, and reversibility of gene ablation. Overexpression of the targeted gene may be viewed as an advantage or disadvantage. However, complications may arise due to disruption of unknown endogenous regulatory domains, yielding alleles that are not regulated or are null even in the absence of drug. Future generations of the tTA protein and the tet cassette are being developed by several laboratories in efforts to maximize the benefits and minimize problems in this simple but elegant approach to conditional gene regulation. Combinations of regulatory elements are being developed that will allow titration of gene expression [171].

Insertion of recombinase recognition sites flanking coding exons remains the simplest, yet most flexible, method of achieving tissue- and/or timing-specific gene ablation. Sophistication in the specificities of knockout is provided by control of expression of the recombinase. Future developments in the use of mutant recognition sites and enzymes may even yield recombinase-mediated gene knockouts that are reversible by relying on inversions of intervening

sequences rather than excision. Our imagination is the only limit to what we will ultimately be able to accomplish in targeted gene regulation in animal models, and perhaps even in humans for treatment of genetic diseases.

3. *SK Physiology and SK transgenic mice.*

SK3 in the brain

Studies employing the *SK3 tTA* mice, which over express SK3 mRNA and protein 3-5 fold over wild type animals in the absence of administration of doxycycline, or which can be acutely knocked out for SK3 by doxycycline in the diet, have lent understanding of SK3 function in several different physiologies. Overexpression of SK3 results in a compromised ability to respond to hypoxia. Under normal conditions, the respiratory timing in the SK3 overexpressing mice was not different than wild type. In the presence of 8% oxygen (hypoxia), wild type animals exhibit sustained tachycardia, with breathing rates ~150% of normal. In contrast, mice overexpressing SK3 showed a brief (30 sec) tachycardia to ~122%, followed by a decline in frequency to 68% of baseline. In some cases, apneic episodes (no respiration) necessitated termination of the hypoxia [114]. Respiration frequencies and response to hypoxia were not tested in the *SK3 tTA* mice after long term dox administration (knock out condition). However, studies of respiratory neurons in brainstem slice preparations showed that application of apamin only minimally affected respiration, weakening rather than abolishing the normal rhythm. In contrast, blockade of glycinergic inhibition

and BK together completely eliminated respiratory discharges [172]. SK3 is also expressed in muscle cells of the diaphragm (unpublished observation). The possible contribution of overexpression of SK3 at peripheral sites was not addressed in assessing their response to hypoxia. However, the *SK3 tTA* mouse offers a model within which to study the role of SK3 channels in generation and maintenance of respiratory rhythm, and responses within the rhythm-generating nuclei to changes in synaptic input from sensory systems.

Systemic apamin injection facilitates hippocampal-dependent learning [24]. Behavioral studies of *SK3 tTA* mice following longterm administration of dox, (knockout condition), did not recapitulate the apamin effect, indicating that SK3 subunits do not mediate control over synaptic plasticity. SK3 channels have been reported to be in presynaptic terminals of the hippocampus [149]. However, no presynaptic effect on synaptic plasticity, as assayed by paired pulse facilitation, was found in response to apamin application to hippocampal brain slice preparations [24].

SK3 in the periphery

Studies of the *SK3 tTA* mouse have yielded greater understanding of SK channel function in many peripheral physiologies. SK3 expression in endothelial cells of the vasculature contributes to maintenance of vascular smooth muscle tone and blood pressure [12]. Control of vascular tone and hence blood pressure has long been ascribed to hypothetical factor(s) termed EDHF for endothelial-cell

derived hyperpolarizing factor. Both nitric oxide (NO) and prostacyclin (PGI₂) from endothelium have been shown to affect vascular smooth muscle function. However, an additional non-NO, non-PGI₂ EDHF function has also been characterized, but the identity of the factor has been elusive [173]. Studies of the SK3 tTA mice have revealed that SK3-mediated hyperpolarization of the endothelium results in hyperpolarization of the smooth muscle, possibly through gap junctions between endothelial and muscle cells. Thus SK channel activation may be that elusive EDHF. The observation that the SK3 gene is regulated by estrogen [120, 174] leads to the hypothesis that SK3 expression may underlie the cardiovascular effects of estrogen. No additional effect of apamin was detected in mice where SK3 expression was eliminated by dox, indicating neither SK1 nor SK2 directly effect vascular tone.

SK3 overexpression resulted in enlargement of hollow organs, such as mesenteric and coronary arteries and bladder [11, 12]. Although the mechanism underlying these structural modifications is unknown, a role for SK3 in vascular development may provide another mechanism by which SK3 contributes to control of cardiovascular function.

The significance of the role of SK3 in cardiovascular function is enhanced by the observations of altered SK3 expression in some pathological states. For example, following balloon catheter injury of the carotid artery, endothelium-dependent vasodilation is blunted. This effect has recently been linked to decreased SK3 expression in the regenerated endothelial cells [175]. Further,

elevated endothelial SK3 expression in rats with cirrhosis was associated with attenuated vasoconstrictor responses [176]. These results all support the idea that manipulation of SK3 channel expression and/or activity may provide novel therapeutic approaches for the treatment of vascular disorders, including hypertension.

Study of bladder function in the *SK3 tTA* mice revealed a role for SK3 in control of bladder contraction and also revealed high affinity apamin binding in the absence of SK3 expression, indicating a role for another SK subunit, likely SK2. [11] Overexpression of SK3 resulted in excess urine production, however the mechanism of this effect was not determined. Suppression of SK3 expression resulted in a marked increase in non-voiding contractions, a condition that characterizes many types of urinary bladder dysfunctions, including incontinence. Thus, since SK3 is not expressed in the smooth muscle cells of the vasculature, targeting of agents to smooth muscle that activate SK channels may allow therapeutic intervention in bladder function without deleterious side effects on blood pressure and cardiovascular function [11].

SK knockouts and regulation of excitability

SK channel activity has been implicated in the regulation of excitability in many brain regions and systems. Activation of SK channels through direct coupling to various sources of calcium influx, such as voltage-dependent calcium

channels or ionotropic neurotransmitter receptors, specifies which stimuli will be most affected by SK channel mediated inhibition.

In the pyramidal cell of the CA1 region of the hippocampus, calcium-dependent potassium currents mediate afterhyperpolarizations (AHP) that modulate the level of postsynaptic response. The AHP in these neurons has three kinetically and pharmacologically distinguishable components. As described in Chapter III, SK2 subunits are essential for formation of channels underlying the apamin-sensitive medium AHP. Experiments performed on the three known *SK* gene knockout mice clearly demonstrate that none of these subunits are essential for the slow AHP, leading to the conclusion that SK channels are not involved in the sAHP current. However, as this manuscript is being written, a new *SK* gene has been discovered in the mouse genome database. This new gene is not represented in the sequences compiled in EST databases, so nothing is known yet about sites of expression or channel function. The computationally predicted translation product has an extended amino-terminal domain of over 600 amino acids (for comparison, the long amino terminus of SK3 is only 265 amino acids). The pore domain encoded by this new gene has the three amino acids found in SK1 that mediate the reduced affinity of apamin for the SK1 channel [144]. Future experiments will determine if and where the gene is in fact expressed, whether the predicted protein is indeed the gene product, and what are the functional characteristics and pharmacological

profile. Only after these preliminary data are obtained can any hypothesis about the role of this new sequence be formulated.

Systemic apamin injection speeds the acquisition of hippocampal dependent memory [24], and also shifts the synaptic plasticity threshold to the left, resulting in long term potentiation at lower stimulus frequencies.

Acetylcholine and noradrenaline, through elevation of cAMP and activation of protein kinase A, inhibit the slow AHP [135], also enhancing learning [177].

Future experiments with *SK2* null mice, or *SK2* CA1 null mice may shed new light on possible mixed influences of medium AHP, mediated by *SK2* channels and perhaps modulated by cholinergic tone as in other regions of the brain, and the slow AHP in acquisition and retention of hippocampal dependent memory.

Future experiments on mice null for *SK2* in only CA1, or only in hippocampus, compared to animals null for *SK2* throughout all the brain (*SK2* Δ/Δ) may be useful in understanding separately the mechanisms for memory acquisition, consolidation and retention.

Of the three *SK* knockout mice, only *SK2* Δ/Δ animals display an overt behavioral phenotype, exhibiting a developmentally limited ataxia and a whole body tremor. In fact, the *SK2* Δ/Δ phenotype correlates remarkably with the description of the effect of injection of mild doses of apamin, mild hyperactivity, resting tremor and ataxia. This limited phenotypic expression is consistent with the observation that *SK2* is the predominant, if not only, *SK* expressed in the principle neurons of the cortex, cerebellum and hippocampus. Cerebellar function

is important to motor coordination. Purkinje neurons supply the sole output from the cerebellum. Purkinje neurons exhibit complex spontaneous firing patterns consisting of at least three modes: rapid firing, burst firing, or silent, with transitions from mode to mode affected by application of apamin [128]. The significance of these firing modes to the output of the purkinje cells onto deep cerebellar nuclei is not known. SK2 is expressed in purkinje neurons in a developmentally regulated pattern [127]. SK2 is also expressed in the principle neurons of motor cortex [82]. Studies of animals null for SK2 in only the purkinje neurons of the cerebellum will provide understanding of the balance of cerebellar and cortical SK activity responsible for the ataxic phenotype of the *SK2 Δ/Δ* mice. Further studies of region-specific knockout of SK2 in the brain will shed light on the structures underlying the tremor seen in the *SK2 Δ/Δ* animals.

CHAPTER VI: Summary and Conclusions

Transgenic mice in which expression of each of the three known small-conductance calcium-activated potassium channel genes can be conditionally regulated were created by homologous recombination. Studies of these mice have demonstrated a role for SK3 in regulation of vascular tone and blood pressure, bladder control and respiration. Further studies have demonstrated that SK2 subunits are essential to formation of channels underlying the medium component of the AHP in hippocampal CA1 pyramidal neurons. It is likely that SK2 mediates afterhyperpolarization in other principle neurons of the brain, and likely underlies the apamin-mediated effects on synaptic plasticity. Studies of the SK null mice demonstrated that none of these three SK channels are necessary for the slowAHP. SK1 knockout mice did not exhibit an overt phenotype to give hints to understanding the role of SK1. However, more detailed examination of these mice may reveal functions served by the SK1 gene.

We have already learned a great deal about SK function throughout the organism by the study of SK transgenic mice. But this is just the beginning. Future studies on these mice, in conjunction with a wealth of region-specific Cre expressing mice currently available, will make it possible to understand the role of each SK in different brain and organ physiologies. Ultimately, the ability to modulate brain or organ function by manipulation of SK gene expression will

enhance our basic understanding of complex systems that underlie specific physiologies.

References

1. Bootman, M.D., M.J. Berridge, and H.L. Roderick, *Calcium signalling: more messengers, more channels, more complexity*. Curr Biol, 2002. **12**(16): p. R563-5.
2. Gardos, G., *The function of calcium in the potassium permeability of human erythrocytes*. Biochim Biophys Acta, 1958. **30**(3): p. 653-4.
3. Meech, R.W., *Intracellular calcium injection causes increased potassium conductance in Aplysia nerve cells*. Comp Biochem Physiol A, 1972. **42**(2): p. 493-9.
4. Hamill, O.P., A. Marty, E. Neher, B. Sakmann, and F.J. Sigworth, *Improved patch-clamp techniques for high-resolution current recording from cells and cell-free membrane patches*. Pflugers Arch, 1981. **391**(2): p. 85-100.
5. Latorre, R., A. Oberhauser, P. Labarca, and O. Alvarez, *Varieties of calcium-activated potassium channels*. Annu Rev Physiol, 1989. **51**: p. 385-99.
6. Mourre, C., H. Schmid-Antomarchi, M. Hugues, and M. Lazdunski, *Autoradiographic localization of apamin-sensitive Ca^{2+} -dependent K^{+} channels in rat brain*. Eur J Pharmacol, 1984. **100**(1): p. 135-6.
7. Wu, K., R. Carlin, L. Sachs, and P. Siekevitz, *Existence of a Ca^{2+} -dependent K^{+} channel in synaptic membrane and postsynaptic density*

- fractions isolated from canine cerebral cortex and cerebellum, as determined by apamin binding. Brain Res, 1985. 360(1-2): p. 183-94.*
8. Seagar, M.J., P. Deprez, N. Martin-Moutot, and F. Couraud, *Detection and photoaffinity labeling of the Ca²⁺-activated K⁺ channel-associated apamin receptor in cultured astrocytes from rat brain. Brain Res, 1987. 411(2): p. 226-30.*
 9. Burckhardt, B.C. and H. Gogelein, *Small and maxi K⁺ channels in the basolateral membrane of isolated crypts from rat distal colon: single-channel and slow whole-cell recordings. Pflugers Arch, 1992. 420(1): p. 54-60.*
 10. Herrera, G.M., T.J. Heppner, and M.T. Nelson, *Regulation of urinary bladder smooth muscle contractions by ryanodine receptors and BK and SK channels. Am J Physiol Regul Integr Comp Physiol, 2000. 279(1): p. R60-8.*
 11. Herrera, G.M., M.J. Pozo, P. Zvara, G.V. Petkov, C.T. Bond, J.P. Adelman, and M.T. Nelson, *Urinary bladder instability induced by selective suppression of the murine small conductance calcium-activated potassium (SK3) channel. J Physiol, 2003. 551(Pt 3): p. 893-903.*
 12. Taylor, M.S., A.D. Bonev, T.P. Gross, D.M. Eckman, J.E. Brayden, C.T. Bond, J.P. Adelman, and M.T. Nelson, *Altered expression of small-conductance Ca²⁺-activated K⁺ (SK3) channels modulates arterial tone and blood pressure. Circ Res, 2003. 93(2): p. 124-31.*

13. Burnham, M.P., R. Bychkov, M. Feletou, G.R. Richards, P.M. Vanhoutte, A.H. Weston, and G. Edwards, *Characterization of an apamin-sensitive small-conductance Ca^{2+} -activated K^{+} channel in porcine coronary artery endothelium: relevance to EDHF*. Br J Pharmacol, 2002. **135**(5): p. 1133-43.
14. Ohta, T., S. Ito, and Y. Nakazato, *Ca^{2+} -dependent K^{+} currents induced by muscarinic receptor activation in guinea pig adrenal chromaffin cells*. J Neurochem, 1998. **70**(3): p. 1280-8.
15. Tse, A. and A.K. Lee, *Arginine vasopressin triggers intracellular calcium release, a calcium-activated potassium current and exocytosis in identified rat corticotropes*. Endocrinology, 1998. **139**(5): p. 2246-52.
16. Tse, A. and B. Hille, *GnRH-induced Ca^{2+} oscillations and rhythmic hyperpolarizations of pituitary gonadotropes*. Science, 1992. **255**(5043): p. 462-4.
17. Capiod, T. and D.C. Ogden, *The properties of calcium-activated potassium ion channels in guinea-pig isolated hepatocytes*. J Physiol, 1989. **409**: p. 285-95.
18. Hugues, M., H. Schmid, G. Romey, D. Duval, C. Frelin, and M. Lazdunski, *The Ca^{2+} -dependent slow K^{+} conductance in cultured rat muscle cells: characterization with apamin*. Embo J, 1982. **1**(9): p. 1039-42.
19. Hallworth, N.E., C.J. Wilson, and M.D. Bevan, *Apamin-sensitive small conductance calcium-activated potassium channels, through their*

- selective coupling to voltage-gated calcium channels, are critical determinants of the precision, pace, and pattern of action potential generation in rat subthalamic nucleus neurons in vitro.* J Neurosci, 2003. **23**(20): p. 7525-42.
20. Szente, M.B., A. Baranyi, and C.D. Woody, *Intracellular injection of apamin reduces a slow potassium current mediating afterhyperpolarizations and IPSPs in neocortical neurons of cats.* Brain Res, 1988. **461**(1): p. 64-74.
 21. Stocker, M., M. Krause, and P. Pedarzani, *An apamin-sensitive Ca^{2+} -activated K^{+} current in hippocampal pyramidal neurons.* Proc Natl Acad Sci U S A, 1999. **96**(8): p. 4662-7.
 22. Messier, C., C. Murre, B. Bontempi, J. Sif, M. Lazdunski, and C. Destrade, *Effect of apamin, a toxin that inhibits Ca^{2+} -dependent K^{+} channels, on learning and memory processes.* Brain Res, 1991. **551**(1-2): p. 322-6.
 23. Deschaux, O., J.C. Bizot, and M. Goyffon, *Apamin improves learning in an object recognition task in rats.* Neurosci Lett, 1997. **222**(3): p. 159-62.
 24. Stackman, R.W., R.S. Hammond, E. Linardatos, A. Gerlach, J. Maylie, J.P. Adelman, and T. Tzounopoulos, *Small conductance Ca^{2+} -activated K^{+} channels modulate synaptic plasticity and memory encoding.* J Neurosci, 2002. **22**(23): p. 10163-71.

25. Fiorillo, C.D. and J.T. Williams, *Cholinergic inhibition of ventral midbrain dopamine neurons*. J Neurosci, 2000. **20**(20): p. 7855-60.
26. Yamada, S.I., H. Takechi, I. Kanchiku, T. Kita, and N. Kato, *Small conductance Ca^{2+} -dependent K^{+} channels are the target of spike-induced Ca^{2+} release in a feedback regulation of pyramidal cell excitability*. J Neurophysiol, 2003 91 :2322-2329
27. Glowatzki, E. and P.A. Fuchs, *Cholinergic synaptic inhibition of inner hair cells in the neonatal mammalian cochlea*. Science, 2000. **288**(5475): p. 2366-8.
28. Oliver, D., N. Klocker, J. Schuck, T. Baukrowitz, J.P. Ruppersberg, and B. Fakler, *Gating of Ca^{2+} -activated K^{+} channels controls fast inhibitory synaptic transmission at auditory outer hair cells*. Neuron, 2000. **26**(3): p. 595-601.
29. Frolenkov, G.I., F. Mammano, I.A. Belyantseva, D. Coling, and B. Kachar, *Two distinct Ca^{2+} -dependent signaling pathways regulate the motor output of cochlear outer hair cells*. J Neurosci, 2000. **20**(16): p. 5940-8.
30. Wolfart, J., H. Neuhoff, O. Franz, and J. Roeper, *Differential expression of the small-conductance, calcium-activated potassium channel SK3 is critical for pacemaker control in dopaminergic midbrain neurons*. J Neurosci, 2001. **21**(10): p. 3443-56.

31. Nguyen, T., W.C. Chin, and P. Verdugo, *Role of Ca^{2+}/K^{+} ion exchange in intracellular storage and release of Ca^{2+}* . *Nature*, 1998. **395**(6705): p. 908-12.
32. Vigh, J., E. Solessio, C.W. Morgans, and E.M. Lasater, *Ionic mechanisms mediating oscillatory membrane potentials in wide-field retinal amacrine cells*. *J Neurophysiol*, 2003. **90**(1): p. 431-43.
33. Benington, J.H. and H.C. Heller, *Does the function of REM sleep concern non-REM sleep or waking?* *Prog Neurobiol*, 1994. **44**(5): p. 433-49.
34. Steriade, M. and J. Hobson, *Neuronal activity during the sleep-waking cycle*. *Prog Neurobiol*, 1976. **6**(3-4): p. 155-376.
35. Benington, J.H., M.C. Woudenberg, and H.C. Heller, *Apamin, a selective SK potassium channel blocker, suppresses REM sleep without a compensatory rebound*. *Brain Res*, 1995. **692**(1-2): p. 86-92.
36. Renaud, J.F., C. Desnuelle, H. Schmid-Antomarchi, M. Hugues, G. Serratrice, and M. Lazdunski, *Expression of apamin receptor in muscles of patients with myotonic muscular dystrophy*. *Nature*, 1986. **319**(6055): p. 678-80.
37. Behrens, M.I., P. Jalil, A. Serani, F. Vergara, and O. Alvarez, *Possible role of apamin-sensitive K^{+} channels in myotonic dystrophy*. *Muscle Nerve*, 1994. **17**(11): p. 1264-70.
38. Pribnow, D., T. Johnson-Pais, C.T. Bond, J. Keen, R.A. Johnson, A. Janowsky, C. Silvia, M. Thayer, J. Maylie, and J.P. Adelman, *Skeletal*

- muscle and small-conductance calcium-activated potassium channels.*
Muscle Nerve, 1999. **22**(6): p. 742-50.
39. Park, Y.B., *Ion selectivity and gating of small conductance $\text{Ca}(2+)\text{-}$ activated K^+ channels in cultured rat adrenal chromaffin cells.* J Physiol, 1994. **481**(Pt 3): p. 555-70.
40. Lara, B., P. Zapater, C. Montiel, M.T. de la Fuente, R. Martinez-Sierra, J.J. Ballesta, L. Gandia, and A.G. Garcia, *Density of apamin-sensitive $\text{Ca}(2+)\text{-}$ dependent K^+ channels in bovine chromaffin cells: relevance to secretion.* Biochem Pharmacol, 1995. **49**(10): p. 1459-68.
41. Sah, P., *$\text{Ca}(2+)\text{-}$ activated K^+ currents in neurones: types, physiological roles and modulation.* Trends Neurosci, 1996. **19**(4): p. 150-4.
42. Marrion, N.V. and S.J. Tavalin, *Selective activation of Ca^{2+} -activated K^+ channels by co-localized Ca^{2+} channels in hippocampal neurons.* Nature, 1998. **395**(6705): p. 900-5.
43. Shah, M.M. and D.G. Haylett, *K^+ currents generated by NMDA receptor activation in rat hippocampal pyramidal neurons.* J Neurophysiol, 2002. **87**(6): p. 2983-9.
44. Yuhas, W.A. and P.A. Fuchs, *Apamin-sensitive, small-conductance, calcium-activated potassium channels mediate cholinergic inhibition of chick auditory hair cells.* J Comp Physiol [A], 1999. **185**(5): p. 455-62.

45. Fiorillo, C.D. and J.T. Williams, *Glutamate mediates an inhibitory postsynaptic potential in dopamine neurons*. *Nature*, 1998. **394**(6688): p. 78-82.
46. Novitski, E., *Drosophila Information Service*, 1949(23): p. 61.
47. Timpe, L.J.L., *Gene dosage and complementation analysis of the Shaker locus in Drosophila*. *J Neurosci*, 1987. **7**(5): p. 1307-1317.
48. Papazian, D.M., T.L. Schwarz, B.L. Tempel, Y.N. Jan, and L.Y. Jan, *Cloning of genomic and complementary DNA from Shaker, a putative potassium channel gene from Drosophila*. *Science*, 1987. **237**(4816): p. 749-53.
49. Tempel, B.L., Y.N. Jan, and L.Y. Jan, *Cloning of a probable potassium channel gene from mouse brain*. *Nature*, 1988. **332**(6167): p. 837-9.
50. Christie, M.J., J.P. Adelman, J. Douglass, and R.A. North, *Expression of a cloned rat brain potassium channel in Xenopus oocytes*. *Science*, 1989. **244**(4901): p. 221-4.
51. Stuhmer, W., J.P. Ruppersberg, K.H. Schroter, B. Sakmann, M. Stocker, K.P. Giese, A. Perschke, A. Baumann, and O. Pongs, *Molecular basis of functional diversity of voltage-gated potassium channels in mammalian brain*. *Embo J*, 1989. **8**(11): p. 3235-44.
52. Pfaffinger, P.J., Y. Furukawa, B. Zhao, D. Dugan, and E.R. Kandel, *Cloning and expression of an Aplysia K⁺ channel and comparison with native Aplysia K⁺ currents*. *J Neurosci*, 1991. **11**(4): p. 918-27.

53. Trimmer, J.S., *Immunological identification and characterization of a delayed rectifier K⁺ channel polypeptide in rat brain*. Proc Natl Acad Sci U S A, 1991. **88**(23): p. 10764-8.
54. Pak, M.D., K. Baker, M. Covarrubias, A. Butler, A. Ratcliffe, and L. Salkoff, *mShal, a subfamily of A-type K⁺ channel cloned from mammalian brain*. Proc Natl Acad Sci U S A, 1991. **88**(10): p. 4386-90.
55. Atkinson, N.S., G.A. Robertson, and B. Ganetzky, *A component of calcium-activated potassium channels encoded by the Drosophila slo locus*. Science, 1991. **253**(5019): p. 551-5.
56. Adelman, J.P., K.Z. Shen, M.P. Kavanaugh, R.A. Warren, Y.N. Wu, A. Lagrutta, C.T. Bond, and R.A. North, *Calcium-activated potassium channels expressed from cloned complementary DNAs*. Neuron, 1992. **9**(2): p. 209-16.
57. Lagrutta, A., K.Z. Shen, R.A. North, and J.P. Adelman, *Functional differences among alternatively spliced variants of Slowpoke, a Drosophila calcium-activated potassium channel*. J Biol Chem, 1994. **269**(32): p. 20347-51.
58. Heginbotham, L., T. Abramson, and R. MacKinnon, *A functional connection between the pores of distantly related ion channels as revealed by mutant K⁺ channels*. Science, 1992. **258**(5085): p. 1152-5.

59. Liman, E.R., J. Tytgat, and P. Hess, *Subunit stoichiometry of a mammalian K⁺ channel determined by construction of multimeric cDNAs*. Neuron, 1992. **9**(5): p. 861-71.
60. MacKinnon, R., *Determination of the subunit stoichiometry of a voltage-activated potassium channel*. Nature, 1991. **350**(6315): p. 232-5.
61. Covarrubias, M., A.A. Wei, and L. Salkoff, *Shaker, Shal, Shab, and Shaw express independent K⁺ current systems*. Neuron, 1991. **7**(5): p. 763-73.
62. Xu, J., W. Yu, Y.N. Jan, L.Y. Jan, and M. Li, *Assembly of voltage-gated potassium channels. Conserved hydrophilic motifs determine subfamily-specific interactions between the alpha-subunits*. J Biol Chem, 1995. **270**(42): p. 24761-8.
63. Salkoff, L., K. Baker, A. Butler, M. Covarrubias, M.D. Pak, and A. Wei, *An essential 'set' of K⁺ channels conserved in flies, mice and humans*. Trends Neurosci, 1992. **15**(5): p. 161-6.
64. Sakmann, B. and G. Trube, *Conductance properties of single inwardly rectifying potassium channels in ventricular cells from guinea-pig heart*. J Physiol, 1984. **347**: p. 641-57.
65. Constanti, A. and M. Galvan, *Fast inward-rectifying current accounts for anomalous rectification in olfactory cortex neurones*. J Physiol, 1983. **335**: p. 153-78.

66. Silver, M.R. and T.E. DeCoursey, *Intrinsic gating of inward rectifier in bovine pulmonary artery endothelial cells in the presence or absence of internal Mg²⁺*. J Gen Physiol, 1990. **96**(1): p. 109-33.
67. Ho, K., C.G. Nichols, W.J. Lederer, J. Lytton, P.M. Vassilev, M.V. Kanazirska, and S.C. Hebert, *Cloning and expression of an inwardly rectifying ATP-regulated potassium channel*. Nature, 1993. **362**(6415): p. 31-8.
68. Kubo, Y., T.J. Baldwin, Y.N. Jan, and L.Y. Jan, *Primary structure and functional expression of a mouse inward rectifier potassium channel*. Nature, 1993. **362**(6416): p. 127-33.
69. Bond, C.T., M. Pessia, X.M. Xia, A. Lagrutta, M.P. Kavanaugh, and J.P. Adelman, *Cloning and expression of a family of inward rectifier potassium channels [published erratum appears in Receptors Channels 1994;2(4):following 350]*. Receptors Channels, 1994. **2**(3): p. 183-91.
70. Inagaki, N., Y. Tsuura, N. Namba, K. Masuda, T. Gono, M. Horie, Y. Seino, M. Mizuta, and S. Seino, *Cloning and functional characterization of a novel ATP-sensitive potassium channel ubiquitously expressed in rat tissues, including pancreatic islets, pituitary, skeletal muscle, and heart*. J Biol Chem, 1995. **270**(11): p. 5691-4.
71. Sakura, H., C. Bond, M. Warren-Perry, S. Horsley, L. Kearney, S. Tucker, J. Adelman, R. Turner, and F.M. Ashcroft, *Characterization and variation*

- of a human inwardly-rectifying-K-channel gene (KCNJ6): a putative ATP-sensitive K-channel subunit. FEBS Lett, 1995. 367(2): p. 193-7.*
72. Kobayashi, T., K. Ikeda, T. Ichikawa, S. Abe, S. Togashi, and T. Kumanishi, *Molecular cloning of a mouse G-protein-activated K⁺ channel (mGIRK1) and distinct distributions of three GIRK (GIRK1, 2 and 3) mRNAs in mouse brain. Biochem Biophys Res Commun, 1995. 208(3): p. 1166-73.*
73. Lesage, F., E. Guillemare, M. Fink, F. Duprat, C. Heurteaux, M. Fosset, G. Romey, J. Barhanin, and M. Lazdunski, *Molecular properties of neuronal G-protein-activated inwardly rectifying K⁺ channels. J Biol Chem, 1995. 270(48): p. 28660-7.*
74. Pessia, M., C.T. Bond, M.P. Kavanaugh, and J.P. Adelman, *Contributions of the C-terminal domain to gating properties of inward rectifier potassium channels. Neuron, 1995. 14(5): p. 1039-45.*
75. Suzuki, M., K. Takahashi, M. Ikeda, H. Hayakawa, A. Ogawa, Y. Kawaguchi, and O. Sakai, *Cloning of a pH-sensitive K⁺ channel possessing two transmembrane segments. Nature, 1994. 367(6464): p. 642-5.*
76. Kohler, M., B. Hirschberg, C.T. Bond, J.M. Kinzie, N.V. Marrion, J. Maylie, and J.P. Adelman, *Small-conductance, calcium-activated potassium channels from mammalian brain. Science, 1996. 273(5282): p. 1709-14.*

77. Xia, X.M., B. Fakler, A. Rivard, G. Wayman, T. Johnson-Pais, J.E. Keen, T. Ishii, B. Hirschberg, C.T. Bond, S. Lutsenko, J. Maylie, and J.P. Adelman, *Mechanism of calcium gating in small-conductance calcium-activated potassium channels*. *Nature*, 1998. **395**(6701): p. 503-7.
78. Keen, J.E., R. Khawaled, D.L. Farrens, T. Neelands, A. Rivard, C.T. Bond, A. Janowsky, B. Fakler, J.P. Adelman, and J. Maylie, *Domains responsible for constitutive and Ca^{2+} -dependent interactions between calmodulin and small conductance Ca^{2+} -activated potassium channels*. *J Neurosci*, 1999. **19**(20): p. 8830-8.
79. Schumacher, M.A., A.F. Rivard, H.P. Bachinger, and J.P. Adelman, *Structure of the gating domain of a Ca^{2+} -activated K^{+} channel complexed with Ca^{2+} /calmodulin*. *Nature*, 2001. **410**(6832): p. 1120-4.
80. Shah, M. and D.G. Haylett, *The pharmacology of $hSK1$ Ca^{2+} -activated K^{+} channels expressed in mammalian cell lines*. *Br J Pharmacol*, 2000. **129**(4): p. 627-30.
81. Benton, D.C., A.S. Monaghan, R. Hosseini, P.K. Bahia, D.G. Haylett, and G.W. Moss, *Small conductance Ca^{2+} -activated K^{+} channels formed by the expression of rat $SK1$ and $SK2$ genes in HEK 293 cells*. *J Physiol*, 2003. **553**(Pt 1): p. 13-9.
82. Stocker, M. and P. Pedarzani, *Differential distribution of three Ca^{2+} -activated K^{+} channel subunits, $SK1$, $SK2$, and $SK3$, in the adult rat central nervous system*. *Mol Cell Neurosci*, 2000. **15**(5): p. 476-93.

83. Scott, V.E., J. Rettig, D.N. Parcej, J.N. Keen, J.B. Findlay, O. Pongs, and J.O. Dolly, *Primary structure of a beta subunit of alpha-dendrotoxin-sensitive K⁺ channels from bovine brain*. Proc Natl Acad Sci U S A, 1994. **91**(5): p. 1637-41.
84. Rettig, J., S.H. Heinemann, F. Wunder, C. Lorra, D.N. Parcej, J.O. Dolly, and O. Pongs, *Inactivation properties of voltage-gated K⁺ channels altered by presence of beta-subunit*. Nature, 1994. **369**(6478): p. 289-94.
85. Morales, M.J., R.C. Castellino, A.L. Crews, R.L. Rasmusson, and H.C. Strauss, *A novel beta subunit increases rate of inactivation of specific voltage-gated potassium channel alpha subunits*. J Biol Chem, 1995. **270**(11): p. 6272-7.
86. Wang, H.S., Z. Pan, W. Shi, B.S. Brown, R.S. Wymore, I.S. Cohen, J.E. Dixon, and D. McKinnon, *KCNQ2 and KCNQ3 potassium channel subunits: molecular correlates of the M-channel*. Science, 1998. **282**(5395): p. 1890-3.
87. Brenner, R., J.Y. Yu, K. Srinivasan, L. Brewer, J.L. Larimer, J.L. Wilbur, and N.S. Atkinson, *Complementation of physiological and behavioral defects by a slowpoke Ca(2⁺) -activated K(+) channel transgene*. J Neurochem, 2000. **75**(3): p. 1310-9.
88. Koster, J.C., B.A. Marshall, N. Ensor, J.A. Corbett, and C.G. Nichols, *Targeted overactivity of beta cell K(ATP) channels induces profound neonatal diabetes*. Cell, 2000. **100**(6): p. 645-54.

89. Zaritsky, J.J., D.M. Eckman, G.C. Wellman, M.T. Nelson, and T.L. Schwarz, *Targeted disruption of Kir2.1 and Kir2.2 genes reveals the essential role of the inwardly rectifying K(+) current in K(+)-mediated vasodilation*. Circ Res, 2000. **87**(2): p. 160-6.
90. McLerie, M. and A. Lopatin, *Dominant-negative suppression of I(K1) in the mouse heart leads to altered cardiac excitability*. J Mol Cell Cardiol, 2003. **35**(4): p. 367-78.
91. Browne, D.L., S.T. Ganchar, J.G. Nutt, E.R. Brunt, E.A. Smith, P. Kramer, and M. Litt, *Episodic ataxia/myokymia syndrome is associated with point mutations in the human potassium channel gene, KCNA1*. Nat Genet, 1994. **8**(2): p. 136-40.
92. Zerr, P., J.P. Adelman, and J. Maylie, *Episodic ataxia mutations in Kv1.1 alter potassium channel function by dominant negative effects or haploinsufficiency*. J Neurosci, 1998. **18**(8): p. 2842-8.
93. Clark, J.D. and B.L. Tempel, *Hyperalgesia in mice lacking the Kv1.1 potassium channel gene*. Neurosci Lett, 1998. **251**(2): p. 121-4.
94. Herson, P.S., M. Virk, N.R. Rustay, C.T. Bond, J.C. Crabbe, J.P. Adelman, and J. Maylie, *A mouse model of episodic ataxia type-1*. Nat Neurosci, 2003. **6**(4): p. 378-83.
95. Bradley, A., M. Evans, M.H. Kaufman, and E. Robertson, *Formation of germ-line chimaeras from embryo-derived teratocarcinoma cell lines*. Nature, 1984. **309**(5965): p. 255-6.

96. Gossler, A., T. Doetschman, R. Korn, E. Serfling, and R. Kemler, *Transgenesis by means of blastocyst-derived embryonic stem cell lines*. Proc Natl Acad Sci U S A, 1986. **83**(23): p. 9065-9.
97. Doetschman, T., A. Gossler, E. Serfling, W. Schaffner, K. Marcu, L. Stanton, and R. Kemler, *Introduction of genes into mouse embryonic stem cells*. Prog Clin Biol Res, 1986. **217A**: p. 47-50.
98. Thomas, K.R. and M.R. Capecchi, *Site-directed mutagenesis by gene targeting in mouse embryo-derived stem cells*. Cell, 1987. **51**(3): p. 503-12.
99. Nelson, R.J. and K.A. Young, *Behavior in mice with targeted disruption of single genes*. Neurosci Biobehav Rev, 1998. **22**(3): p. 453-62.
100. Silva, A.J., A.M. Smith, and K.P. Giese, *Gene targeting and the biology of learning and memory*. Annu Rev Genet, 1997. **31**: p. 527-46.
101. Umanoff, H., W. Edelmann, A. Pellicer, and R. Kucherlapati, *The murine N-ras gene is not essential for growth and development*. Proc Natl Acad Sci U S A, 1995. **92**(5): p. 1709-13.
102. Chang, H., A.L. Lau, and M.M. Matzuk, *Studying TGF-beta superfamily signaling by knockouts and knockins*. Mol Cell Endocrinol, 2001. **180**(1-2): p. 39-46.
103. Conway, S.J., A. Kruzynska-Frejtag, P.L. Kneer, M. Machnicki, and S.V. Koushik, *What cardiovascular defect does my prenatal mouse mutant have, and why?* Genesis, 2003. **35**(1): p. 1-21.

104. Lewandoski, M., *Conditional control of gene expression in the mouse*. Nat Rev Genet, 2001. **2**(10): p. 743-55.
105. Misra, R.P. and S.A. Duncan, *Gene targeting in the mouse: advances in introduction of transgenes into the genome by homologous recombination*. Endocrine, 2002. **19**(3): p. 229-38.
106. Gossen, M. and H. Bujard, *Tight control of gene expression in mammalian cells by tetracycline-responsive promoters*. Proc Natl Acad Sci U S A, 1992. **89**(12): p. 5547-51.
107. Kistner, A., M. Gossen, F. Zimmermann, J. Jerecic, C. Ullmer, H. Lubbert, and H. Bujard, *Doxycycline-mediated quantitative and tissue-specific control of gene expression in transgenic mice*. Proc Natl Acad Sci U S A, 1996. **93**(20): p. 10933-8.
108. Jerecic, J., F. Single, U. Kruth, H. Krestel, R. Kolhekar, T. Storck, K. Kask, M. Higuchi, R. Sprengel, and P.H. Seeburg, *Studies on conditional gene expression in the brain*. Ann N Y Acad Sci, 1999. **868**: p. 27-37.
109. Storck, T., U. Kruth, R. Kolhekar, R. Sprengel, and P.H. Seeburg, *Rapid construction in yeast of complex targeting vectors for gene manipulation in the mouse*. Nucleic Acids Res, 1996. **24**(22): p. 4594-6.
110. Sternberg, N., D. Hamilton, S. Austin, M. Yarmolinsky, and R. Hoess, *Site-specific recombination and its role in the life cycle of bacteriophage P1*. Cold Spring Harb Symp Quant Biol, 1981. **45 Pt 1**: p. 297-309.

111. Cox, M.M., *The FLP protein of the yeast 2-microns plasmid: expression of a eukaryotic genetic recombination system in Escherichia coli*. Proc Natl Acad Sci U S A, 1983. **80**(14): p. 4223-7.
112. Sauer, B. and N. Henderson, *Site-specific DNA recombination in mammalian cells by the Cre recombinase of bacteriophage P1*. Proc Natl Acad Sci U S A, 1988. **85**(14): p. 5166-70.
113. Nakano, M., M. Ishimura, J. Chiba, Y. Kanegae, and I. Saito, *DNA substrates influence the recombination efficiency mediated by FLP recombinase expressed in mammalian cells*. Microbiol Immunol, 2001. **45**(9): p. 657-65.
114. Bond, C.T., R. Sprengel, J.M. Bissonnette, W.A. Kaufmann, D. Pribnow, T. Neelands, T. Storck, M. Baetscher, J. Jerecic, J. Maylie, H.G. Knaus, P.H. Seeburg, and J.P. Adelman, *Respiration and parturition affected by conditional overexpression of the Ca²⁺-activated K⁺ channel subunit, SK3*. Science, 2000. **289**(5486): p. 1942-6.
115. Schwenk, F., U. Baron, and K. Rajewsky, *A cre-transgenic mouse strain for the ubiquitous deletion of loxP-flanked gene segments including deletion in germ cells*. Nucleic Acids Res, 1995. **23**(24): p. 5080-1.
116. Uusi-Oukari, M., J. Heikkila, S.T. Sinkkonen, R. Makela, B. Hauer, G.E. Homanics, W. Sieghart, W. Wisden, and E.R. Korpi, *Long-range interactions in neuronal gene expression: evidence from gene targeting in*

- the GABA(A) receptor beta2-alpha6-alpha1-gamma2 subunit gene cluster.*
Mol Cell Neurosci, 2000. **16**(1): p. 34-41.
117. Pham, C.T., D.M. MacIvor, B.A. Hug, J.W. Heusel, and T.J. Ley, *Long-range disruption of gene expression by a selectable marker cassette.* Proc Natl Acad Sci U S A, 1996. **93**(23): p. 13090-5.
118. Nakamura, A. and T. Kuwaki, *Sleep apnea in mice: a useful animal model for study of SIDS?* Early Hum Dev, 2003. **75 Suppl**: p. S167-74.
119. Morley Kotchen, J. and T.A. Kotchen, *Impact of female hormones on blood pressure: review of potential mechanisms and clinical studies.* Curr Hypertens Rep, 2003. **5**(6): p. 505-12.
120. Bosch, M.A., M.J. Kelly, and O.K. Ronnekleiv, *Distribution, neuronal colocalization, and 17beta-E2 modulation of small conductance calcium-activated K(+) channel (SK3) mRNA in the guinea pig brain.* Endocrinology, 2002. **143**(3): p. 1097-107.
121. Tamarina, N.A., Y. Wang, L. Mariotto, A. Kuznetsov, C. Bond, J. Adelman, and L.H. Philipson, *Small-conductance calcium-activated K⁺ channels are expressed in pancreatic islets and regulate glucose responses.* Diabetes, 2003. **52**(8): p. 2000-6.
122. Gossen, M. and H. Bujard, *Studying gene function in eukaryotes by conditional gene inactivation.* Annu Rev Genet, 2002. **36**: p. 153-73.
123. Leneuve, P., S. Colnot, G. Hamard, F. Francis, M. Niwa-Kawakita, M. Giovannini, and M. Holzenberger, *Cre-mediated germline mosaicism: a*

- new transgenic mouse for the selective removal of residual markers from tri-lox conditional alleles. Nucleic Acids Res, 2003. 31(5): p. e21.*
124. Clemens, B., *Ictal electroencephalography in a case of benign centrotemporal epilepsy. J Child Neurol, 2002. 17(4): p. 297-300.*
125. Zakharenko, S.S., S.L. Patterson, I. Dragatsis, S.O. Zeitlin, S.A. Siegelbaum, E.R. Kandel, and A. Morozov, *Presynaptic BDNF required for a presynaptic but not postsynaptic component of LTP at hippocampal CA1-CA3 synapses. Neuron, 2003. 39(6): p. 975-90.*
126. Fournier, C., S. Kourrich, B. Soumireu-Mourat, and C. Mourre, *Apamin improves reference memory but not procedural memory in rats by blocking small conductance Ca(2+)-activated K(+) channels in an olfactory discrimination task. Behav Brain Res, 2001. 121(1-2): p. 81-93.*
127. Cingolani, L.A., M. Gymnopoulos, A. Boccaccio, M. Stocker, and P. Pedarzani, *Developmental regulation of small-conductance Ca2+-activated K+ channel expression and function in rat Purkinje neurons. J Neurosci, 2002. 22(11): p. 4456-67.*
128. Womack, M.D. and K. Khodakhah, *Somatic and dendritic small-conductance calcium-activated potassium channels regulate the output of cerebellar purkinje neurons. J Neurosci, 2003. 23(7): p. 2600-7.*
129. Edgerton, J.R. and P.H. Reinhart, *Distinct contributions of small and large conductance Ca2+-activated K+ channels to rat Purkinje neuron function. J Physiol, 2003. 548(Pt 1): p. 53-69.*

130. Brockhaus, J. and J.W. Deitmer, *Long-lasting modulation of synaptic input to Purkinje neurons by Bergmann glia stimulation in rat brain slices*. J Physiol, 2002. **545**(Pt 2): p. 581-93.
131. Barski, J.J., K. Dethleffsen, and M. Meyer, *Cre recombinase expression in cerebellar Purkinje cells*. Genesis, 2000. **28**(3-4): p. 93-8.
132. Branda, C.S. and S.M. Dymecki, *Talking about a revolution: The impact of site-specific recombinases on genetic analyses in mice*. Dev Cell, 2004. **6**(1): p. 7-28.
133. Lancaster, B. and P.R. Adams, *Calcium-dependent current generating the afterhyperpolarization of hippocampal neurons*. J Neurophysiol, 1986. **55**(6): p. 1268-82.
134. Shao, L.R., R. Halvorsrud, L. Borg-Graham, and J.F. Storm, *The role of BK-type Ca²⁺-dependent K⁺ channels in spike broadening during repetitive firing in rat hippocampal pyramidal cells*. J Physiol, 1999. **521 Pt 1**: p. 135-46.
135. Sah, P. and E.S. Faber, *Channels underlying neuronal calcium-activated potassium currents*. Prog Neurobiol, 2002. **66**(5): p. 345-53.
136. Gerlach, A.C., C.A. Syme, L. Giltinan, J.P. Adelman, and D.C. Devors, *ATP-dependent activation of the intermediate conductance, Ca²⁺-activated K⁺ channel, hIK1, is conferred by a C-terminal domain*. J Biol Chem, 2001. **276**(24): p. 10963-70.

137. Storm, J.F., *An after-hyperpolarization of medium duration in rat hippocampal pyramidal cells*. J Physiol, 1989. **409**: p. 171-90.
138. Sah, P. and J.D. Clements, *Photolytic manipulation of $[Ca^{2+}]_i$ reveals slow kinetics of potassium channels underlying the afterhyperpolarization in hippocampal pyramidal neurons*. J Neurosci, 1999. **19**(10): p. 3657-64.
139. Bowden, S.E., S. Fletcher, D.J. Loane, and N.V. Marrion, *Somatic colocalization of rat SK1 and D class (Ca(v)1.2) L-type calcium channels in rat CA1 hippocampal pyramidal neurons*. J Neurosci, 2001. **21**(20): p. RC175.
140. Madison, D.V. and R.A. Nicoll, *Noradrenaline blocks accommodation of pyramidal cell discharge in the hippocampus*. Nature, 1982. **299**(5884): p. 636-8.
141. Pedarzani, P. and J.F. Storm, *PKA mediates the effects of monoamine transmitters on the K^+ current underlying the slow spike frequency adaptation in hippocampal neurons*. Neuron, 1993. **11**(6): p. 1023-35.
142. Ishii, T.M., C. Silvia, B. Hirschberg, C.T. Bond, J.P. Adelman, and J. Maylie, *A human intermediate conductance calcium-activated potassium channel*. Proc Natl Acad Sci U S A, 1997. **94**(21): p. 11651-6.
143. Joiner, W.J., L.Y. Wang, M.D. Tang, and L.K. Kaczmarek, *hSK4, a member of a novel subfamily of calcium-activated potassium channels*. Proc Natl Acad Sci U S A, 1997. **94**(20): p. 11013-8.

144. Ishii, T.M., J. Maylie, and J.P. Adelman, *Determinants of apamin and d-tubocurarine block in SK potassium channels*. J Biol Chem, 1997. **272**(37): p. 23195-200.
145. Sailer, C.A., H. Hu, W.A. Kaufmann, M. Trieb, C. Schwarzer, J.F. Storm, and H.G. Knaus, *Regional differences in distribution and functional expression of small-conductance Ca^{2+} -activated K^{+} channels in rat brain*. J Neurosci, 2002. **22**(22): p. 9698-707.
146. Monaghan, A.S., D.C. Benton, P.K. Bahia, R. Hosseini, Y.A. Shah, D.G. Haylett, and G.W. Moss, *The SK3 subunit of small conductance Ca^{2+} -activated K^{+} channels interacts with both SK1 and SK2 subunits in a heterologous expression system*. J Biol Chem, 2004. **279**(2): p. 1003-9.
147. Bond, C.T., R. Sprengel, J.M. Bissonnette, W.A. Kaufmann, D. Pribnow, T. Neelands, T. Storck, M. Baetscher, J. Jerecic, J. Maylie, H.G. Knaus, P.H. Seeburg, and J.P. Adelman, *Respiration and parturition affected by conditional overexpression of the Ca^{2+} -activated K^{+} channel subunit, SK3*. Science, 2000. **289**(5486): p. 1942-6.
148. Shmukler, B.E., C.T. Bond, S. Wilhelm, A. Bruening-Wright, J. Maylie, J.P. Adelman, and S.L. Alper, *Structure and complex transcription pattern of the mouse SK1 K(Ca) channel gene, KCNN1*. Biochim Biophys Acta, 2001. **1518**(1-2): p. 36-46.
149. Obermair, G.J., W.A. Kaufmann, H.G. Knaus, and B.E. Flucher, *The small conductance Ca^{2+} -activated K^{+} channel SK3 is localized in nerve*

- terminals of excitatory synapses of cultured mouse hippocampal neurons.*
Eur J Neurosci, 2003. **17**(4): p. 721-31.
150. Xia, X.-M., B. Fakler, A. Rivard, G. Wayman, T. Johnson-Pais, J.E. Keen, T. Ishii, B. Hirschberg, C.T. Bond, S. Lutsenko, J. Maylie, and J.P. Adelman, *Mechanism of calcium gating in small-conductance calcium-activated potassium channels.* Nature, 1998. **395**: p. 503-507.
 151. Sah, P. and J.D. Clements, *Photolytic manipulation of $[Ca^{2+}]$ reveals slow kinetics of potassium channels underlying the afterhyperpolarization in hippocampal pyramidal neurons.* J. Neurosci., 1999. **19**: p. 3657-3664.
 152. Vogalis, F., J.F. Storm, and B. Lancaster, *SK channels and the varieties of slow after-hyperpolarizations in neurons.* Eur J Neurosci, 2003. **18**(12): p. 3155-66.
 153. Gerlach, A.C., J. Maylie, and J.P. Adelman, *Activation kinetics of the slow afterhyperpolarization in hippocampal CA1 neurons.* Pflugers Arch, 2004 January 16.
 154. Lee, W.S., T.J. Ngo-Anh, A. Bruening-Wright, J. Maylie, and J.P. Adelman, *Small conductance Ca^{2+} -activated K^{+} channels and calmodulin: cell surface expression and gating.* J Biol Chem, 2003. **278**(28): p. 25940-6.
 155. D'Hoedt, D., K. Hirzel, P. Pedarzani, and M. Stocker, *Domain analysis of the calcium-activated potassium channel SK1 from rat brain: Functional expression and toxin sensitivity.* J Biol Chem, 2004. **279**(13):12088-92

156. Langer, P., S. Grunder, and A. Rusch, *Expression of Ca²⁺-activated BK channel mRNA and its splice variants in the rat cochlea*. J Comp Neurol, 2003. **455**(2): p. 198-209.
157. Burke, N.A., K. Takimoto, D. Li, W. Han, S.C. Watkins, and E.S. Levitan, *Distinct structural requirements for clustering and immobilization of K⁺ channels by PSD-95*. J Gen Physiol, 1999. **113**(1): p. 71-80.
158. Zhang, B.M., V. Kohli, R. Adachi, J.A. Lopez, M.M. Udden, and R. Sullivan, *Calmodulin binding to the C-terminus of the small-conductance Ca²⁺-activated K⁺ channel hSK1 is affected by alternative splicing*. Biochemistry, 2001. **40**(10): p. 3189-95.
159. Jiang, Y., A. Lee, J. Chen, M. Cadene, B.T. Chait, and R. MacKinnon, *The open pore conformation of potassium channels*. Nature, 2002. **417**(6888): p. 523-6.
160. Jospin, M., M.C. Mariol, L. Segalat, and B. Allard, *Characterization of K(+) currents using an in situ patch clamp technique in body wall muscle cells from Caenorhabditis elegans*. J Physiol, 2002. **544**(Pt 2): p. 373-84.
161. Desai, R., A. Peretz, H. Idelson, P. Lazarovici, and B. Attali, *Ca²⁺-activated K⁺ channels in human leukemic Jurkat T cells. Molecular cloning, biochemical and functional characterization*. J Biol Chem, 2000. **275**(51): p. 39954-63.
162. Litt, M., D. LaMorticella, C.T. Bond, and J.P. Adelman, *Gene structure and chromosome mapping of the human small-conductance calcium-activated*

- potassium channel SK1 gene (KCNN1)*. Cytogenet Cell Genet, 1999. **86**(1): p. 70-3.
163. Tsai, S.Y., B.W. O'Malley, F.J. DeMayo, Y. Wang, and S.S. Chua, *A novel RU486 inducible system for the activation and repression of genes*. Adv Drug Deliv Rev, 1998. **30**(1-3): p. 23-31.
 164. Schnutgen, F., N. Doerflinger, C. Calleja, O. Wendling, P. Chambon, and N.B. Ghyselinck, *A directional strategy for monitoring Cre-mediated recombination at the cellular level in the mouse*. Nat Biotechnol, 2003. **21**(5): p. 562-5.
 165. Shin, M.K., J.M. Levorse, R.S. Ingram, and S.M. Tilghman, *The temporal requirement for endothelin receptor-B signalling during neural crest development*. Nature, 1999. **402**(6761): p. 496-501.
 166. Yamamoto, A., J.J. Lucas, and R. Hen, *Reversal of neuropathology and motor dysfunction in a conditional model of Huntington's disease*. Cell, 2000. **101**(1): p. 57-66.
 167. Safran, M., W.Y. Kim, A.L. Kung, J.W. Horner, R.A. DePinho, and W.G. Kaelin, Jr., *Mouse reporter strain for noninvasive bioluminescent imaging of cells that have undergone Cre-mediated recombination*. Mol Imaging, 2003. **2**(4): p. 297-302.
 168. Cormack, B.P., R.H. Valdivia, and S. Falkow, *FACS-optimized mutants of the green fluorescent protein (GFP)*. Gene, 1996. **173**(1 Spec No): p. 33-8.

169. Haas, J., E.C. Park, and B. Seed, *Codon usage limitation in the expression of HIV-1 envelope glycoprotein*. Curr Biol, 1996. **6**(3): p. 315-24.
170. Kozak, M., *An analysis of 5'-noncoding sequences from 699 vertebrate messenger RNAs*. Nucleic Acids Res, 1987. **15**(20): p. 8125-48.
171. Kramer, B.P., W. Weber, and M. Fussenegger, *Artificial regulatory networks and cascades for discrete multilevel transgene control in mammalian cells*. Biotechnol Bioeng, 2003. **83**(7): p. 810-20.
172. Busselberg, D., A.M. Bischoff, and D.W. Richter, *A combined blockade of glycine and calcium-dependent potassium channels abolishes the respiratory rhythm*. Neuroscience, 2003. **122**(3): p. 831-41.
173. Griffith, T.M., *Endothelium-dependent smooth muscle hyperpolarization: do gap junctions provide a unifying hypothesis?* Br J Pharmacol, 2004. **141**(6): p. 881-903.
174. Jacobson, D., D. Pribnow, P.S. Herson, J. Maylie, and J.P. Adelman, *Determinants contributing to estrogen-regulated expression of SK3*. Biochem Biophys Res Commun, 2003. **303**(2): p. 660-8.
175. Kohler, R., S. Brakemeier, M. Kuhn, C. Behrens, R. Real, C. Degenhardt, H.D. Orzechowski, A.R. Pries, M. Paul, and J. Hoyer, *Impaired hyperpolarization in regenerated endothelium after balloon catheter injury*. Circ Res, 2001. **89**(2): p. 174-9.

176. Barriere, E., K.A. Tazi, F. Pessione, J. Heller, O. Poiriel, D. Lebrech, and R. Moreau, *Role of small-conductance Ca^{2+} -dependent K^{+} channels in in vitro nitric oxide-mediated aortic hyporeactivity to alpha-adrenergic vasoconstriction in rats with cirrhosis*. J Hepatol, 2001. **35**(3): p. 350-7.
177. Power, J.M., M.M. Oh, and J.F. Disterhoft, *Metrifonate decreases $sl(AHP)$ in CA1 pyramidal neurons in vitro*. J Neurophysiol, 2001. **85**(1): p. 319-22.

Appendix A

Listed are publications resulting from studies of SK transgenic mice or that were published during my graduate student tenure.

1. **Bond CT**, Sprengel R, Bissonnette JM, Kaufmann WA, Pribnow D, Neelands T, Storck T, Baetscher M, Jerecic J, Maylie J, Knaus HG, Seeburg PH, Adelman JP. Respiration and parturition affected by conditional overexpression of the Ca^{2+} -activated K^{+} channel subunit, SK3.

Science. 289:1942-6, 2000

2. Shmukler BE, **Bond CT**, Wilhelm S, Bruening-Wright A, Maylie J, Adelman JP, Alper SL. Structure and complex transcription pattern of the mouse SK1 K(Ca) channel gene, KCNN1.

Biochim Biophys Acta. 1518:36-46, 2001

3. Taylor MS, Bonev AD, Gross TP, Eckman DM, Brayden JE, **Bond CT**, Adelman JP, Nelson MT. Altered expression of small-conductance Ca^{2+} -activated K^{+} (SK3) channels modulates arterial tone and blood pressure.

Circ Res. 2003 Jul 25;93(2):124-31

4. Herrera GM, Pozo MJ, Zvara P, Petkov GV, **Bond CT**, Adelman JP, Nelson MT. Urinary bladder instability induced by selective suppression of the murine small conductance calcium-activated potassium (SK3) channel. J Physiol. 2003 Jun 17 551:893-903

5. Tamarina NA, Wang Y, Mariotto L, Kuznetsov A, **Bond C**, Adelman J, Philipson LH. Small-conductance calcium-activated K(+) channels are expressed in pancreatic islets and regulate glucose responses. Diabetes. 2003 Aug;52(8):2000-6.

6. Herson PS, Virk M, Rustay NR, **Bond CT**, Crabbe JC, Adelman JP, Maylie J. A mouse model of episodic ataxia type-1. Nat Neurosci. 2003 Apr;6(4):378-83.

7. **Bond CT**, Herson PS, Strassmaier T, Hammond R, Stackman R, Maylie J, Adelman JP. SK Knockout Mice Reveal the Identity of Calcium-dependent AHP Currents. J Neurosci. Submitted Jan. 2004, resubmitted Mar 2004

Appendix B.

Derivation of the formula for comparative C_T method for quantitative PCR.

Amount of target, normalized to an internal reference and relative to a calibrator is given by: $2^{-\Delta\Delta C_t}$

The exponential amplification of PCR is given by:

$$X_n = X_0 \times (1 + E_x)^n$$

where X_n =number of target molecules at cycle n , X_0 =initial number of target molecules, E_x =efficiency of amplification, and n =number of cycles.

The threshold cycle (C_t) indicates the fractional cycle number at which the amount of amplified target reaches a fixed threshold. Thus

$$X_T = X_0 \times (1 + E_x)^{C_{t,x}} = K_x$$

where X_T =threshold number of target molecules, $C_{t,x}$ =threshold cycle for target amplification, and K_x =constant.

The corollary equation for the endogenous reference reaction is

$$R_T = R_0 \times (1 + E_R)^{C_{t,R}} = K_R$$

where R_T =threshold number of reference molecules, R_0 =initial number of reference molecules, E_R =efficiency of reference amplification, $C_{t,R}$ =threshold cycle for reference, and K_R =constant.

Dividing X_T by R_T gives:

$$X_T / R_T = X_0 \times (1+E_x)^{Ct,x} / R_0 \times (1+E_R)^{Ct,R} = K_x / K_R = K$$

Assuming the efficiencies of target and reference are the same: $E_x = E_R = E$, gives

$$X_0 / R_0 \times (1+E)^{Ct,x-Ct,R} = K \text{ or } X_N \times (1+E)^{\Delta Ct} = K$$

where $X_N = X_0 / R_0$, the normalized amount of target and $\Delta Ct = Ct,x - Ct,R$.

Rearranging gives the following equation:

$$X_N = K \times (1+E)^{-\Delta Ct}$$

Dividing X_N for any sample q by X_N for the calibrator (cb) yields:

$$X_{N,q} / X_{N,cb} = (K \times (1+E)^{-\Delta Ct,q}) / (K \times (1+E)^{-\Delta Ct,cb}) = (1+E)^{-\Delta \Delta Ct}$$

where $\Delta \Delta Ct = \Delta Ct,q - \Delta Ct,cb$

For optimized amplicons < 150 base pairs, the efficiency of amplification per round is close to one. Thus the amount of target, normalized to an endogenous reference and relative to a calibrator is given by:

$$2^{-\Delta \Delta Ct}$$